(NASA-TM-X-74600) FUNDAMENTAL ANALYSIS OF THE LINEAR MULTIPLE REGRESSION TECHNIQUE FOR QUANTIFICATION OF WATER QUALITY PARAMETERS FROM REMOTE SENSING DATA Ph.D. Thesis - Old Dominion Univ. (NASA) 185 p HC A09/MF A01 N77-20546

Unclas
G3/43 23907

FUNDAMENTAL ANALYSIS OF THE LINEAR MULTIPLE REGRESSION TECHNIQUE FOR QUANTIFICATION OF WATER QUALITY PARAMETERS FROM REMOTE SENSING DATA

by

Charles Henry Whitlock III
B.A.E. June 1961, University of Virginia
M.A.E. June 1965, University of Virginia
M.B.A. June 1970, College of William and Mary

A Dissertation Submitted to the Faculty of
Old Dominion University in Partial Fulfillment of the
Requirements for the Degree of

DOCTOR OF PHILOSOPHY

CIVIL ENGINEERING

OLD DOMINION UNIVERSITY
May, 1977

Approved by:

Chin Y. Kuo (Director)

ABSTRACT

FUNDAMENTAL ANALYSIS OF THE
LINEAR MULTIPLE REGRESSION TECHNIQUE FOR
QUANTIFICATION OF WATER QUALITY PARAMETERS
FROM REMOTE SENSING DATA

Charles Henry Whitlock III
Old Dominion University, 1977
Director: Dr. Chin Y. Kuo

Inconsistent results have been obtained from previous experiments which have applied linear multiple regression techniques to remote sensing data for quantification of water quality parameters. The objective of this investigation is to define optical physics and/or environmental conditions under which the linear multiple regression should be applicable. To achieve this objective, an investigation of the signal response equations is conducted and the concept is tested by application to both analytical test cases and actual remote sensing data from a laboratory under controlled conditions.

Investigation of the signal response equations shows that the exact solution for a number of optical physics conditions is of the same form as a linearized multiple regression equation, even if nonlinear contributions are made by such factors as surface reflections, atmospheric constituents, or other water pollutants. Limitations on achieving this type of solution are defined. Since the exact solution is in the form of a linear multiple regression equation, application of multiple regression techniques to remote sensing and ground truth data is viewed as a calibration of the exact solution to account for

daily variations in background constituents.

Least-squares and statistical concepts for performing the multiple regression analysis are examined. A test for evaluating the applicability of least-squares techniques to a particular set of data is defined and criteria for selection of "good" data are established.

From analytical test case results, it is concluded that constituents with linear radiance gradients with concentration may be quantified from signals which contain nonlinear atmospheric and surface reflection effects for both homogeneous and non-homogeneous water bodies provided accurate data can be obtained and nonlinearities are constant with wavelength. It is also concluded that statistical parameters must be used which give an indication of bias as well as total squared error to insure that an equation with an optimum combination of bands is selected for utilization.

From application to laboratory data, it is concluded that the effect of error in upwelled radiance measurements is to reduce the accuracy of the least-squares fitting process and to increase the number of points required to obtain a satisfactory fit. The problem of obtaining a multiple regression equation that is extremely sensitive to error is discussed. It is also concluded that the linearized multiple regression is applicable in situations in which some types of optical interaction occur between constituents.

The result of this investigation is an increased understanding of technique limitations, mathematical requirements, ground truth

requirements, and error effects which should aid in the obtaining of consistent results from future remote sensing experiments.

TABLE OF CONTENTS

ACKNOWLEDGEMENTS

I owe a debt of gratitude to many people whose aid enabled the completion of this investigation. My Ph.D. committee consisting of Dr. Chin Kuo, Dr. George Ofelt, Dr. Robert Cheng, Dr. John Kuhlman, Dr. Sidney Roberts, and (from Virginia Commonwealth University) Dr. George Canavos provided both intellectual and technical support. In addition, their unusual interest in this particular problem area provided a degree of encouragement and moral support which cannot be measured. Much credit must also go to a number of persons at the NASA Langley Research Center where the author is employed. Mr. Donald P. Hearth, Director of the Langley Research Center, personally approved the use of his contingency budget for fiscal year 1976 for the construction of the laboratory facility used in this investigation. A special debt is owed to Mr. Ernest A. Gurganus for electrical and mechanical support which allowed laboratory construction and testing to proceed at a rapid pace in spite of a limited budget. The tests could not have been conducted without the assistance of Mr. Jimmy W. Usry and Mr. William G. Witte Jr. who provided important criticism at various stages of construction and sorted out numerous problems associated with the spectrometer instrument. Sincere appreciation must also go to Mr. William H. Guy III, a summer employee and student from the University of Virginia, who assisted the author in the hand-reading of numerous Polaroid images to obtain the measurements required for this investigation. Finally, I am eternally grateful

for the encouragement and patience provided me by my supervisor at the Langley Research Center, Mr. Albin O. Pearson, and my wife, Jean, who sacrificed much to make this effort possible.

Charles H. Whitlock

Norfolk, Virginia
March, 1977

CHAPTER I

INTRODUCTION

Large amounts of sediments and other pollutants are carried annually in the rivers, lakes, estuaries, and coastal waters of the United States. These sediments and pollutants are major determinates of water quality. Measurement of marine sediment and pollutant concentrations is a tedious and expensive effort usually involving both in situ and laboratory work. Efforts have been directed towards the development of more rapid and economical methods for monitoring sediment and pollutant concentration in the nation's waters. Many agencies are investigating the potential of using remote sensing techniques to monitor various water quality parameters because of the ability of remote sensing to provide synoptic views over large areas.

Specific data needs usually vary among different user organizations (Kuo and Cheng 1976). Typical water quality parameters of interest to user organizations include chlorophyll, phytoplankton, organic compounds, toxic chemicals, heavy metals, clays, silt, and sand. For these parameters, the types of information desired are concentration, composition, size distribution, etc. for biological, geological, oceanographic, and sanitation uses. Advanced monitoring systems which utilize remote sensing data to its fullest advantage are desired for assessment of the effects of both man-made and natural events such as storms, floods, etc.. While much has been done toward the use of

remote sensing data for monitoring of water quality parameters ("Satellites Helping-----Problems" 1975), it is clear that additional research and development of improved data analysis procedures is desired by many users (Howells 1975, for example). Generally the desired use of remote sensing data is either identification or quantification of surface sediments and pollutants. In the long term, both identification and quantification are desired simultaneously from the same data. At the present time, however, these two processes are approached by different techniques. This dissertation is concerned with data analysis procedures for quantification of water quality parameters that have already been identified and are known to exist within the water body. Specifically, the study deals with the linear multiple regression technique as a procedure for defining and calibrating data analysis algorithms for such instruments as spectrometers and multispectral scanners. The technique has been utilized by Johnson (1975 and 1976), and Rogers et al (October 1975) with some apparent success. A more complete understanding of the limitations, requirements, and precision of the linear multiple regression technique is required before it can be applied by user agencies in an operational manner. In an effort to gain some insight into these questions, it is the objective of this investigation to define optical physics and/or environmental conditions under which the linear multiple regression analysis should apply for quantification of water quality parameters. To achieve this objective, an investigation of the signal response equations is conducted, and the concept is tested by application to both analytical test cases and

actual remote sensing data from a laboratory under controlled conditions. An improved understanding of technique limitations, mathematical requirements, ground truth requirements, and error effects is desired as a result of this study.

CHAPTER II

REMOTE SENSING CONCEPTS AND PRESENT SYSTEMS

There are two types of remote sensing systems capable of monitoring water characteristics. Active systems are those which emit their own energy source and monitor variances in the return signal. Radars, lasers, and microwave radiometers are examples of active remote sensing systems. Passive systems are those which depend upon the sun's radiation as the energy source and measure variations in the upwelled signal radiated back from the surface of the Earth. Aerial photography, spectrometers, and multispectral scanners are examples of passive remote sensing systems. This investigation is concerned with use of passive systems, in particular spectrometers and multispectral scanners, as a means for remote sensing of water quality parameters.

Passive remote sensors measure the total upwelled radiance emitted from the water-atmospheric system as shown in figure 1. Components which make up the total upwelled radiance include (1) upwelled radiance from the water, (2) reflected light, and (3) diffuse skylight. Of these components, only the upwelled light from the water is normally a function of the constituents in the water, although in some cases, surface films as a result of water pollutants may influence reflected radiance. The upwelled light from the water is the result of a multiple scattering and absorption process in which a small fraction

(usually less than one percent) of the downwelling light is back-scattered back up through the water surface. Constituents which introduce particles or dissolved substances alter the scattering and absorption characteristics of the mixture which in turn alter the upwelled radiance emitted through the surface of the water. The upwelled radiance is further modified by diffuse skylight and reflected sunlight before it reaches the remote sensor. Researchers are presently seeking methods to separate atmospheric and surface reflection effects from total remote sensing signals in an effort to deduce variations in upwelled spectra caused by variations in water constituents. The ultimate goal is to devise data analysis procedures from which water constituents may be identified and quantified by computerized processes.

For ease of computerized analysis, remote sensing systems which have digital radiance output are desired. For this reason, multi-spectral scanners or spectrometers are normally used to monitor upwelled radiance whenever economic conditions allow such systems. As sketched in figure 2, a spectrometer normally measures the total radiance (or power) spectrum over the wavelength range of interest. The measurement is for only one location within the scene of interest, however. To overcome this limitation, multispectral scanners have spanwise rotating optics systems such that upwelled radiance may be measured over a total scene as the aircraft or satellite progresses along its flight path. Unfortunately, multispectral scanners measure only a portion of the total upwelled radiance spectrum. Total radiance

values at specified bands over the wavelength range of interest are the output of these instruments. Most research is presently centered on the use of multispectral scanners from either aircraft or satellite for the monitoring of water constituents. It must be noted, however, that spectrometers may also be utilized for identification and quantification of marine parameters if one does not require values over a total scene.

A number of multispectral scanner systems are presently available. Unfortunately, each system has different band locations and band widths from the other systems available. Figure 3 shows band locations and band widths for several of the more well-known systems. It must also be noted that each system has a different ability to resolve features on the surface of the earth (spacial resolution). LANDSAT A and B have spacial resolutions of 70 meters, and LANDSAT D will have a value near 30 meters. NIMBUS G has narrow bandwidths (high spectral resolution), but its spacial resolution is expected to be near 200 meters. Aircraft systems normally have lower spacial resolutions as a result of lower flight altitude. From a 2.4 km altitude, the Bendix Modular Multispectral Scanner (M2S) has a spacial resolution of 7 meters. The NASA Ocean Color Scanner (OCS) has a spacial resolution of 70 meters from the U-2 aircraft at an altitude of 18.3 km. It must also be noted that the various scanners have different amounts of instrument noise in the radiance measurements. Noise in the data may range from 2 percent to 30 plus percent of the water radiance values depending on the particular scanner being used, the particular

band under analysis, the instrument gain setting, and the stability of associated equipment on the day of the experiment. The effects of noise on the analysis of remote sensing data will be discussed in a later section.

CHAPTER III

HISTORY AND RELATED WORK

It has been known for a number of years that differences in water turbidity or light transmission characteristics can often be detected by certain aerial photography systems. Some efforts have been successful at quantifying the surface concentrations of some water quality parameters from photographic data in a limited number of cases (see Lillesand 1973 and Link 1973, for example). With the launch of the ERTS-1 satellite (now known as LANDSAT-A), it was recognized by a number of agencies that the potential exists for monitoring water quality parameters on a large scale. The use of multispectral scanners such as that used on LANDSAT-A provide digital radiance data which is susceptible to computerized processing in large volumes. If computerized algorithms can be developed which relate remotely-sensed radiance values to water constituent concentrations, then certain water quality parameters may be monitored over large geographic areas on a rapid time scale which is not possible with photographic data.

One of the major difficulties in evaluating the potential for remote sensing of water constituents is the fact that only limited optical theory is presently available to relate the remote sensing measurements to concentrations of specific water parameters. Jerlov (1968) gives the precise formulation of the radiative transfer equation in an absorbing and scattering medium from which the radiance

upwelled from the water may be calculated. The radiative transfer process is treated as a function of the losses caused by absorption added to the gain caused by scattering. Various approximate solutions have been formulated (see Jerlov 1968 and McCluney 1974, for example) for relatively clear ocean waters, but an exact solution to the radiative transfer equation applicable to all classes of water is believed to be extremely difficult (Jerlov 1968). Because of this difficulty, various researchers (Gordon et al 1975 and Ghovanlou 1976, for example) have developed optical theory models which use Monte Carlo techniques to trace movement of photons after entry into the water from the atmosphere. Such models are often prohibitive for practical investigations because 100,000 separate computer cases may be required to define the upwelled radiance spectra over a reasonable wavelength range.

Optical models are also limited at the present time in that they relate the upwelled radiance to only the optical properties of the water and not specific constituent concentrations. Monte Carlo optical models generally compute the upwelled radiance based on the beam attenuation coefficient, the scattering coefficient, and the probability scattering function of the water mixture. Only limited work has been done to relate these specific optical parameters as a group to concentrations of specific water constituents for the more turbid waters as found in the coastal and inland United States. For example, Ghovanlou et al (1973) collected samples from a number of East Coast locations and made laser transmission measurements in a

laboratory. This study was successful in relating beam attenuation coefficient to constituent concentration and defined the scattering to absorption ratio for a number of different sediments. Whitlock (1976) used these data to estimate scattering and absorption coefficients as a function of sediment type and concentration. Unfortunately, the results are limited to one wavelength (540 nm) and values for the probability scattering function are not available. Thus a complete set of optical parameters is not available for input to a Monte Carlo model without estimating one parameter. The problem of not having measured values of all optical parameters over a wavelength range for various constituent concentrations is typical and is a major reason for the present lack of theoretical relations between water constituent concentration values and upwelled remote sensing radiance measurements.

As a result of the above unknowns, most LANDSAT and other multispectral scanner investigations have approached the problem from a statistical point of view. The usual analysis is one in which the radiance values of various wavelengths (or bands) are correlated with ground truth concentration values of a particular parameter in a linearized, least-squares-fit manner. When a high value of correlation coefficient (approaching 1.0) and a low value of standard error (68 percent of all points for a normally-distributed error band about the fitted curve) is obtained, it is often assumed that the regression equation obtained from the least-squares fit can be used to estimate water constituent concentrations in other areas of the remote sensing image where no ground truth measurements exist. In the simplest case,

the regression equation is linear and of the following form:

$$C = J + K_X(Rad_X) \qquad (3\text{-}1)$$

where: C = water constituent concentration

J = empirical constant

K_X = empirical constant for wavelength X

Rad_X = radiance at wavelength X (or band X)

When a linearized, least-squares fit is made to more than one parameter, the resulting relation is known as a linearized multiple regression equation which might be of the following form:

$$C = J + K_X(RadX) + K_Y(Rad_Y) + ... \qquad (3\text{-}2)$$

While statistical data analysis techniques provide only limited understanding of the optical process being monitored, the approach has been successful in providing useful information to agencies which monitor various water quality parameters. Developments which have led to multiple regression concepts for analysis of marine remote sensing data are reviewed in the following paragraphs.

Klemas et al (1973) noted the ability of the LANDSAT-A multispectral scanner to detect sediment plumes and aquatic fronts with band 5. At the same time, Wezernak and Roller (1973) demonstrated that both LANDSAT and aircraft multispectral scanners had the ability to see

acid-iron wastes, sewage sludge, suspended solids, and major water mass boundaries in the New York Bight area. Maul (1973) noted the ability to detect chlorophyll-A in the ocean and concluded that sea state is a significant variable that can dominate the upwelled radiance when weather conditions introduce bubbles, white caps, and foam. Grew (1973) concluded that it was feasible to distinguish between algae and sediment from tests conducted at Clear Lake, California. Yarger et al (March 1973) showed that LANDSAT bands 5 and 6 showed strong correlation with suspended load in two Kansas reservoirs but noted possible problems with atmospheric scatter. Scherz et al (1973) made simple laboratory measurements of upwelled spectral signatures of various water samples and concluded that upwelled radiance positively correlates with water turbidity. Ritchie et al (1974) made spectrometer measurements of six Mississippi lakes and showed a high linear correlation coefficient ($r = 0.90$) between upwelled radiation and total suspended solids in the 28 to 242 ppm range. The data were from a number of different water bodies, and there was a large amount of scatter in the results (probably the result of different dissolved substances and particle compositions in the various lakes). It was later found (Ritchie et al 1975) that the sun angle had an effect on the correlation of upwelled radiance to total suspended solids. Turner (1974) made a study of atmospheric effects and concluded that variations in atmospheric absorption and multiple scattering have a significant nonlinear effect on values obtained from an aircraft or satellite remote sensing system. Of particular concern was data taken

under hazy conditions in which aerosol or moisture content might vary over the remote sensing scene of interest. In spite of these difficulties, Christensen and Wezernak (1975) concluded that remote sensing could serve as an important addition to techniques available to a regulatory agency for environmental monitoring. Images give good maps of overall features of turbid and thermal plumes, and surface films could be detected at wavelengths between 320 and 380 nm. The above results indicate that remotely-sensed spectral measurements are quite useful for qualitative evaluation of circulation and transport patterns.

Of particular concern to agencies charged with environmental monitoring responsibilities is the requirement to quantify surface concentration values using remote sensing data. One early attempt at quantification was by Yost et al (1973) which developed additive color algorithms of the form:

$$C = J + K(Rad_X + Rad_Y) \qquad (3\text{-}3)$$

The algorithms produced good results for quantification of suspended solids for two days in the New York Bight area but were unsuccessful in quantification of extinction coefficient, chlorophyll-A, and total particle counts. Yarger et al (1973) showed that sun angle had a significant effect on upwelled radiance signals and formulated a band-ratio technique which nearly surpressed the effect of unequal illumination. The band-ratio algorithm was of the form:

$$C = J + K\left(\frac{Rad_X}{Rad_Y}\right) \qquad (3\text{-}4)$$

It was also demonstrated that for a concrete target on the ground, the band-ratio technique eliminated the effects of variable atmospheric scattering and absorption. It was noted, however, that the band-ratio algorithm did not produce consistent results for experiments conducted on different days. The reason for the anomalous behavior was unexplained, and it was believed that variations in water constituents and surface conditions between days were not significant. Bennett and Sydor (1974) utilized a linear regression algorithm of the form of equation (3-1) with LANDSAT band 5 to map turbidity in Lake Superior to an accuracy of 20 percent. It was noted, however, that factors which changed the absorption coefficient of the water caused the upwelled radiance for Superior Bay to be four times lower than that from Lake Superior water bearing equivalent suspended load. One of the most complete investigations recently reported is that conducted by Yarger and McCauley (1975). That investigation made correlation studies with 16 LANDSAT overpasses over three Kansas reservoirs collecting a total of 170 water samples for ground truth data. It was concluded that the band-ratio type of algorithm depressed the effect of seasonal sun angle variation, and that suspended solids could be quantified with a linear algorithm (equation (3-4)) to a standard error of 12 ppm over a range of 0 to 80 ppm. The radiance-concentration relationship was nonlinear for concentrations above

80 ppm. A good fit to the higher concentration data was obtained with a smooth polynomial algorithm of the following form:

$$C = J + K_1\left(\frac{Rad_X}{Rad_Y}\right) + K_2\left(\frac{Rad_X}{Rad_Y}\right)^2 + K_3\left(\frac{Rad_X}{Rad_Y}\right)^3 \qquad (3\text{-}5)$$

A standard error of 35 ppm over a range of 0 - 900 ppm was obtained for suspended solids. Correlation studies with the SKYLAB multispectral scanner produced similar results, however, these experiments were limited to suspended solids concentrations less than 100 ppm. The investigation was unsuccessful in detecting dissolved solids (ranging to 500 ppm) and algal nutrients (ranging to 20 ppm). Total chlorophyll was not detectable below 8 µg/ℓ but showed a weak correlation for higher values. Also potassium, phosphate, and nitrate were not detectable. Bowker and Witte (1975) also made repetitive investigations with several LANDSAT passes over the lower Chesapeake Bay in Virginia. Their analysis included linearized correlation studies using a number of different types of algorithms including single band (equation (3-1)), color addition (equation (3-3)), color substraction, band ratios (equation (3-4)), and band multiplication ($C = J + K(Rad_X Rad_Y)$) forms. While the experimental data suffered from tidal and meteorological effects as a result of time lag between the satellite overpass and ground truth sampling, it was concluded that good linear correlations with sediment could be obtained with LANDSAT band 5 or combinations of band 5 and band 4. Only low correlations for chlorophyll could be obtained. Results from individual days were

quite variable indicating the effects of atmospheric, tidal, and seasonal variations. Unlike the studies of Yarger and McCauley (1975), the band-ratio type of algorithm did not improve this situation. Later analysis (Bowker et al 1975) indicated that a color substraction algorithm (using ($Rad_5 - Rad_6$)) was highly correlated with total particles if a daily calibration could be obtained. Band 5 also had high correlation with water attenuation coefficient at a wavelength of 535 nm.

It must be noted that several non-statistical approaches have been attempted in the effort to quantify certain water constituents from remote sensing data. Williamson et al (1973) developed automatic data processing routines using only limited computer capability for mapping of suspended sediment classes. The technique matched reference spectra from known ground truth to satellite data (after corrections for a standard atmosphere) assuming the following parameters are constant over the scene of interest:

1. Water constituents
2. Water surface conditions
3. Solar geometry
4. Atmospheric composition

(It should be noted that many of the statistical analysis techniques make these same assumptions.) It was noted that the technique was unable to discriminate between various sediment types for concentrations below 25 ppm, but some measure of discrimination was possible for higher concentrations. Scherz et al (1975) developed a technique

in which the atmosphere and water surface noise effects on LANDSAT data can be removed using distilled water laboratory measurements and field measurement of signals from very clear lakes. The approach made a number of optical and physical assumptions, but a quantitative calculation for turbidity is made and used for classification of Wisconsin Lakes.

Most recently, linearized multiple regression analysis procedures have been applied to marine remote sensing data. This technique provides data analysis algorithms of the form of equation (3-2). The first known use of multiple regression procedures for marine data was by Mueller (1974) in performing correlations of ocean color spectra off the Oregon coast. The technique was used in an indirect manner in that dummy variables were correlated in the regression analysis instead of radiance levels from various wavelengths or bands. The measured upwelled radiance spectra was transformed into four principle components where the principle components are projections of the observed spectra on coordinate axes defined by the first four orthonormal eigenvectors. The purpose of the transformation was to reduce 55 bands of spectrometer data to four variables for ease of manipulation. Two algorithms were developed for Secchi-depth and Net Equivalent Color concentration with correlation coefficients of 0.89 and 0.87, respectively. It was noted that the assumption of linearity of upwelled radiance with concentration was questionable.

Johnson (March 1975) was apparently the first to apply multiple regression analysis in a direct manner using actual LANDSAT radiance

values. Using four data points from the Delaware Bay, an algorithm was formulated and applied to the Potomac River to produce a continuously variable map of suspended sediment concentrations. Unfortunately no ground truth data were available from the Potomac to test the accuracy of the algorithm. This study served to introduce the concept of direct application of multiple regression analysis for developing data analysis algorithms for quantifying surface concentrations of water constituents. The concept was applied to aircraft multispectral scanner data in a later experiment in the James River of Virginia in which 54 ground truth data points were taken near the time of overpass (Johnson et al June 1975). Linearized radiance-concentration relationships were assumed and multiple regression algorithms were developed for suspended sediment and chlorophyll concentrations (Johnson June 1975). For suspended sediment, the multiple regression algorithm of the form of equation (3-2) had a standard error of 4.31 ppm over a range of 0 to 50 ppm. The correlation coefficient was 0.93. This represented an improvement over the single band regression algorithm (equation (3-1)) which had a standard error of 4.76 ppm and a correlation coefficient of 0.89. Use of multiple regression analysis produced a more dramatic improvement for the chlorophyll-A parameter. Over a range of 0 to 20 mg/m^3, the multiple regression algorithm had a standard error of 1.56 mg/m^3 and a correlation coefficient of 0.97, while the single band regression algorithm had a standard error of 2.64 mg/m^3 and a correlation coefficient of 0.89. This study suggested the potential

for multiple regression concepts as an analysis technique for separating various water constituents from the total water scene. Conducting a more refined analysis of the same James River data set (Johnson May 1976 and Johnson and Bahn August 1976), it was found that correlation coefficients and standard error values were not as good as the earlier analysis had indicated. For suspended sediment, a single band regression equation (using band 8) produced a standard error of 7.16 ppm ($r = 0.79$), but a multiple regression equation (using bands 8 and 1) again improved the analysis reducing the standard error to 5.86 ppm ($r = 0.87$). Use of the refined data produced only a slight degradation in the chlorophyll-A results. A standard error of 1.78 mg/m^3 ($r = 0.96$) was obtained for this parameter using a multiple regression equation. It was also found that multiple regression algorithms could be derived which gave high correlations for Secchi-depth ($r = 0.92$), inorganic NO_3 ($r = 0.98$), inorganic NO_2 ($r = 0.99$), acidity ($r = 0.99$), and salinity ($r = 0.97$). The high correlation of many of these parameters were not believed to be a direct result of the scattering attenuation optical process but rather because of indirect chemical or physical relationships between the particular parameter and sediment or chlorophyll properties. Unfortunately the results are for only one data set, and there is no evidence of the reliability of the analysis technique for different days on the same water body.

The multiple regression concept has now been accepted by other investigators and applied to other water bodies. Rogers et al (1975)

applied the concept to define algorithms for 12 water quality parameters in Saginaw Bay, Michigan. LANDSAT data were then input to these algorithms to map the surface concentrations of the 12 water quality parameters. The particular parameters mapped were Secchi-depth, temperature, conductivity, chloride, chlorophyll, sodium, potassium, magnesium, calcium, total dissolved phosphorus, total phosphorus, and total kjeldahl nitrogen. Correlation coefficients ranged from 0.99 for total phosphorus to 0.72 for chlorophyll-A. The data were from a one-day experiment (June 3, 1974) with 31 ground truth stations, however, ground truth were not synchronous with the satellite overpass. (Samples were from 3 hours before overpass to 8 hours after.) These results also suggest that the multiple regression concept has the capability of monitoring water quality parameters which may not directly influence water optical characteristics (attenuation coefficient, scattering coefficient or volume scattering function). More recent work has applied the concept to a second data set (July 31, 1975) over Saginaw Bay (Rogers et al 1976). In the second application, the concept was modified to incorporate the results of Yarger et al (1973) in which band ratios were believed to suppress the effects of atmospheric and solar illumination variations. Instead of performing the linear multiple regression analysis with LANDSAT bands 4, 5, 6, and 7, the analysis also included the parameters band 4/band 5, band 4/band 6, band 4/band 7, band 5/band 6, band 5/band 7, and band 6/band 7. Thus ten independent variables were correlated against the ground truth data. In some cases the optimum

multiple regression algorithm utilized only band radiances and in other cases the optimum utilized ratios of band radiances. Seven water quality parameters were correlated which included Secchi-depth, temperature, chloride, conductivity, total kjeldahl nitrogen, total phosphorus, and chlorophyll-A. Correlation coefficients ranged from 0.94 for temperature to 0.71 for Secchi-depth. Also it was reported that the June 3, 1974 data set had been reanalyzed using the modified multiple regression procedure. Specific results were not given, however, it was reported that the modified multiple regression procedure gave improved results over the direct multiple regression analysis for most water quality parameters for that particular data set.

In addition to the James River and Saginaw Bay tests, additional experiments have been conducted in the New York Bight and off the Delaware coast to test linearized multiple regression procedures for quantification of water constituent concentrations. Two joint NOAA-NASA experiments have been conducted in the New York Bight (Johnson September 1976). The first experiment was conducted on April 13, 1975 in which ground truth were collected at 24 stations within 2 hours of aircraft scanner overpass. Suspended sediment and chlorophyll-A data were subjected to direct multiple regression procedures. For suspended sediment, a single-band regression equation proved optimum having a standard error of 1.39 mg/ℓ ($r = 0.79$) over a range of 0.56 to 8.38 mg/ℓ. A two-band multiple regression equation proved optimum for chlorophyll-A giving a standard error of 3.87 mg/m^3 ($r = 0.83$) over a range of 2.2 to

17.8 mg/m^3. These results are somewhat worse than those from the James River experiment. The reason for the deterioration is not known, however, a different multispectral scanner with poorer spacial resolution (but improved signal to noise ratio) was used. Also the fact that the New York Bight has less turbid waters than the James River allows deeper penetration depths for remote sensing purposes (see Whitlock 1976). Deeper penetration depths may allow vertical concentration gradients to confuse the results. The second New York Bight experiment was conducted September 22, 1975 for purposes of testing multiple regression procedures for quantification of sewage sludge surface concentrations. For suspended solids in the sludge dumping area, a standard error of 4.11 mg/ℓ ($r = 0.96$) over a range of 1.1 to 32.2 mg/ℓ was obtained using a multiple regression equation with two bands.

One problem with all of the above multiple regression analysis experiments was that they required a high number of field data samples nearly synchronous with the multispectral scanner overpass. On August 28, 1975, an acid waste remote sensing experiment was conducted off the Delaware coast with only one ground truth boat (Ohlhorst 1976). In order to obtain data for performing multiple regression procedures, a number of aircraft overpasses were made as the boat moved to different concentrations of acid waste. Each overpass was precisely synchronous with ground truth sampling, but the process took nearly 8 hours meaning that each ground truth - remote sensing data pair was for a different solar angle as well as different meteorological and

atmospheric conditions (the wind and waves increased during the last half of the experiment). Iron precipate concentrations from seven stations at a 0.6 m depth were correlated with the multispectral scanner data. Both direct and modified multiple regression procedures were used to correlate the data. Use of band radiances alone gave results which indicated that the multiple regression equation offered no improvement over a single-band linear regression equation of the form of equation (3-1). A standard error of 0.172 mg/ℓ ($r = 0.88$) over a range from 0.05 to 1.1 mg/ℓ was obtained. In an attempt to account for the effects of different illuminations, a normalizing procedure similar to that suggested by Mueller (1974) was applied. For each ground truth location, the radiance levels in all bands were summarized and then the radiance in each individual band was divided by this sum. The values for this ratio were then input to the process, and a multiple regression equation was developed which had a standard error of 0.096 mg/ℓ and a correlation coefficient of 0.97. Multiple regression correlation with band ratios as suggested by Rogers et al (1976) had not been attempted.

Considering all of the above investigations, it may be concluded that quantification of surface concentrations of marine constituents from remote sensing spectral data is presently a somewhat unreliable process. Various types of algorithms have been attempted which seem to give good results in some cases and poor results in others. It must be noted, however, that present-day remote sensing data often contains an appreciable amount of instrument noise. Few of the above

investigators discussed the problem, but Williamson et al (1973) did indicate noise of from 7 to 16 percent of the water signal for early LANDSAT data. Bahn (1976) has indicated that more recent LANDSAT data has noise levels from 5 to 10 percent of the water signal. (It should be noted that signals from land objects are seldom badly influenced by this problem because the received radiance is usually a high percentage of the dynamic range of the instrument whereas signals from water bodies are low in magnitude.) Data from aircraft multispectral scanners is quite variable. Depending on the particular scanner used, noise levels may range from 2 percent to values in excess of 30 percent of the water signal (Bahn 1976). In many cases, smoothing processes are applied to the remote sensing data to suppress noise, but most published results generally do not discuss this aspect of the investigation. Also little is published concerning uncertainties in ground truth values used in the various correlation studies. Tidal and meteorological effects cause uncertainties when there is a time lapse between the remote sensor overpass and the taking of the water sample. Variations in sampling technique and the present state of art of laboratory analysis introduce additional sources of error. It is clear that more highly controlled experiments and additional indepth investigations must be conducted to test those data analysis concepts which show promise.

CHAPTER IV

THEORY

The basic processes which occur during multiple regression analysis of spectral radiance data can best be examined by analysis of the problem from a signal response point of view. The objective of this analysis is to define those optical physics conditions for which the linearized multiple regression equation (equation (3-2)) represents an exact solution to the problem. A single-constituent water mixture is first discussed with multi-constituent cases analyzed in subsequent sections.

Single-Constituent Water Mixtures

It is assumed that the polluting constituent (pollutant A) has an upwelled radiance spectra similar to that shown by Schiebe and Ritchie (1975) for sediment. It is also assumed that at any wavelength, the reflected radiance varies in a linear manner with pollutant A concentration. Assuming linear superposition, the upwelled radiance near the water surface, Rad, for filtered seawater plus pollutant A may be expressed as,

$$Rad = A + B P_A \qquad (4\text{-}1)$$

where:

A = upwelled radiance of filtered seawater.

B = constant giving change in upwelled radiance due to P_A.

P_A = pollutant A concentration.

For a given water mixture of fixed pollutant A concentration, the constants A and B both vary over the spectral range but are assumed constant at any particular wavelength. Thus for a single wavelength band or channel in the spectra, Rad is a linear function of P_A.

From these assumptions a hypothetical radiance spectra can be constructed as shown in figure 4. The upwelled radiance scale is in arbitrary units for simplicity of analysis in this study. Also pollutant A concentration values are in arbitrary units (different from radiance units) for ease of analysis. The spectral profile for pure water (filtered seawater) was taken from Grew (1973). Also shown in figure 4 are 5 spectral bands which will be used in this analysis.

Equation (4-1) can be rewritten in terms of sediment concentration for any one band.

$$P_A = j + k(\text{Rad}) \qquad (4\text{-}2)$$

where:

$$j = \frac{-A}{B}$$

$$k = \frac{1}{B}$$

In the general case where j and k vary with wavelength λ,

$$P_A = j(\lambda) + k(\lambda)\ \mathrm{Rad}(\lambda) \tag{4-3}$$

Equations (4-2) and (4-3) indicate that in the single-constituent case, sediment concentration may be obtained from measurements in only one spectral band assuming the constants j and k are known.

Dual-Constituent Water Mixtures

If it is now assumed that the filtered seawater contains two constituents, pollutant A and pollutant B, the upwelled radiance at any wavelength X may be written as:

$$\mathrm{Rad}_X = A_X + B_X P_A + E_X P_B \tag{4-4}$$

Equation (4-4) assumes that there are no chemical, electrical, or optical interactions between pollutant A and pollutant B, and that the upwelled radiance varies linearly with concentration of each constituent. If it is further assumed that the radiance linearity with concentration is consistent over the wavelength range of interest and that the spectra of pollutant B (in filtered seawater) is different than that of pollutant A (see figure 5), then the upwelled radiance at wavelength Y may be written as:

$$\mathrm{Rad}_Y = A_Y + B_Y P_A + E_Y P_B \tag{4-5}$$

The requirement that the spectra of pollutant A be different than that of pollutant B means that:

$$\left.\begin{array}{l} B_X \neq B_Y \\ \\ E_X \neq E_Y \end{array}\right\} \qquad (4\text{-}6)$$

If upwelled radiance values are known at wavelengths X and Y, equations (4-4) and (4-5) represent two equations with two unknowns (P_A and P_B). Multiplying (4-4) by B_Y and (4-5) by B_X and substracting,

$$B_Y(Rad_X) - B_X(Rad_Y) = B_YA_X - B_XA_Y + (B_YE_X - B_XE_Y)P_B \qquad (4\text{-}7)$$

Solving for P_B:

$$P_B = \frac{B_YA_X - B_XA_Y}{B_XE_Y - B_YE_X} - \frac{B_Y}{B_XE_Y - B_YE_X}(Rad_X) + \frac{B_X}{B_XE_Y - B_YE_X}(Rad_Y) \qquad (4\text{-}8)$$

Remembering that A_X, A_Y, B_X, B_Y, E_X and E_Y are constants, equation (4-8) can be written as:

$$P_B = J' + K'_X(Rad_X) + K'_Y(Rad_Y) \qquad (4\text{-}9)$$

where:

$$J' = \frac{B_Y A_X - B_X A_Y}{B_X E_Y - B_Y E_X} = \text{constant}$$

$$K'_X = \frac{-B_Y}{B_X E_Y - B_Y E_X} = \text{constant}$$

$$K'_Y = \frac{B_X}{B_X E_Y - B_Y E_X} = \text{constant}$$

Solving for P_A:

$$P_A = J + K_X(Rad_X) + K_Y(Rad_Y) \qquad (4\text{-}10)$$

where:

$$J = -\frac{A_X}{B_X} - \frac{E_X B_Y A_X}{B_X^2 E_Y - B_Y B_X E_X} + \frac{E_X A_Y}{B_X E_Y - B_Y E_X} = \text{constant}$$

$$K_X = \frac{1}{B_X} + \frac{1}{B_X^2 E_Y - B_Y B_X E_X} = \text{constant}$$

$$K_Y = \frac{-1}{B_X E_Y - B_Y E_X} = \text{constant}$$

Thus the exact solutions for P_A and P_B (equations (4-9) and (4-10)) are linear multi-parameter equations of the same form as the statistician's multiple regression equation (equation (3-2)) if each constituent has a linear radiance gradient with concentration and there are no chemical, electrical, or optical interactions.

Dual-Constituent Water Mixtures in the Presence of Nonlinear Surface and Atmospheric Effects

The total radiance value received by a remote sensing instrument includes both surface reflection and atmospheric diffusion effects in addition to the radiance upwelled through the surface of the water (see figure 1). Such surface and atmospheric effects may be either linear or nonlinear with various parameters such as pointing angle, wind speed, aerosol content, and moisture content. Thus one may be faced with the problem of trying to extract pollutant concentrations for pollutants with linear radiance gradients from total radiance measurements which contain nonlinear components as a result of variations in unknown surface and atmospheric parameters. For purposes of this analysis, it is assumed that these nonlinear radiance components are independent of the radiance upwelled from the water. Atmospheric and surface effects may then be superimposed upon the upwelled radiance from the water to obtain a total signal. At any wavelength, the total radiance received by the remote sensing instrument may be expressed as:

$$Rad = A + BP_A + EP_B + H\phi^M + I + LX_A^N \qquad (4\text{-}11)$$

where:

A = upwelled radiance of filtered seawater

BP_A = upwelled radiance of pollutant A

EP_B = upwelled radiance of pollutant B

$H\phi^M$ = radiance component from surface reflection (assumed as a function of some variable such as ϕ which is related to the instrument pointing angle and the solar elevation angle).

I = radiance component from clear atmosphere.

LX_A^N = radiance component from atmospheric pollutant X_A (assumed as function of X_A to the Nth power).

Equation (4-11) assumes that atmospheric and surface reflection variations are small over the scene of interest and that their effects may be approximated by power law functions over small variations. If it is further assumed that all nonlinearities are consistent (M and N values are constant) over the wavelength range of the remote sensing measurements, then the total radiance for wavelengths W, X, Y, and Z may be written:

$$Rad_W = A_W + B_W P_A + E_W P_B + H_W \phi^M + I_W + L_W X_A^N \qquad (4\text{-}12)$$

$$Rad_X = A_X + B_X P_A + E_X P_B + H_X \phi^M + I_X + L_X X_A^N \qquad (4\text{-}13)$$

$$Rad_Y = A_Y + B_Y P_A + E_Y P_B + H_Y \phi^M + I_Y + L_Y X_A^N \qquad (4\text{-}14)$$

$$Rad_Z = A_Z + B_Z P_A + E_Z P_B + H_Z \phi^M + I_Z + L_Z X_A^N \qquad (4\text{-}15)$$

Equations (4-12) through (4-15) are four equations with four unknowns (P_A, P_B, ϕ^M, X_A^N). Solving these equations simultaneously (see Appendix C), it can be shown that:

$$P_A = J + K_W(Rad_W) + K_X(Rad_X) + K_Y(Rad_Y) + K_Z(Rad_Z) \qquad (4\text{-}16)$$

where:

$$J = \frac{1}{\theta}\,[-(\beta_X\alpha_{Y,Z}L_X + \beta_W\alpha_{Y,Z}L_Y)(A_W + I_W)$$

$$+ (\beta_X\alpha_{Y,Z}L_X)(A_X + I_X)$$

$$+ (\beta_X\alpha_{W,X}L_Z + \beta_W\alpha_{W,Y}L_Z + \beta_W\alpha_{Y,Z}L_W)(A_Y + I_Y)$$

$$- (\beta_X\alpha_{W,X}L_Y + \beta_W\alpha_{W,Y}L_Y)(A_Z + I_Z)]$$

$$= \text{constant}$$

$$= f(A,B,E,H,I,L)$$

$$K_W = \frac{1}{\theta}\,[\beta_X\alpha_{Y,Z}L_X + \beta_W\alpha_{Y,Z}L_Y] = \text{constant}$$

$$= f(B,E,H,L)$$

$$K_X = \frac{1}{\theta}\,[-\beta_X\alpha_{Y,Z}N_W] = \text{constant}$$

$$= f(B,E,H,L)$$

$$K_Y = \frac{1}{\theta}\left[-\beta_X\alpha_{W,X}L_Z - \beta_W\alpha_{W,Y}L_Z - \beta_W\alpha_{Y,Z}L_W\right] = \text{constant}$$

$$= f(B,E,H,L)$$

$$K_Z = \frac{1}{\theta}\left[\beta_X\alpha_{W,X}L_Y + \beta_W\alpha_{W,Y}L_Y\right] = \text{constant}$$

$$= f(B,E,H,L)$$

$$\theta = (\beta_X\alpha_{Y,Z}L_XB_W - \beta_X\alpha_{Y,Z}L_WB_X - \beta_X\alpha_{W,X}L_ZB_Y$$

$$+ \beta_X\alpha_{W,X}L_YB_Z - \beta_W\alpha_{W,Y}L_ZB_Y + \beta_W\alpha_{W,Y}L_YB_Z$$

$$+ \beta_W\alpha_{Y,Z}L_YB_W - \beta_W\alpha_{Y,Z}L_WB_Y)$$

$$\beta_W = (\alpha_{Y,Z}L_XE_W - \alpha_{Y,Z}L_WE_X - \alpha_{W,X}L_ZE_Y + \alpha_{W,X}L_YE_Z)$$

$$\beta_X = (\alpha_{W,Y}L_ZE_Y - \alpha_{W,Y}L_YE_Z - \alpha_{Y,Z}L_YE_W + \alpha_{Y,Z}L_WE_Y)$$

$$\alpha_{W,X} = (L_XH_W - L_WH_X)$$

$$\alpha_{Y,Z} = (L_ZH_Y - L_YH_Z)$$

$$\alpha_{W,Y} = (L_YH_W - L_WH_Y)$$

and,

$$P_B = J' + K'_W(Rad_W) + K'_X(Rad_X) + K'_Y(Rad_Y) + K'_Z(Rad_Z) \qquad (4\text{-}17)$$

where:

J' = constant = f(A,B,E,H,I,L)

K'_W = constant = f(B,E,H,L)

K'_X = constant = f(B,E,H,L)

K'_Y = constant = f(B,E,H,L)

K'_Z = constant = f(B,E,H,L)

Equations (4-16) and (4-17) are significant in that they show that the exact solutions for P_A and P_B are again linear multi-parameter equations of the same form as the statistician's multiple regression equation even if nonlinear atmospheric and surface reflection variations are present. A major assumption of this analysis is that the atmospheric and surface nonlinearities are consistent over the wavelength range of the measurements and can be approximated by power-law variations. Again each water constituent is assumed to have a linear radiance gradient with concentration and there are no chemical, electrical, or optical interactions between constituents. Another important point to note is that if the J,K constants of equations

(4-16) and (4-17) can be obtained, the concentrations P_A and P_B can be computed without knowledge of the atmospheric and surface reflection variables, ϕ and X_A. If the nonlinear radiance components do not follow power law variations, but instead follow other relations independent of P_A and P_B (such as power series expansions), procedures similar to Appendix C can be followed and the exact solutions for P_A and P_B will still be in the form of linear multi-parameter equations.

Multi-Constituent Water Mixtures with Nonlinear Constituents and Atmospheric Effects

In this case, one is dealing with a situation that is analytically similar to the previous case with nonlinear surface reflection and atmospheric effects. In both cases, the total radiance received by the remote sensor is composed of components with linear variations and components with nonlinear variations. If the water constituent with a nonlinear radiance variation with concentration is independent of other constituents (no chemical, electrical, or optical interactions) and the nonlinearity may be approximated as a power law variation, the total radiance may be expressed as:

$$Rad = A + BP_A + EP_B + SP_C^Q + I + LX_A^N \qquad (4\text{-}18)$$

where:

A = upwelled radiance of filtered seawater

BP_A = upwelled radiance of pollutant A

EP_B = upwelled radiance of pollutant B

SP_C^Q = upwelled radiance of pollutant C (assumed as a function of concentration, P_C, to the Qth power)

I = radiance component from clear atmosphere

LX_A^N = radiance component from atmospheric pollutant X_A.

If it is assumed that the nonlinearity of P_C radiance (as well as that of X_A) is consistent over the wavelength range of interest, then equation (4-18) can be written for the wavelengths W, X, Y, and Z. The resulting equations are identical to equations (4-12) through (4-15) except SP_C^Q terms are substituted for the $H\phi^M$ terms. If the procedures of Appendix C are followed, it can again be shown that:

$$P_A = J + K_W(Rad_W) + K_X(Rad_X) + K_Y(Rad_Y) + K_Z(Rad_Z) \qquad (4\text{-}19)$$

$$P_B = J' + K'_W(Rad_W) + K'_X(Rad_X) + K'_Y(Rad_Y) + K'_Z(Rad_Z) \qquad (4\text{-}20)$$

The J,J' terms are a function of A, B, E, S, I, and L and the K,K' terms are a function of B, E, S, and L. Again it must be noted that it is not necessary that the nonlinearity of P_C obey a power law relation as used in this example. Equations of the same form as (4-19) and (4-20) would result so long as the nonlinearity is consistent with wavelength and independent of P_A and P_B. A knowledge of P_C or

X_A is not required to compute P_A and P_B from equations (4-19) and (4-20) if the J,K constants can be obtained by some means.

Multi-Constituent Water Mixtures with Optical Interactions

The above analyses have assumed mutual independence with no optical interactions between water constituents. While many types of optical interactions may occur, there is at least one type for which the solution to the signal response equations is still in the form of a linearized multiple regression equation. That is the case when a constituent with a linear radiance gradient has its radiance component modified by the presence of another component because of chemical or physical processes. Assume, for example, the component of total radiance contributed by P_B is EP_B (see equation (4-4)). Assume also that there is a constituent P_C which when added to the water modifies the radiance contributed by P_B such that the new P_B component is $EP_B + G(P_B^R)(P_C^T)$, where R and T represent power-law approximations of the nonlinear modifications which may occur. The total radiance from the water mixture with this type of interaction would have the following form (ignoring atmospheric and surface nonlinear components):

$$Rad = A + BP_A + EP_B + G(P_B^R)(P_C^T) \qquad (4\text{-}21)$$

If it is assumed that the nonlinear modification terms, R and T, are constant over wavelength, then the total radiance for various wavelengths may be expressed:

$$Rad_W = A_W + B_W P_A + E_W P_B + G_W(P_B^R)(P_C^T) \tag{4-22}$$

$$Rad_X = A_X + B_X P_A + E_X P_B + G_X(P_B^R)(P_C^T) \tag{4-23}$$

$$Rad_Y = A_Y + B_Y P_A + E_Y P_B + G_Y(P_B^R)(P_C^T) \tag{4-24}$$

Multiplying (4-22) by G_X and (4-23) by G_W and subtracting:

$$G_X(Rad_W) - G_W(Rad_X) = (G_X A_W - G_W A_X) + (G_X B_W - G_W B_X)P_A + (G_X E_W - G_W E_X)P_B \tag{4-25}$$

Multiplying (4-22) by G_Y and (4-24) by G_W and subtracting:

$$G_Y(Rad_W) - G_W(Rad_Y) = (G_Y A_W - G_W A_Y) + (G_Y B_W - G_W B_Y)P_A + (G_Y E_W - G_W E_Y)P_B \tag{4-26}$$

Multiplying (4-25) by $(G_Y B_W - G_W B_Y)$ and (4-26) by $(G_X B_W - G_W B_X)$ and subtracting:

$$(G_X G_Y B_W - G_X G_W B_Y)Rad_W - (G_W G_Y B_W - G_W^2 B_Y)Rad_X$$

$$- (G_Y G_X B_W - G_Y G_W B_X)Rad_W + (G_W G_X B_W - G_W^2 B_X)Rad_Y$$

$$= (G_X A_W - G_W A_X)(G_Y B_W - G_W B_Y)$$

$$-(G_Y A_W - G_W A_Y)(G_X B_W - G_W B_X)$$

$$+[(G_X E_W - G_W E_X)(G_Y B_W - G_W B_Y)$$

$$- (G_Y E_W - G_W E_Y)(G_X B_W - G_W B_X)]P_B \qquad (4\text{-}27)$$

Solving for P_B, the solution is also of the form:

$$P_B = J' + K'_W(Rad_W) + K'_X(Rad_X) + K'_Y(Rad_Y) \qquad (4\text{-}28)$$

Thus it can be seen that some types of optical interaction may occur and the exact solution to the signal response equations is still of the form of a linearized multiple regression equation. It is expected that many types of optical interactions may occur in nature, and it is beyond the scope of this investigation to study the effects of all possible situations. Rather it is the purpose of this section to simply note that mutual independence between water constituents is a desirable but not a strict requirement for application of multiple regression concepts.

The above analyses have defined some optical physics conditions for which the exact solution to the signal response equations is in the same form as a linearized multiple regression equation. To summarize, these conditions are:

1. The constituents of interest must have a linear or near-linear upwelled radiance gradient with concentration.
2. The degree of nonlinearity in each radiance component must remain constant at the wavelengths which are used in the multiple regression equation.
3. Mutual independence between constituents (no electrical, chemical, or optical interactions) is desirable but not always required.

An additional assumption of the analysis is that the mixture concentration is constant to the depth of penetration of the remote sensing signal (see Whitlock, 1976). (The impact of this assumption will be discussed in a later section.) For those situations in which the above assumptions approximate real-world conditions, the linearized multiple regression equation is the appropriate form for computation of constituent concentration from multispectral remote sensing data in spite of the presence of nonlinear effects from other water constituents, surface effects, and atmospheric effects.

CHAPTER V

LEAST-SQUARES AND STATISTICAL CONCEPTS

Estimation of Coefficients

It is generally considered that independent variables in a mathematical equation cause a change in the dependent variables of the equation. From an optical physics point of view, a change in pollutant concentration is believed to cause a change in upwelled radiance such as that given in equation (5-1).

$$Rad = A + BP_A \tag{5-1}$$

From a physical viewpoint, P_A is the independent variable and Rad is the dependent variable expressing the actual cause-and-effect relationship.

From a data analysis viewpoint, the problem must be viewed in an opposite manner. The regression task is to estimate the j,K coefficients in which Rad is assumed as the independent variable and P_A is the dependent variable such as given in equation (5-2).

$$P_A = j + K(Rad) \tag{5-2}$$

For a multiple regression analysis, the task is to estimate the J,K coefficients in the following multi-parameter equation.

$$P_A = J + K_X(Rad_X) + K_Y(Rad_Y) + \ldots \qquad (5\text{-}3)$$

In this case, Rad_X, Rad_Y, etc. are treated as independent variables. In many real life observations, the so-called "independent variables" are positively correlated with each other as well as with the dependent variable which make the answers more difficult to interprete (Snedecor and Cochran 1967, p. 398). For the remote sensing situation, high correlations between the independent variables should be expected if the pollutant of interest has a broad spectral signature such as those shown in figures 4 and 5.

Because of experimental error and a limited number of sample pairs, a precise estimate of the J,K coefficients is usually not possible. In this case, the multiple regression equation is represented as:

$$P_A = J + K_X(Rad_X) + K_Y(Rad_Y) + \ldots + e \qquad (5\text{-}4)$$

where e = deviation from the true value of P_A

If there are n concentration-radiance sample pairs, the sum of the squares (SS) of the deviations from the true values is:

$$SS = \sum_{i=1}^{n} e_i^2 = \sum_{i=1}^{n} [P_{A_i} - J - K_X(Rad_X)_i - K_Y(Rad_Y)_i - \ldots]^2 \qquad (5\text{-}5)$$

The least-squares procedure chooses the J,K constants such that SS is a minimum. Taking the derivative of SS with respect to J and K and setting it equal to zero, it can be shown in matrix form (see Draper and Smith 1966, p. 9-59):

$$b = (Rad' Rad)^{-1} Rad' P_A \tag{5-6}$$

where:

$$b = \begin{bmatrix} J \\ K_X \\ K_Y \\ \cdot \\ \cdot \\ \cdot \\ \cdot \end{bmatrix}$$

$$P_A = \begin{bmatrix} \hat{P}_{A_1} \\ \hat{P}_{A_2} \\ \cdot \\ \cdot \\ \cdot \\ \cdot \\ \hat{P}_{A_n} \end{bmatrix}$$

$$Rad = \begin{bmatrix} 1 & Rad_{X_1} & Rad_{Y_1} & \cdots \\ 1 & Rad_{X_2} & Rad_{Y_2} & \cdots \\ \cdot & \cdot & \cdot & \\ \cdot & \cdot & \cdot & \\ \cdot & \cdot & \cdot & \\ 1 & Rad_{X_n} & Rad_{Y_n} & \cdots \end{bmatrix}$$

Thus given radiance values from several wavelengths (say Rad_X and Rad_Y) taken over n points where P_A values were measured ($\hat{P}_A$), values for the J,K constants can be estimated using matrix transpose, multiplication, and inversion procedures. In performing the least squares process, three major assumptions concerning the remote sensing and ground truth data are involved (Daniel and Wood 1971, p. 7). They are:

1. The correct form of equation has been chosen. (Rad is linear with concentration for all wavelengths involved.)
2. The data are typical and are a representative sample from the whole range of environmental combinations.
3. The observations of ground truth concentration values (dependent variables) are uncorrelated and statistically independent.

Three minor assumptions are:

1. All observations of concentration have the same (but unknown) variance.
2. The distribution of uncontrolled error is a normal one.
3. All independent variables (Rad values) are known without error.

An unwritten assumption is that all the data are "good" without physical or instrumentation deficiencies. In the remote sensing case, this generally means that only those data synchronous with the remote sensor overpass should be utilized in the least-squares process.

Time lags between the overpass and ground truth collection cause the data to be hydraulically inappropriate because of wind and tidal effects. It may be possible to correct the ground truth data to account for small time lags (see Kuo and Blair 1976), but such procedures have not yet been demonstrated valid in field experiments. An additional problem is that measurements of the independent variable (Rad) do contain error. Daniel and Wood (1971, p. 32) note that when the independent variables have considerable error variance, the estimate of the K coefficients is biased toward zero. As a rule of thumb, Daniel (1976) recommends that the least squares analysis be used if the error variance of the independent variables, $(\sigma_{Rad})^2$, is less than 0.1 of the mean square scatter about the mean value of Rad of the experiment. For any wavelength, X, this is expressed:

$$(\sigma_{Rad_X})^2 < 0.1 \left\{ \frac{\sum_{i=1}^{n} [(Rad_X)_i - \overline{Rad_X}]^2}{n} \right\} \qquad (5\text{-}7)$$

where:

$$\overline{Rad_X} = \frac{\sum_{i=1}^{n} Rad_X}{n}$$

Given an experiment with n observations, straightforward computation yields the mean square scatter about the mean of Rad. It is often difficult to estimate the error variance of the Rad measurements, however. Instrument calibration data may be required. Another

possibility is to examine the noise in the data. If the data noise is assumed random with a normal distribution about the true value, then the maximum deviation from the true value is $3.9(\sigma_{Rad})$. The full range of noise on both sides of the true value is $7.8(\sigma_{Rad})_e$. The error variance is $(\sigma_{Rad})^2$. An estimate of the error variance is then:

$$(\sigma_{Rad})^2 = \frac{(\text{full range of noise})^2}{60.8} \qquad (5\text{-}8)$$

Equation (5-8) assumes no bias in the measurement of Rad. If equation (5-7) is satisfied for all wavelengths to be considered in the regression analysis, the independent variables, Rad, are assumed to contain minimal error and least-squares estimates of the J,K coefficients are appropriate.

Measures of Precision

Unfortunately experimental radiance and concentration data contain errors which in turn cause uncertainties in the estimated values for the J,K coefficients. While errors in the individual coefficients are of some concern, the precision of the total regression equation is of prime concern. The uncertainty in prediction of concentration values in other portions of a remote sensing scene using the least-squares-fitted equation is required by the environmental engineer. Various measures of precision will be discussed in the following sections.

Correlation Coefficient

If least-squares estimates are used for the J,K coefficients, then the predicted value for P_A at any point i is P_{A_i}. The measured value at point i used in the least-squares process is $\hat{P}_{A_i}$. The mean value of all $\hat{P}_{A_i}$ is $\bar{P}_A$. From Draper and Smith (1966, p. 14), the following three statistical parameters are related as:

$$\sum_{i=1}^{n} (\hat{P}_{A_i} - \bar{P}_A)^2 = \sum_{i=1}^{n} (\hat{P}_{A_i} - P_{A_i})^2 + \sum_{i=1}^{n} (P_{A_i} - \bar{P}_A)^2 \qquad (5\text{-}9)$$

where:

$$\sum_{i=1}^{n} (\hat{P}_{A_i} - \bar{P}_A)^2 = \text{SS about mean}$$

$$\sum_{i=1}^{n} (\hat{P}_{A_i} - P_{A_i})^2 = \text{SS about regression}$$

$$\sum_{i=1}^{n} (P_{A_i} - \bar{P}_A)^2 = \text{SS due to regression}$$

The SS about regression are those deviations between the predicted values, P_{A_i}, and the measured values, $\hat{P}_A$. If the coefficients are correct and the total equation is a good fit to the data, then SS about regression should approach zero. The ratio r^2 is defined as:

$$r^2 = \frac{\text{SS due to regression}}{\text{SS about mean}} = \frac{\sum_{i=1}^{n} (P_{A_i} - \bar{P}_{A_i})^2}{\sum_{i=1}^{n} (\hat{P}_{A_i} - \bar{P}_A)^2} \qquad (5\text{-}10)$$

If r^2 approaches 1.0, then SS about regression must approach zero from equation (5-9). Thus r^2 is one statistical measure of the adequacy of the least-squares-fitting process. Draper and Smith (1966, p. 26) state that r^2 measures the proportion of total variation about the mean value of P_A, $\bar{P}_A$, that is explained by the regression equation. It is often expressed as a percentage after multiplication by 100. The square root of r^2, r, is defined as the correlation coefficient (multiple correlation coefficient for a multiple regression equation) and is a statistical parameter which is often used as a measure of adequacy. A correlation coefficient of 0.9 means that 81 percent of the total variation about the mean value is explained by the regression equation. Similarly, an r value equal 1.0 indicates a precise fit of the predictive equation to the measured data. One must be careful not to rely too heavily on r as a measure of equation precision, however. When the number of estimated coefficients in the regression equation equals the number of experimental observations, an exact solution for the coefficients is obtained. In this case, r will equal 1.0. If, however, there are errors in the experimental data, the coefficients will be in error. Thus r is not a good measure of precision as the number of estimated J,K coefficients approach the number of experimental observations. For the remote sensing situations, this means that the number of ground truth observations should exceed the number of radiance wavelengths (or bands) in the regression equation by two or more.

Standard Error

To arrive at other measures of precision, additional statistical terminology must be introduced. The number of independent pieces of information that are required to obtain the SS is defined as the degrees of freedom. If p equals the number of estimated J,K parameters and n equals the number of independent observations, then the degrees of freedom are as follows:

Source	Degrees of Freedom
SS due to regression	$p - 1$
SS about regression	$n - p$

Mean square values are obtained by dividing SS values by the appropriate degrees of freedom. The mean square about regression is known as the variance, σ^2, and may be expressed as:

$$\sigma^2 = \frac{\sum_{i=1}^{n} (\hat{P}_{A_i} - P_{A_i})^2}{n - p} \qquad (5\text{-}11)$$

The variance is a measure of the deviation between the predicted values from the least-squares equation and the measured values. The square root of the variance is known as the standard deviation or the standard error, σ. The standard error is a second measure of the precision of the least-squares estimation process for estimating the J,K coefficients. From equation (5-11), it is clear that the smaller the value, the more precise the fitted equation. If an error

is a sum of errors from several sources, then no matter what the probability distribution of separate errors may be, their sum will have a distribution that will tend more and more to the normal distribution as the number of error components increase by the Central Limit Theorem (Draper and Smith 1966, p. 17). Thus the standard error, σ, is usually assumed to represent a value within which 68 percent of all errors are expected to fall <u>if</u> (1) there are an infinite number of observations and (2) there is minimal error in the independent variables. Unfortunately there are usually only a small number of ground truth observations that are synchronous with the remote sensor overpass for most water quality remote sensing experiments.

F-Test

The F-test is a third method of evaluating the adequacy of the least-squares-estimation process. Fortunately, the technique is also believed to give an indication as to the capability of the regression equation as a predictive tool. The F-ratio is defined as:

$$F = \frac{(\text{mean square due to regression})}{(\text{mean square about regression})} \tag{5-12}$$

For a multiple regression equation with p estimated coefficients and n experimental observations:

$$F = \frac{(n - p)}{(p - 1)} \frac{\sum_{i=1}^{n} (P_{A_i} - \bar{P}_A)^2}{\sum_{i=1}^{n} (\hat{P}_{A_i} - P_{A_i})^2} \tag{5-13}$$

An alternative expression for F is (from Snedecor and Cochran 1967, p. 402):

$$F = \frac{(n - p)}{(p - 1)} \left[\frac{r^2}{1 - r^2}\right] \qquad (5\text{-}14)$$

There is also a critical F value available from tables which is based on the degree of freedom parameters as well as the confidence limit. A confidence limit of 0.95 means that the risk of being incorrect is no more than 5 percent. The F-test is one in which the calculated F value from equations (5-13) or (5-14) must be greater than the critical value for the regression process to be judged significant within the confidence limit. For example, if the multiple regression equation $P_A = J + K_X(Rad_X) + K_Y(Rad_Y)$ has been obtained from 12 sets of independent observations, the critical F value for a 95 percent confidence level ($F(p - 1, n - p, 0.95)$) would be 4.26 from a F-distribution table (Draper and Smith 1966, p. 306). If the computed F value were greater than 4.26, the regression equation would be judged significant within a 95 percent confidence level. Draper and Smith (1966, p. 64) state that the obtaining of a statistically significant regression does not necessarily mean that the resulting equation will be useful for predictive purposes. They note that J.M. Wetz suggests the calculated F value should be at least four times the critical F value if the regression equation is to be regarded as a satisfactory predictor. Thus the F-test for predictive capability is:

$$\frac{F}{F_{cr}} \geq 4.0 \qquad (5\text{-}15)$$

Total Squared Error

Daniel and Wood (1971, p. 86) recommend the total squared error as a criterion for goodness of fit. This statistic, called C_p, measures the sum of the squared biases plus the sum of the squared random errors for the dependent variables at all n data points. Given a multiple regression equation with p estimated J,K coefficients:

$$C_p = \frac{RSS_p}{s^2} - (n - 2p) \qquad (5\text{-}16)$$

where:

RSS_p = sum of squares of residuals p-term equation

s^2 = unbiased estimate of σ^2

For purposes of this analysis, the procedures of Daniel and Wood (1971, p. 87) are followed. It is assumed that the mean square of the residual of the multiple regression equation containing radiances from all possible wavelengths ($p = p_{max}$) is an unbiased estimate of σ^2. Equation (5-16) may then be expressed:

$$C_p = \frac{\left[\sum_{i=1}^{n} (\hat{P}_{A_i} - P_{A_i})^2\right]}{\left[\frac{\sum_{i=1}^{n} (\hat{P}_{A_i} - P_{A_i})^2}{n - p_{max}}\right]_{P_{max}}} - (n - 2p) \qquad (5\text{-}17)$$

An equation with a minimum value of C_p would have a minimum total variance (and average error) when used for predictive purposes. If the p-term multiple regression equation has negligible bias, then the expected value of RSS_p is $[(n - p)s^2]$. From equation (5-16), $C_p = p$ when there is zero bias in the fitted equation. When there is substantial bias, C_p is much larger than p (Daniel and Wood 1971, p. 87). A multiple regression equation which has a low value of C_p and the ratio $C_p/p \leq 1.0$ is considered by Daniel to be a good fit with negligible bias and useful for prediction purposes.

Selection of Wavelength Combinations

It is usually not known precisely what atmospheric and water parameters are present when a remote sensing experiment is performed. It is impossible to measure all parameters which might influence the total upwelled radiance received by the remote sensor. The usual case is one in which ground truth measurements are made for only those parameters of interest. Since all the factors present which make up the total signal are unknown, it is not possible to predict how many wavelengths will be required to separate the desired parameter from the total mix of factors influencing the signal. Previous

authors who have utilized direct multiple regression analysis (Johnson 1975 and Rogers et al 1975) have performed least-squares fits to various combinations of wavelengths (or bands) using the stepwise regression process to select a "best" equation for the parameter of interest. The stepwise regression process (see Draper and Smith 1966, p. 171) introduces independent variables one at a time to the regression equation to reduce the residual sum of squares. An F-test is used to judge the need for adding additional terms. Daniel and Wood (1971, p. 85) note that stepwise regression can lead to confusing results whenever the independent variables are highly correlated (as they are in this case). There are often better equations with different sets of independent variables that are overlooked by the stepwise procedure. Daniel and Wood (1971, p. 86) recommend that the C_p statistic be used to select the equation with the optimum combination of wavelengths or bands. For purposes of this investigation, regression equations will be computed for all combinations of wavelengths or bands for which upwelled radiance values are available. Correlation coefficients, standard errors, F-tests, C_p values, and C_p/p ratios will be computed for each combination. The selection of a "best" equation will be based on minimum C_p values if the C_p/p ratio indicates an unbiased fit and if values for correlation coefficient, standard error, and F-ratio are reasonable.

CHAPTER VI

ANALYTICAL VALIDATION

It is desirable to validate application of the linearized multiple regression analysis in the presence of known nonlinearities. In the usual experimental situation, it is often difficult to know exactly what nonlinearities are present. For this reason, several hypothetical sets of data with known nonlinearities were constructed. Linearized multiple regression analyses were then applied to these data for both homogeneous and non-homogeneous test cases. The following sections describe the hypothetical data and results from the analyses.

Hypothetical Data

For purposes of this analysis, the situation described by equation (4-11) was assumed. The spectral characteristics assumed for pollutants A and B are shown in figures 4 and 5, respectively. As noted previously, the spectra assumed for pollutant A is typical of a sediment. The spectra for pollutant B is typical of an algae species (see Grew 1973). The upwelled radiation component assumed for surface reflection is shown in figure 6. For this component it was assumed that the upwelled radiance varies as the cube of ϕ where ϕ is related to the solar elevation angle and the instrument pointing angle. High values of ϕ indicate the instrument is looking near the

sun glitter and low values are looking away from the glitter area. The spectral peaks shown might be caused by a surface film on the water. The component of upwelled radiance assumed from atmospheric effects (diffuse skylight) is shown in figure 7. It was further assumed that X_A represents the concentration of some type of fluorescent pollutant which absorbs atmospheric scattering in the blue region and enhances it in the infrared. The modification to clear atmosphere scattering was assumed to vary as the square of X_A concentration.

It was next assumed that the concentrations of pollutant A, pollutant B, and aerosol X_A varied over a remote sensing scene of interest. The instrument pointing angle, hence ϕ, was also assumed to vary. For the homogeneous case, values for these parameters at eight locations within the scene were assumed as follows:

Location	P_A	P_B	ϕ	X_A
1	20	20	20	20
2	10	20	30	40
3	30	40	20	10
4	20	30	10	40
5	40	10	30	20
6	10	40	10	30
7	20	10	40	30
8	40	30	40	10

For each of these eight locations, a hypothetical total upwelled radiance spectra was constructed using equation (4-11) and the components from figures 4 through 7. Figure 8 shows a typical total upwelled radiance spectra constructed during this process. Table 1 shows total upwelled radiance values computed for each of the eight

locations. Also shown are concentration values for P_A and P_B which were assumed to have been measured. (Values for ϕ and X_A were assumed not to be known.)

Analysis Results for Homogeneous Case

The data in table 1 were used in the linearized multiple regression analysis. Least-squares estimates of the J,K coefficients for all possible combinations of bands were computed. Since there were 5 radiance bands, there are $2^5 - 1$ or 31 possible combinations for each parameter of interest. The J,K coefficient estimates for P_A for each regression equation are shown in table 2. The various statistical estimates of precision for each combination of bands is shown in table 3. From table 3, it is evident that there are a number of band combinations which provide high correlation coefficient, small standard error, and an F-test greater than 4.0 (at the 95 percent confidence level). In this case, there are several combinations which show negligible bias (C_p/p near 1.0 or lower). The optimum combination of bands according to Daniel and Wood (1971) is the one with the lowest value of C_p (bands 1, 3, 4, 5). The correlation coefficient, the standard error, and the F-test ratio are all satisfactory for this combination. Referring back to table 2, the optimum linear multiple regression equation for extracting P_A from the upwelled radiance data of this scene is:

$$P_A = -26.2 - 0.90(Rad_1) + 3.73(Rad_3) - 0.17\ (Rad_4) - 1.89(Rad_5) \quad (6\text{-}1)$$

It took four wavelengths to extract P_A from a scene which contained four variables as expected based on theoretical considerations.

Estimates of the J,K coefficients for P_B are given in table 4. The statistical estimates of precision for P_B are given in table 5. In this case there are two combinations of four bands which are unbiased. Both have approximately the same value of C_p so the combination with the highest F-test is considered optimum (bands 2, 3, 4, 5). Referring to table 4, the equation for extracting P_B from the scene is:

$$P_B = -3.5 + 1.18(Rad_2) - 4.34(Rad_3) + 4.28(Rad_4) - 1.04(Rad_5) \qquad (6\text{-}2)$$

Both equations (6-1) and (6-2) should be accurate predictors. The standard error for P_A is 0.5 units over a total range of values of 30 units. This means that all predicted values of P_A using equation (6-1) should fall within ± 1.95 units (3.9σ) of the true value. The standard error for P_B is 1.1 units indicating that all predicted values of P_B from equation (6-2) should be within ± 4.29 units of the true value. To test these hypotheses, radiance values for ten additional locations have been generated. Values assumed for the variables which influence upwelled radiance at each location are given below:

Location	P_A	P_B	ϕ	X_A
9	15	38	12	23
10	22	23	18	16
11	37	14	29	27
12	23	11	33	13
13	38	16	39	34
14	12	29	28	37
15	32	34	23	27
16	29	17	17	12
17	14	23	14	17
18	35	32	11	39

Values for the radiances at each location were computed again using equation (4-11) and the components from figures 4 through 7. Table 6 gives the radiance values for each location. The values from tables 6 and 1 were input to equations (5-1) and (5-2) for computation of P_A and P_B at each location. Predicted P_A and P_B values are compared with the assumed true values in figures 9 and 10. Since all predicted values are within $\pm 3.9\sigma$ of true values, it is concluded that the linear multiple regression analysis is a valid approach for extracting linear water quality parameters in the presence of nonlinear effects in homogeneous waters provided radiance components are mutually independent and linearity is constant with wavelength.

Analysis Results for Non-Homogeneous Case

A water body may be considered non-homogeneous if a portion of it contains constituents which are not contained in other parts. An industrial effluent in a non-tidal, flowing river represents a typical non-homogeneous situation. The river may be flowing with various concentrations of P_A upstream of the industrial plant and outside

the effluent plume. Within the plume, the waters would contain various concentrations of both P_A and the effluent P_B. To simulate such a situation, a set of hypothetical data has been formulated for the case when P_B is zero. Values assumed for other parameters are as follows:

Location	P_A	P_B	ϕ	X_A
19	15	0	12	23
20	22	0	18	16
21	37	0	29	27
22	23	0	33	13
23	38	0	39	34
24	12	0	28	37
25	32	0	23	27
26	29	0	17	12
27	14	0	14	17
28	35	0	11	39

Values for upwelled radiances were again computed using equation (4-11) and the components from figures 4 through 7. Table 7 shows the radiance values computed which were assumed to exist for river locations upstream of the industrial plant and outside the effluent plume. Next it was assumed that a remote sensing experiment had taken place in which five ground truth data points were taken outside the plume (locations 19 through 23 from table 7) and eight points were taken inside the plume (locations 1 through 8 from table 1). The linearized multiple regression analysis was then applied to these 13 data points.

Estimates of the J,K coefficients and statistical measures of precision are given in tables 8 and 9, respectively, for the river constituent, P_A. The combination of bands 2, 3, 4, and 5 gives the

lowest value of C_p and is an unbiased estimate. The equation for extracting P_A from the non-homogeneous scene is:

$$P_A = -22.63 - 1.56(Rad_2) + 4.29(Rad_3) - 0.28(Rad_4) - 1.76(Rad_5) \quad (6\text{-}3)$$

Tables 10 and 11 give estimates of coefficients and statistical measures of precision for the industrial effluent, P_B. Band combination 1, 3, 4, and 5 gives the lowest value of C_p with an unbiased estimate. The equation for P_B is:

$$P_B = -3.93 + 0.55(Rad_1) - 3.85(Rad_3) + 4.23(Rad_4) - 0.82(Rad_5) \quad (6\text{-}4)$$

To validate the adequacy of equations (6-3) and (6-4), it was assumed that locations 24 through 28 from table 7 represented independent points from the river outside the plume and that locations 9 through 18 (table 6) represented independent points from within the plume. Equations (6-3) and (6-4) were then applied to the 15 independent points as well as to the 13 points used in the fitting process. Figures 11 and 12 compare predicted and assumed values for P_A and P_B; respectively. In many cases, the independent points fell on top of the solid symbols and are hidden from view. Since all predicted values are within $\pm 3.9\sigma$ of assumed true values, it is concluded that the linear multiple regression analysis is valid for non-homogeneous water situations as well as homogeneous cases. The data used in the fitting process must contain several points from each different water

mass, however, to insure that a correct correlation is performed for the total scene.

CHAPTER VII

LABORATORY VALIDATION

The analytical test cases provided validation of the linearized multiple regression analysis when the data contain nonlinear background effects. The hypothetical data set assumed that radiances from various sources could be superimposed upon each other (mutual independence) and the data contained minimal experimental error. In practice, the radiance contributions from various sources are not always totally independent, and remote sensing experiments always contain significant errors in the measured ground truth and radiance values. As a result of these problems, it is desirable to validate application of the linearized multiple regression technique with actual remote sensing data under controlled conditions. To achieve this result, a laboratory facility was constructed such that upwelled radiance measurements could be made over various controlled water mixes in the presence of light from a solar simulator. Experimental error in the measurements was analyzed, and the linearized multiple regression analysis was applied to the data. The following sections describe the laboratory facility, the test program, and results of the analysis.

Description of Laboratory Facility

A sketch of the laboratory set-up is shown in figure 13. The enclosure shown had not been completed at the time of these tests. To restrict the amount of diffuse light being input to the water, all tests were conducted at night with the solar simulator as the only light source. Figures 14 and 15 show photographs of the tank assembly and solar simulator. The laboratory was designed and constructed to satisfy the following objectives:

1. Measurement of upwelled radiance spectra under controlled conditions to determine at which wavelengths signals are emitted by various marine pollutants.
2. Measurements at various concentration levels to determine the degree of linearity of upwelled radiance with pollutant concentration.

It was recognized from the start that the laboratory would not provide a precise simulation of real-world spectra because (1) the solar simulator uses a xenon light source with a slightly different spectra than that of the sun and (2) diffuse skylight is not simulated. It was believed, however, that the design objectives could be met if the radiance values were normalized against the input solar simulator spectrum.

An initial study was conducted (Whitlock 1976) to estimate the range of concentration values for which tank tests are applicable. Figure 16 shows the results of that study. Z_{90} is the penetration depth from which 90 percent of the upwelled radiance is emitted.

Figure 16 indicates that sediment concentrations should be greater than 4 ppm if bottom reflection effects are to be minimized for a tank which is 3 meters deep.

The illumination geometry on the water surface is shown in figure 17. There was some concern as to whether or not the 35 cm diameter of the solar spot is adequate to enable the full underwater multiple scattering process to occur. In a separate study, Ghovanlou (1976) conducted a study using a Monte Carlo optical model. Results of that study are shown in figure 18. Upwelled radiance is shown as a function of solar spot size for three sediment concentrations. For concentrations of 4 and 6 ppm, the curves are flat for solar diameters 35 cm or larger indicating that the true underwater multiple scattering process is allowed to occur. Results show that the 35 cm solar spot size is not quite large enough for the 2 ppm concentration. Optical modeling results indicate that the 35 cm spot size (dictated by mirror diameter) is compatable with tank depth in that both limit applicability of the laboratory to test concentrations 4 ppm or greater.

Another design problem was that of maintaining a uniform, homogeneous mixture without significant vertical or horizontal concentration gradients in the tank. The problem is that the larger-size particles of a sediment mixture tend to settle quite rapidly unless an adequate degree of turbulence is maintained. Figure 19 is a schematic diagram showing the circulation system finally selected

for the tank. Tests were conducted using tracer techniques which indicate that particle sizes up to 140μ (with specific gravity = 2.6) are maintained in suspension. Transmission measurements with two concentrations of feldspar soil (particle size less than 60μ) indicate that the maximum deviation at any location in the tank was less than 0.5 ppm. Tests with larger size particles have not yet been conducted so the maximum capacity of the laboratory in terms of particle size is not presently known.

In order to be able to compare data taken from different days, a consistent water mixture is required as a base to which pollutants are added to achieve various concentrations. The tank holds 3,063 gallons so distilled water is prohibitively expensive. Also tap water at the Langley Research Center is quite variable, depending upon the amount and frequency of rain and the building from which the water is being drawn. To overcome these problems, a filtering-deionization system has been inserted into the plumbing such that consistent base water can be achieved. Figure 20 shows the performance of that system. For suspended solids, the fiber filter removes large sediments and iron particles, and the carbon filter removes small particles. Suspended solids concentrations are consistently less than 0.5 ppm. Dissolved substances such as minerals and chlorine are also quite high in tap water. The deionization system in use with the laboratory reduces the combined concentration of these constituents to less than 1.0 ppm.

The spectrometer used to make upwelled radiance measurements was the Tektronix J20/7J20 unit with the 7313/R7313 oscilliscope accessory. A photograph of the instrument is shown in figure 21. The spectrometer measures power/bandwidth (watts/nm) over a range from 380 to 980 nm. Bandwidths (spectral resolution) from 4 to 160 nm may be selected depending on the intensity level of the radiation being measured. For purposes of this investigation, power/bandwidth values were divided (normalized) by gray-card reflectance measurements of the input light source. The result is a normalized upwelled radiance spectra which is dimensionless. At the time of the tests described herein, automatic data read-out equipment were not available. Photographs of the oscilliscope images were read by hand. The hand reduction of data in combination with instrument-oscilliscope noise introduced several sources for measurement error. Estimates were made of the effects of various error sources on final normalized radiance values and are shown below:

Error Source	Effect on Normalized Radiance
1. Instrument noise during water mixture measurements	$\pm$0.0212
2. Inability to discriminate center of line of water measurements	$\pm$0.0106
3. Instrument noise during gray card measurements	$\pm$0.0222
4. Inability to discriminate center of line of gray card measurements	$\pm$0.0109

If the above errors are assumed random, independent, and equal the standard error, then the standard error of all combined effects is 0.0343. The range of normalized radiance values for water mixtures is from 0 to 0.6 so the estimated standard error of the laboratory data is 5.7 percent of the range of measurement values. While automated data read-out equipment would reduce the error, it must be noted that the level of uncertainty of these particular laboratory measurements is compatable with instrument noise values from present-day aircraft and satellite remote sensing systems as previously discussed.

For this investigation, specific values of concentration were obtained by addition of weighed, dry samples of the constituent to the water volume of the system (3063 gallons). The system was then allowed to circulate for approximately 15 minutes so that an even distribution of material would exist throughout the tank. The estimated standard error of concentration values used in this study is 5 percent of the quoted value. Quoted values were obtained by dividing the dry material weight by the water volume.

Test Program

In order to select test materials which had near-linear radiance gradients with concentration, a series of single-constituent tests were first conducted. Figures 22, 23, and 24 show wide-band spectra (spectral resolution = 160 nm) for the three materials selected for this investigation. Ball Clay and Feldspar sediments were selected because of their small particle sizes (Chapman 1976) and their relative

inertness when mixed both in tap water and with each other (Gjardo 1976). Rhodamine WT dye was selected because of its wide use in the environmental engineering field for dispersion and transport studies.

Figure 22 shows a broad spectra in the visible wavelength range for various concentrations of Ball Clay sediment. The value at each wavelength represents the average of all radiances 80 nm both to the left and right of the wavelength being read. Measurements were made at the 160 nm spectral resolution such that maximum light could be absorbed by the spectrometer in its "factory calibrated" mode. (The spectrometer can also be operated in a time-delay integration mode for measurements under low-light conditions to obtain narrower spectral resolution. Such a mode requires portable calibration equipment which was not available for these tests.) Figure 23 for Feldspar sediment shows (1) a pronounced signal at the lower wavelengths and (2) a much weaker signal than Ball Clay for any given concentration. Figure 24 for Rhodamine WT dye shows a signal which is also quite weak in comparison to Ball Clay but has a very pronounced peak at red wavelengths. The inconsistent curves below 500 nm and above 780 nm are believed to be the result of measurement uncertainty. The standard error of measurement, σ_{Rad}, is estimated to be approximately 0.0343 for these tests as previously discussed.

The radiance values of figures 22 through 24 were cross-plotted versus concentration at various wavelengths. Figure 25 indicates that Ball Clay sediments are near-linear at all wavelengths for concentrations greater than 9 mg/ℓ. Figure 26 shows Feldspar to be quite

linear for all concentrations at all wavelengths. Rhodamine WT dye (figure 27) is nonlinear at all wavelengths where it has a signal.

Following the single-constituent tests, a series of dual-constituent tests were conducted using various concentrations of Ball Clay and Feldspar sediments. It was believed that these two sediments in combination would provide an interesting test of the linearized multiple regression analysis because (1) both sediments have near-linear radiance gradients, and (2) the Feldspar has a low signal magnitude in comparison to the Ball Clay. While both sediments have different spectra and for that reason should be easy to separate, it was believed that these data would provide a somewhat severe test of the multiple regression process. The radiance measurement uncertainty ($\sigma_{Rad} = 0.0343$) is an appreciable portion of the upwelled radiance component caused by Feldspar sediments (compare σ_{Rad} with figure 23). The analytical test case previously discussed showed that a constituent with a low magnitude of radiance (P_B) could be accurately separated in the presence of one with high radiance values (P_A) if near-perfect data are available. It was questionable as to whether the linearized multiple regression process would operate as well on constituents with low upwelled radiation in the presence of significant measurement errors. The mixtures selected for testing and analysis are shown below:

Test Number	Ball Clay (ppm)	Feldspar (ppm)
1	129	17
2	173	17
3	9	35
4	9	69
5	52	69
6	52	173
7	173	173
8	9	17
9	17	17
10	129	73
11	52	17
12	173	35
13	17	69
14	17	35
15	52	35
16	173	52

Over the total wavelength range, five bands were selected at which to measure upwelled radiance. The bands selected were:

Band Number	Wavelength Range (nm)	Center Wavelength (nm)
1	340-500	420
2	460-620	540
3	540-700	620
4	620-780	700
5	700-860	780

A limited number of bands was selected because both present and near-future satellite systems will have only a few bands in the visible and near-infrared wavelength regions (figure 3). The measured values for normalized radiance in each of the five bands for each mixture combination is shown in table 12.

Following the dual-constituent measurements, a series of tests were conducted with various mixtures of three constituents, Ball Clay, Feldspar, and Rhodamine WT dyes. The objective was to add a third constituent which had nonlinear radiance gradients with concentration and was known to also have some optical interaction with the sediments. The mixtures selected for testing and analysis are shown below:

Test Number	Ball Clay (ppm)	Feldspar (ppm)	Rhodamine WT (ppb)
1	9	17	34
2	9	17	1052
3	9	35	34
4	17	35	34
5	9	35	1052
6	17	35	1052
7	17	35	190
8	17	52	190
9	17	52	535
10	52	52	535
11	17	52	1052
12	52	52	1052
13	173	129	34
14	173	129	190
15	52	129	535
16	129	129	535
17	173	129	535
18	52	129	1052
19	129	129	1052
20	173	129	1052
21	173	173	34
22	173	173	190
23	173	173	535
24	129	173	1052
25	173	173	1052

Values for the normalized upwelled radiance at the same five bands as the dual-constituent tests are shown in table 13.

Results of Analysis

Dual-Constituent Mixtures

Before analysis of the dual-constituent data could proceed, a test was first be made to see if measurements were accurate enough for application of the least-squares technique. Following the recommendation of Daniel (1976), a comparison of the error variance with the mean square scatter about the mean of the independent variables was used for this purpose. Using table 12 data, the mean square scatter about the mean was computed for the various bands and compared with $(\sigma_{Rad})^2$. For example in band 1, the calculations are:

$$\frac{\sum_{i=1}^{16} [(Rad_1)_i - \overline{Rad_1}]^2}{16} = 0.017315 \qquad (7\text{-}1)$$

From previous discussion, $(\sigma_{Rad})^2 = 0.00117$. The ratio of the error variance to the mean square scatter about the mean for this band equals 0.067. Since this value (and values for other bands) is less than 0.1, it is concluded that the measurement uncertainty is small enough in comparison to the range of values for least squares techniques to be used.

On analysis of the data, a general philosophy was adapted in which it was decided that only a minimum number of points would be

be used in estimating the J,K coefficients. The resulting multiple regression equation would then be applied to the unused data in an effort to test the predictive accuracy of the equation. For the dual-constituent laboratory data, eight of the test points in table 12 were first selected for analysis. Least-squares estimates of the J,K coefficients were performed and the various statistical measures of precision were computed. These results were discarded, however, because the correlations with Feldspar concentration were so poor that the F-test ratio never exceeded 1.0. It was concluded that the experimental error associated with these tests was large enough such that eight points were not enough for an adequate least-squares estimate of the J,K coefficients for Feldspar.

A multiple regression analysis using 12 of the 16 points was next attempted. All points in table 12 were used except test numbers 1, 3, 7 and 15. Again the regression was performed on all band combinations. Estimates of the J,K coefficients and statistical measures of precision for Ball Clay sediment are given in tables 14 and 15, respectively. Coefficient estimates and statistical parameters for Feldspar sediment are given in tables 16 and 17, respectively. These data were considered acceptable because some band combinations did give F-test ratios greater than 1.0 for both sediments.

Considering first the results obtained for Ball Clay sediment, review of table 15 indicates that high correlation coefficients, reasonable standard error values, and high F-test ratios may be obtained for a number of band combinations, but the fits may contain large

amounts of bias as indicated by C_p/p. The combination of bands 2, 4, and 5 contains the lowest total squared error which is unbiased. Referring to table 14, the multiple regression equation for Ball Clay concentration using this combination of bands is:

$$C = -56.8 + 1537.4(Rad_2) + 7167.1(Rad_4) - 12198.9(Rad_5) \qquad (7\text{-}2)$$

The statistical estimates of precision for this equation are:

$$r = 0.98$$

$$\sigma = 15.6 \text{ ppm}$$

$$(F/F_{cr})_{.95} = 16.9$$

$$C_p = 2.0$$

$$C_p/p = 0.5$$

All of these values are considered acceptable so it is assumed the equation (7-2) will have good predictive capability. Equation (7-2) was then applied to the radiance data in table 12 (including those points not used in the fit) and the results are shown in figure 28. Most points are within the $\pm 3.9\sigma$ limits and it would usually be concluded that equation (7-2) is a reasonable predictive equation. The one point which falls outside the 3.9σ limit brings up an interesting point when dealing with a low number of data points. The fitting of a multiple regression equation to a set of data does not

preclude the possibility that the equation which is obtained may be quite sensitive to small errors in measurement of the independent variables. Equations which compute differences between measured parameters sometimes have this problem. When one is dealing with a small size data set, it is possible that some measurements outside the set may have a slightly larger error than those points used in the fitting process. If the derived multiple regression equation has very large coefficients, then it is possible that a predicted point will fall outside the $\pm 3.9\sigma$ limit. If, however, a larger number of points is used in the fitting process, the points with maximum error would presumably be included, and the calculated value of σ would be larger and more accurate. In the case of the point (test number 7) which falls outside the limit in figure 28, simple calculations indicate an error in Rad_5 of 0.004 would give a predicted value of $\hat{C} = 141$ ppm which is well with the $\pm 3.9\sigma$ limit. Such a value of measurement error is quite possible since the estimated value of $\sigma_{Rad} = 0.0343$. It is concluded that equation (7-2) is quite sensitive to errors in the independent variables. The fact that the other three independent points fell within the band may be a strong indicator that equation (7-2) is a good predictive equation if accurate radiance data can be obtained.

Review of table 17 for Feldspar sediment indicates that the combination of bands 3, 4, and 5 produce an equation which contains the lowest total squared error and is unbiased. From table 16, the equation for Feldspar concentration using this band combination is:

$$C = 62.2 - 2242.6(Rad_3) - 10981.2(Rad_4) + 19674.3(Rad_5) \qquad (7\text{-}3)$$

The statistical estimates of precision for this equation are:

$$r = 0.89$$

$$\sigma = 24.0 \text{ ppm}$$

$$(F/F_{cr})_{.95} = 2.39$$

$$C_p = 3.0$$

$$C_p/p = 0.8$$

The effect of instrument error on a low-radiating constituent like Feldspar appears to be one in which reduced values of the correlation coefficient and higher values for standard error are obtained. The F-test ratio is greater than 1.0 but does not meet the Wetz criteria (see Draper and Smith 1966, p. 64) for being a good predictor at the 95 percent confidence level. (The confidence level could be reduced to some value below 90 percent to produce $F/F_{cr} \geq 4.0$, however.) The radiance data in table 12 were applied to equation (7-3), and the results are shown in figure 29. All values fall within the $\pm 3.9\sigma$ limits in spite of the fact that equation (7-3) is sensitive to small measurement errors as was the equation for Ball Clay. It should be noted that if Rad_5 is changed by 0.004 to improve the Ball Clay prediction, the calculation for Feldspar is also improved further suggesting that test number 7 may contain a bad data point.

Summarizing the results of analysis of the dual-constituent laboratory data, the effect of instrument error in measurement of the radiance data is to degrade the accuracy obtained from the multiple regression analysis. The inaccuracies obtained in these tests are not believed to be caused by lack of fit because the radiance gradients for both constituents are known to be linear with concentration (figures 25 and 26). The constituents are non-reactive with each other in tap water (Gjardo 1976), and the principle of linear superposition seems to give a fair approximation to their total combined signal (Ofelt 1976). It should be noted that values of standard error in comparison to the range of values of the experiment are similar to those obtained by Johnson (May 1976) in an actual field experiment. Whether or not such levels of uncertainty are acceptable to the environmental engineering community depends upon the particular use to which the data will be put. Accuracy requirements for various data uses are beyond the scope of this investigation.

Three-Constituent Mixtures

A comparison of the error variance with the mean square scatter about the mean for the independent variables was made using the data in table 13. Mean square scatter values about the mean are larger than for the dual-constituent tests while the estimated error variance is the same. The criteria for use of least-squares procedures is easily satisfied.

A multiple regression analysis using 12 of the 25 points in table 13 was performed. The points used in the least-squares fitting process were test numbers 1, 3, 5, 6, 8, 10, 13, 15, 18, 20, 21 and 23. The regression was performed on all band combinations. Estimates of the J,K coefficients and statistical measures of precision for both the Ball Clay and Feldspar sediments are given in tables 18 through 21. The 12-point regression analysis was considered acceptable because band combinations existed which gave good estimates of precision for all statistical parameters for both sediments.

Review of table 19 for Ball Clay sediment indicates that the lowest value of total squared error is obtained for band combinations 2, 3, and 4. The fit is also unbiased for this combination which has for its multiple regression equation (table 18):

$$C = -4.1 + 243.4(Rad_2) - 613.7(Rad_3) + 918.0(Rad_4) \qquad (7\text{-}4)$$

The statistical estimates of precision for this equation are:

$$r = 0.98$$

$$\sigma = 6.8 \text{ ppm}$$

$$(F/F_{cr})_{.95} = 105.7$$

$$C_p = 3.0$$

$$C_p/p = 0.8$$

All values are acceptable so it is assumed that equation (7-4) will have good predictive capability. It should be noted that the K coefficients of equation (7-4) are not as large as those for the dual-constituent results so the equation should not be as sensitive to small errors in radiance values. Results of applying the radiance data from table 13 to equation (7-4) are shown in figure 30. All 13 independent data points fall within $\pm 3.9\sigma$ (some are hidden by the dark symbols). It is thus concluded that equation (7-4) is a good predictive equation and that the linearized multiple regression analysis apparently works in spite of the fact that there is a reaction between Ball Clay and Rhodamine WT dye (Loper 1976). Sorption of the dye by the clay probably changes the absorption and scattering characteristics of the clay which in turn cause a change in the upwelled radiance spectra. The precise nature of the optical interaction is presently not known and would be difficult to measure (Loper 1976). A probable change in the upwelled radiance spectra is the only reason known at this time for the obtaining of a reduced value of standard error under that of the dual-constituent tests.

As a result of the Rhodamine WT dye, application of linearized multiple regression analysis to the Feldspar data proves quite interesting. Review of table 21 indicates that an unbiased estimate with minimum total squared error is obtained when only band 3 is present. The regression equation in this case is (table 20):

$$C = -8.0 + 361.4(Rad_3) \qquad (7\text{-}5)$$

The statistics for this equation are:

$$r = 0.92$$

$$\sigma = 23.8 \text{ ppm}$$

$$(F/F_{cr})_{.95} = 11.2$$

$$C_p \approx 0$$

$$C_p/p \approx 0$$

Results of applying the radiance data from table 13 to equation (7-5) are shown in figure 31. Again all 13 independent points fall within $\pm 3.9\sigma$ (four points are completely hidden by the black symbols). It must be concluded that equation (7-5) is a good predictor and that application of the linearized multiple regression analysis is a success.

It is somewhat troublesome to understand why only one band was required to quantify Feldspar when there were three constituents in the water. According to previously developed theory, at least three bands should be required to separate the effects of Feldspar from those of the rest of the mixture. The issue is further complicated by the fact that Band 3 (540 nm to 700 nm) is in the precise region where Rhodamine WT has its strongest signal (figure 24) and where Ball Clay is also quite strong (figure 22). Without optical interactions, the Feldspar signal in band 3 should be completely

confused by Rhodamine WT and Ball Clay effects since there are not strong correlations between the concentration values of each constituent. Loper (1976) notes that quartz-like materials such as Feldspar have negligible sorption of Rhodamine WT in comparison to the sorption by clay soils. He suggests that the modification to scattering and absorption characteristics of the Ball Clay may make it such that Ball Clay upwelled radiance is reduced at band 3 wavelengths enabling the presence of Feldspar to be more clearly seen. While such an explanation may be physically possible, detailed high-spectral-resolution tests of Rhodamine WT dye in the presence of a number of different sediments are required to define the optical interactions which are occurring. Such studies are beyond the scope of this investigation although they would probably be of national benefit because of the heavy use of Rhodamine WT dye in pollution studies. The important point to be made from the three-constituent test results is that the linearized multiple regression technique apparently works in the presence of at least some optical interactions. It is believed that a number of different types of interaction may occur, and it is beyond the scope of this investigation to determine and test all possible situations as discussed previously.

As an additional exercise, it was decided to test application of the multiple regression technique for quantification of a pollutant with a nonlinear radiance gradient. Referring back to equation (4-18), it can be seen that the signal response equation is linear in P_C^Q. Review of the single-constituent data for Rhodamine WT dye (figure 27)

suggests that an approximate value for Q might be obtained by fitting a power law equation to the measured values. Upon performing such an operation, it was found that values from Q = 0.1 to 0.25 could be fitted through the data because of experimental uncertainty. A value of Q = 0.2 appeared to give the best fit to the data for bands 2, 3, and 4 where Rhodamine has a strong signal. Results showing this fit are presented in figure 32.

The Rhodamine WT dye values previously presented for the three-constituent tests were used for the nonlinear multiple regression analyses. The same 12 points as for Ball Clay and Feldspar sediment analysis were utilized to estimate coefficients and statistical parameters for an equation of the following form:

$$C^Q = J + K_1(Rad_1) + K_2(Rad_2) + \text{------} \qquad (7\text{-}6)$$

Since an optical interaction had apparently occurred, it was not assured that Q = 0.2 was the correct value. Therefore, Q was varied from 0.25 to 0.05. Nondimensional statistical parameters for the "best" equation for each value of Q are shown below:

Q	0.25	0.20	0.15	0.10	0.05
r	0.99	0.99	0.99	0.99	0.99
$(F/F_{cr})_{.95}$	20.12	20.43	20.64	20.52	20.19
C_p	4.0	4.0	4.0	4.0	4.0
C_p/p	0.8	0.8	0.8	0.8	0.8

While no significant differences exist between the statistical parameters, the equation for $Q = 0.15$ was arbitrarily selected because of its slightly larger F-test value. Tables 22 and 23 give estimates of equation coefficients and statistical measures of precision for Rhodamine WT dye concentrations to the 0.15 power. The equation with the "best" fit is:

$$C^{0.15} = 1.605 - 7.679(Rad_1) - 3.972(Rad_2) + 17.582(Rad_3) - 7.376(Rad_4) \quad (7\text{-}7)$$

Results of applying equation (7-7) to the 25 three-constituent test points are shown in figure 33. With such a large nonlinearity, figure 33 presents a distorted picture of predictive accuracy. Raising the computed and actual Rhodamine WT concentrations to unity power gives a more accurate picture as shown in figure 34. From figures 33 and 34, it is concluded that multiple regression procedures can be used to quantify constituents with nonlinear radiance gradients, and the technique may be applied to any number of constituents so long as each constituent is related to optical changes in the water body and other technique limitations are not violated.

CHAPTER VIII

FIELD EXPERIMENT CONSIDERATIONS

Analytical and laboratory cases have been used to perform a limited validation of linearized multiple regression analysis for quantification of marine constituents under a variety of environmental and optical conditions. Both analytical and laboratory tests are quite valuable for investigating specific areas of concern under controlled conditions. No matter how many controlled tests are conducted, final validation of the technique must come through use of field experiments. Unfortunately such experiments are quite expensive and beyond the scope of this investigation. As previously discussed, field experiments which utilize multiple regression analysis have been conducted by several investigators (Johnson, May 1976, Rogers et al 1976, Johnson, September 1976, and Ohlhorst 1976). Only mixed success has been obtained from these experiments. Some of the inconsistent field results may in fact be explainable based on various limitations which have been uncovered by the investigation described herein. It is the purpose of this section to recommend procedures which should be used for future field experiments to improve the opportunity for consistent results.

The linearized multiple regression analysis should never be applied blindly to a set of data without a background knowledge concerning the constituent of interest, hydraulics of the water body, and

measurement uncertainties. This extreme caution is recommended so that false results are not published concerning the technique. The linearized multiple regression analysis has strong theoretical foundation for a number of environmental conditions and careful application should yield useful results. The technique should be applied only to those constituents for which accurate ground truth values can be obtained. The present state of art of laboratory analysis may eliminate multiple regression analysis as a possibility for some constituents of interest. Also the technique should only be applied to those constituents whose radiance gradients are known to be near-linear with concentration. Controlled laboratory or field tests may be required to determine this property.

Prior to the remote sensing field experiment, measurements should be made to determine geographic locations to obtain the widest possible range for ground truth measurements of the constituent of interest. A time interval for hydraulic consistency should be established such that ground truth data are not included in the analysis if large water mass movements have occurred between the times of remote sensor overpass and the taking of water samples. Within the time interval for hydraulic consistency, as many points as possible should be obtained with as near a uniform distribution of concentration values as technically feasibility. From a statistics point of view, the number of points should be greater than the number of remote sensor bands plus one. Because of experimental measurement

errors, it is recommended that the number should be much larger than that minimum statistical value. The precise number of points required is a function of the error magnitudes in both the independent and dependent variables. Multi-dimensional parametric studies are required to assess the minimum number of points required for various combinations of error and ranges of values. Until such studies are available, the experimenter must take as many points as possible and hope that enough are obtained. Care should be taken that all ground truth points used in the analysis are from the same water depth. The effect of vertical concentration gradients will be minimized, and the resulting multiple regression equation will be an algorithm for concentration at a particular depth if the assumption is made that vertical concentration gradients near the surface are constant over the scene of interest. For the situation in which a substance is introduced into part of the water body (such as an industrial outfall), a number of points both inside and outside the plume must be obtained to insure against false correlation as a result of non-homogeneity.

Once remote sensing data are in hand, an analysis to estimate error variance of the remote sensing measurements based on instrument noise and calibration data is required. The estimate of error variance must then be compared with the mean square scatter about the mean of the experimental radiance values as previously discussed. Only if an order of magnitude or greater difference exists can the linearized multiple regression analysis using least-squares techniques be utilized.

All data which is outside the time interval for hydraulic consistency and therefore not hydraulically appropriate should be immediately eliminated from the analysis. A review of the sediment levels and water depth of each station should be conducted and compared with order of magnitude estimates of remote sensing penetration depth (see Whitlock 1976). Those points whose remote sensing penetration depth approach the values for water depth must be removed from the analysis to eliminate confusion due to bottom reflection effects. A correlation study should be conducted between the various ground truth parameters measured to understand the possibilities of false correlation. In many cases, the hydraulics of the water body under analysis make it nearly impossible to obtain measurements which are totally uncorrelated with each other.

For analysis of the data, it is recommended that regression equations and statistical parameters be computed for all possible band combinations. The decision as to which equation is optimum should be based on satisfactory values for all statistical parameters, however, the ratio of C_p/p is particularly important because it is an indication of bias in the fitting process. Results obtained in this investigation indicate that good values may be obtained for the correlation coefficient, the standard error, and the F-test ratio but the fit may be extremely biased which is not desirable. If possible, the analysis should be conducted with less than the total number of stations obtained such that some points will be available for independent check calculations. All predicted values in other locations

of the remote sensing scene must be accompanied by the estimated value of standard error. Finally repetitive experiments should be conducted for the constituent of interest in the water body of interest. Confidence must be established in use of the linearized multiple regression analysis under a variety of atmospheric, wind, wave, and seasonal conditions.

CHAPTER IX

SUMMARY AND CONCLUSIONS

The objective of this investigation has been to define optical physics and/or environmental conditions under which the linear multiple regression analysis should apply for quantification of water quality parameters. To achieve this objective, an investigation of the signal response equations has been conducted and the concept has been tested by application to both analytical test cases and actual remote sensing data from a laboratory under controlled conditions. As a result of this investigation, an improved understanding of technique limitations, mathematical requirements, ground truth requirements and error effects has been obtained.

Investigation of the signal response equations shows that the exact solution for a number of optical physics conditions is of the same form as a linearized multiple regression equation, even if nonlinear contributions are made by such factors as surface reflections, atmospheric constituents, or other water pollutants. Limitations on achieving this type of solution and (1) the constituent of interest must have a linear radiance gradient with concentration, (2) the degree of nonlinearity in each of the other components which make up the total signal must be constant for the wavelengths used in the multiple regression equation, and (3) mutual independence between constituents with no electrical, chemical, or optical

interactions is desired but not always required. Mixture concentration also must be constant over the penetration depth of the remote sensing signal, or the vertical concentration gradient must be essentially constant near the surface and all concentrations measured at the same depth. Since the exact solution to the signal response equations under the above conditions is in the form of a linear multiple regression equation, the application of linearized multiple regression analysis to remote sensing and ground truth data may be viewed as a calibration of the exact solution to account for daily variations of background constituents in both the atmosphere and water environment.

To obtain a "calibrated" equation using multiple regression techniques, least-squares procedures are used to estimate coefficients of the equation. In order to use least-squares techniques, the error variance of the upwelled radiance measurements must be at least an order of magnitude smaller than the mean square scatter about the mean of the experimental radiance data. In addition, ground truth observations must be uncorrelated and statistically independent over the range of values for which the final regression equation will be utilized. All data used in the least-squares process must be "good" in that (1) the constituent of interest is measured accurately, (2) the data are hydraulically appropriate, and (3) the remote sensing penetration depth at all points is less than the water depth. For non-homogeneous water bodies such as those with industrial outfalls, a number of ground truth points is required from each water mass to

insure correct correlation of the total scene. From a statistics point-of-view, the minimum number of ground truth locations required is the number of wavelengths (or bands) at which upwelled radiance is being measured plus two. As a result of experimental uncertainty, it is concluded that the total number of ground truth points should be significantly larger than the minimum number if possible.

From analytical test case results, it is concluded that constituents with linear radiance gradients may be quantified from signals which contain nonlinear atmospheric and surface reflection effects for both homogeneous and non-homogeneous mixtures provided accurate data can be obtained and nonlinearities are constant with wavelength. In addition, it was observed that high correlation coefficients, low values of standard error, and acceptable F-test ratios could be obtained for various band combinations, but the fits could contain a large amount of bias. It is concluded that statistical parameters must be used which give an indication of bias as well as total squared error to insure that an equation with the optimum combination of bands is selected for utilization.

From dual-constituent laboratory results, it is concluded that the effect of error in the upwelled radiance measurements is to reduce the accuracy of the least-squares fitting process and to increase the number of ground truth points required to obtain a satisfactory fit. It was also observed that the least-squares fitting process does not preclude the possibility that the multiple regression equation

obtained may have large coefficients and be extremely sensitive to small errors in radiance measurement. If the fit is obtained with a low number of ground truth points, it is possible that the estimated value of standard error is not applicable to predicted values using the equation.

From three-constituent laboratory results, it is concluded that the linearized multiple regression analysis is applicable for constituents with linear radiance gradients which experience some types of optical interaction when combined with other constituents. It definitely can be said that the analysis will not apply for all types of optical interaction; however, it is believed that satisfactory results may be obtained for a number of different situations. The area of optical interactions for usual water pollutants has received only limited attention by the scientific community. It is recommended that fundamental studies be conducted in this area for various constituents of interest. Research on this problem may explain why high correlations have been obtained with certain "invisible" constituents in previous field experiments.

It is recognized that the analytical test cases and analysis of laboratory data conducted in this study have provided only limited validation of the linearized multiple regression concept. While a number of additional laboratory tests could be conducted, the only way to finally validate the concept for use with a particular constituent is with carefully conducted field experiments. Based

on the experience of this study, it is believed that the technique has strong potential for future application. It will be particularly applicable when advanced remote sensing and ground truth systems are developed which have improved accuracy. The concept has strong theoretical support from consideration of the signal response equations and is applicable without precise knowledge of atmospheric and water surface parameters. It further allows for some variation in atmospheric and surface reflection effects over the scene of interest which is a severe limitation for several other data analysis concepts. For those water constituents with nonlinear radiance gradients (versus concentration), the method may be modified and utilized if the nature of the nonlinearity is known.

The most serious problem with the multiple regression concept is the present lack of knowledge concerning possible limitations caused by the requirement that the nonlinearity of various radiance components must be constant over the wavelength range of interest. Based on the success of some of the previous field experiments, it appears that there is a wide range of wind, wave, solar elevation, and atmospheric conditions for which the linearity requirement is satisfied. On the other hand, there may be extremes in environmental conditions or particular water constituents which cause large variations in linearity. Repetitive field experiments under a variety of environmental conditions are required to answer this question.

It is also recommended that multi-dimensional analytical studies be conducted to better define ground truth requirements for application of the multiple regression analysis. Parametric variation of such parameters as dependent variable error, independent variable error, range of values, number of points, degree of homogeneity, and number of constituents may enable the construction of charts based on normalized parameters which would aid the potential experimenter in assessing the number of ground truth stations required for expected levels of uncertainty in both remote sensing and ground truth data. Such information would also be of interest in the development of future in-situ water monitoring systems.

APPENDIX A

REFERENCES

Bahn, G. S. The Vought Corporation. Hampton, Virginia. Interview. 7 September 1976.

Bennett, P., and Sydor, M., "Use of ERTS in Measurements of Water Quality in Lake Superior and the Duluth Superior Harbor." Proceedings of the Conference on Earth Resources Observation and Information Analysis System. Tullahoma, Tennessee: n.p., March 1974.

Bowker, D. E., and Witte, W. G. "Evaluation of ERTS Digital Data for Monitoring Water in the Lower Chesapeake Bay Area." Proceedings of the Fourth Annual Remote Sensing of Earth Resources Conference. Tullahoma, Tennessee: n.p., March 1975.

Bowker, D. E.; Witte, W. G.; Fleischer, P.; Gosink, T. A.; Hanna, W. J.; and Ludwick, J. C. "An Investigation of the Waters in the Lower Chesapeake Bay Area." Proceedings of Tenth International Symposium on Remote Sensing of Environment. Ann Arbor, Michigan: n.p. October 1975.

Chapman, R. S. Particle Size and X-Ray Analysis of Feldspar, Calvert, Ball, and Jordan Soils. NASA TM X-73941. Springfield, Virginia: National Technical Information Service, August 1976.

Christensen, R. J., and Wezernak, C. T. "Use of Remote Sensing for Water Resource Management in Michigan." Proceedings of Tenth International Symposium on Remote Sensing of Environment. Ann Arbor, Michigan: n.p., October 1975.

Daniel, Cuthbert. Consultant, Rhinebeck, New York. Interview. 14 December 1976.

Daniel, C. and Wood, F. S. Fitting Equations to Data. New York: Wiley-Interscience, 1971.

Draper, N. R., and Smith, H. Applied Regression Analysis. New York: John Wiley and Sons, 1966.

Ghovanlou, A. H.; Hickman, G. F.; and Hogg, J. E. Laser Transmission Studies of East Coast Waters. Technical Report No. 2. Alexandria, Virginia: Sparcom Inc., March 1973.

Ghovanlou, A. H. Analytical Model for Remote Sensing of Water Turbidity. NASA CR-145050. Springfield, Virginia: National Technical Information Service, 1976.

Gjardo, Vincent. Williamsburg Pottery Factory. Williamsburg, Virginia. Interview. April 1976.

Gordon, H. R.; Brown, O. B.; and Jacobs, M. M., "Computed Relationships Between the Inherent and Apparent Optical Properties of a Flat Homogeneous Ocean." Applied Optics 14 (February 1975): 417-27.

Grew, G. W. "Signature Analysis of Reflectance Spectra of Phytoplankton and Sediment in Inland Waters." Proceedings of the Second Annual Remote Sensing of Earth Resources Conference. Tullahoma, Tennessee: n.p., March 1973.

Hovis, W. A. "Ocean Color Imagery-Coastal Zone Color Scanner." Proceedings of the NASA Earth Resources Survey Symposium. Houston, Texas: n.p., June 1975.

Howells, D. H. "ERTS: Impractical Image," Civil Engineering-ASCE, November 1975, pp. 26-27.

Jerlov, N. G. Optical Oceanography. New York: Elsevier Publishing Company, 1968.

Johnson, R. W. "Quantitative Sediment Mapping from Remotely Sensed Multispectral Data." Proceedings of the Fourth Annual Remote Sensing of Earth Resources Conference. Tullahoma, Tennessee: n.p., March 1975.

Johnson, R. W.; Batten, C. E.; Bowker, D. E.; Bressette, W. E.; and Grew, G. W. Preliminary Data From the May 28, 1974 Simultaneous Evaluation of Remote Sensors Experiment. NASA TM X-72676. Springfield, Virginia: National Technical Information Service, June 1975.

Johnson, R. W. "Quantitative Suspended Sediment Mapping Using Aircraft Remotely Sensed Multispectral Data." Proceedings of the NASA Earth Resources Survey Symposium. Houston, Texas: n.p., June 1975.

Johnson, R. W. "Quantitative Mapping of Water Quality Parameters in the James River, Virginia, By Aircraft Remote Sensing." Presented at the 1976 Annual Meeting of the Virginia Academy of Science, May 1976.

Johnson, R. W., and Bahn, G. S. National Aeronautics and Space Administration, Langley Research Center. Hampton, Virginia. Interview. 31 August 1976.

Johnson, R. W. National Aeronautics and Space Administration, Langley Research Center. Hampton, Virginia. Interview. 3 September 1976.

Klemas, V.; Srna, R.; Treasure, W.; and Otley, M. "Applicability of ERTS-1 Imagery to the Study of Suspended Sediment and Aquatic Fronts." Proceedings of Symposium on Significant Results Obtained from the Earth Resources Technology Satellite-1. New Carrollton, Maryland: n.p., March 1973.

Klemas, V.; Otley, M.; Philpot, W.; Wethe, C.; and Rogers, R. "Correlation of Coastal Water Turbidity and Circulation With ERTS-1 and Skylab Imagery." Proceedings of the Ninth International Symposium on Remote Sensing of the Environment. Ann Arbor, Michigan: n.p., April 1974.

Klooster, S. A., and Scherz, J. P. "Water Quality Determination by Photographic Analysis." Proceedings of the Second Annual Remote Sensing of Earth Resources Conference. Tullahoma, Tennessee: n.p., March 1973.

Kondrat'ev, K. Y. Radiation Characteristics of the Atmosphere and the Earth's Surface. NASA TT F-678. Springfield, Virginia: National Technology Information Service, 1973.

Kuo, C. Y., and Blair, C. H. Rational Method for Correcting Sea Truth of Suspended Sediment Concentration Related to Remote Sensing. Technical Report 76-C3. Norfolk, Virginia: Old Dominion University, 1976.

Kuo, C. Y., and Cheng, R. Y. K. Laboratory Requirements for In-Situ and Remote Sensing of Suspended Material. Technical Report 76-C2. Norfolk, Virginia: Old Dominion University, 1976.

Lillesand, T. M. "Use of Aerial Photography to Quantitatively Estimate Water Quality Parameters in Surface Mixing Zones." Ph.D. dissertation. University of Wisconsin, 1973.

Link, L. E. "The Use of Remote Sensing Techniques for Detection and Identification of Pollutant Discharges." Master's thesis. Mississippi State University, 1973.

Loper, J. D. E. I. duPont de Nemours and Co. Wilmington, Delaware. Interview. 28 December 1976.

Maul, G. A. "Remote Sensing of Ocean Currents Using ERTS Imagery." Proceedings of Symposium on Significant Results Obtained from the Earth Resources Technology Satellite-1. New Carrollton, Maryland: n.p., March 1973.

McCluney, W. R. "Ocean Color Spectrum Calculations." Applied Optics 13 (October 1974): 2422-29.

Mueller, J. L. "The Influence of Phytoplankton on Ocean Color Spectra." Ph.D. dissertation, Oregon State University, 1974.

Ofelt, G. S. Old Dominion University. Norfolk, Virginia. Interview. November 1976.

Ohlhorst, Craig. National Aeronautics and Space Administration, Langley Research Center. Hampton, Virginia. Interview. 3 September 1976.

Ritchie, J. C.; McHenry, J. R.; Schiebe, F. R.; and Wilson, R. B. "The Relationship of Reflected Solar Radiation and the Concentration of Sediment in the Surface Water of Reservoirs." Proceedings of the Conference on Earth Resources Observation and Information Analysis System. Tullahoma, Tennessee: n.p., March 1974.

Ritchie, J. C.; Schiebe, F. R.; Wilson, R. B.; and May, J. "Sun Angles, Reflected Solar Radiation, and Suspended Sediments in Northern Mississippi Reservoirs." Proceedings of the Fourth Annual Remote Sensing of the Earth Resources Conference. Tullahoma, Tennessee: n.p., March 1975.

Rogers, R. H.; Shah, N. J.; McKeon, J. B.; Wilson, C.; Reed, L.; Smith, V. E.; and Thomas, N. A. "Application of LANDSAT to the Surveillance and Control of Eutrophication in Saginaw Bay." Proceedings of Tenth International Symposium on Remote Sensing of Environment. Ann Arbor, Michigan: n.p., October 1975.

Rogers, R. H.; Shah, N. J.; McKeon, J. B.; and Smith, V. E. "Computer Mapping of Water Quality in Saginaw Bay with LANDSAT Digital Data." Proceedings of the ACSM-ASP Convention. Washington, D.C.: n.p., February 1976.

"Satellites Helping Solve Down-to-Earth Civil Engineering Problems," Civil Engineering-ASCE, August 1975, pp. 49-53.

Scherz, J. P.; Sydor, M.; and Van Domelen, J. F. "Aircraft and Satellite Monitoring of Water Quality." Proceedings of Third Earth Resources Technology Satellite-1 Symposium. Washington, D.C.: n.p., December 1973.

Scherz, J. P.; Crane, D. R.; and Rogers, R: H. "Classifying and Monitoring Water Quality by Use of Satellite Imagery." Proceedings of International Conference on Environmental Sensing and Assessment. Las Vegas, Nevada: n.p., September 1975.

Schiebe, F. R., and Ritchie, J. C. "Color Measurements and Suspended Sediments in North Mississippi Reservoirs." Proceedings of the Fourth Annual Remote Sensing of Earth Resources Conference. Tullahoma, Tennessee: n.p., March 1975.

Schubert, J. S., and MacLeod, N. H. "Digital Analysis of Potomac River Basin ERTS Imagery: Sedimentation Levels at the Potomac-Anacostia Confluence and Strip Mining in Allegheny County, Maryland." Proceedings of Symposium on Significant Results Obtained from the Earth Resources Technology Satellite-1. New Carrollton, Maryland: n.p., March 1973.

Snedecor, G. W., and Cochran, W. G. Statistical Methods. 6th ed. Ames: The Iowa State University Press, 1967.

Turner, R. E. "Contaminated Atmospheres and Remote Sensing." Proceedings of the Conference on Earth Resources Observation and Information Analysis System. Tullahoma, Tennessee: n.p., March 1974.

Wezernak, C. T., and Roller, N. "Monitoring Ocean Dumping With ERTS-1 Data." Proceedings of Symposium on Significant Results Obtained from the Earth Resources Technology Satellite-1. New Carrollton, Maryland: n.p., March 1973.

Wezernak, C. T.; Turner, R. E.; and Lyzenga, D. R. Spectral Reflectance and Radiance Characteristics of Water Pollutants. NASA CR-2665. Springfield, Virginia: National Technical Information Service, June 1975.

Whitlock, C. H. An Estimate of the Influence of Sediment Concentration and Type on Remote Sensing Penetration Depth for Various Coastal Waters. NASA TM X-73906. Springfield, Virginia: National Technical Information Service, March 1976.

Williamson, A. N., and Grabau, W. E. "Sediment Concentration Mapping in Tidal Estuaries." Proceedings of Third Earth Resources Technology Satellite-1 Symposium. Washington, D. C.: n.p., December 1973.

Yarger, H. L.; McCauley, J. R.; James, G. W.; and Magnuson, L. M. "Water Turbidity Detection Using ERTS-1 Imagery." Proceedings of Symposium on Significant Results Obtained from the Earth Resources Technology Satellite-1. New Carrollton, Maryland: n.p., March 1973.

Yarger, H. L.; McCauley, J. R.; James, G. W.; Magnuson, L. M.; and Marzolf, G. R. "Quantitative Water Quality with ERTS-1." Proceedings of Third Earth Resources Technology Satellite-1 Symposium. Washington, D.C.: n.p., December 1973.

Yarger, H. L. and McCauley, J. R. "Quantitative Water Quality with LANDSAT and SKYLAB." Proceedings of the NASA Earth Resources Survey Symposium. Houston, Texas: n.p., June 1975.

Yost, E.; Hollman, R.; Alexander, J.; and Nuzzi, R. "An Interdisciplinary Study of Estuarine and Coastal Oceanography of Block Island Sound and Adjacent New York Coastal Waters." Proceedings of Third Earth Resources Technology Satellite-1 Symposium. Washington, D.C.: n.p., December 1973.

APPENDIX B

LIST OF SYMBOLS

A = upwelled radiance of filtered seawater

B = constant giving change in upwelled radiance due to P_A

b = matrix given by equation (5-6)

C = constituent concentration

C_p = statistical parameter based on sum of squared biases plus the sum of squared random errors as defined in equation (5-17)

E = constant giving change in upwelled radiance due to P_B

e = deviation from true value

F = statistical parameter as defined in equation (5-12)

F_{cr} = critical value of F

G = constant giving change in upwelled radiance due to optical interaction between P_B and P_C as given in equation (4-21)

H = constant giving change in upwelled radiance due to ϕ

I = upwelled radiance from clear atmosphere

J,J',j = constants in regression equation

K,K',k = constants in regression equation

L = constant giving change in upwelled radiance due to atmospheric pollutant X_A

M = arbitrary power expressing upwelled radiance nonlinearity with ϕ

N = arbitrary power expressing upwelled radiance nonlinearity with X_A

n = number of ground truth points with measured concentration and upwelled radiance values

P_A = concentration of pollutant A

$\hat{P}_A$ = measured ground truth value of P_A

$\bar{P}_A$ = mean value of ground truth values of P_A

P_B = concentration of pollutant B

P_C = concentration of pollutant C

p = number of estimated J, K coefficients in regression equation

Q = arbitrary power expressing upwelled radiance nonlinearity with P_C

R = arbitrary power expressing upwelled radiance nonlinearity with P_B in optical interaction with P_C

Rad = upwelled radiance at a particular wavelength or band

RSS_p = sum of square of residuals in p-term regression equation

r = correlation coefficient as defined by the square root of equation (5-10)

S = constant giving change in upwelled radiance due to P_C

SS = sum of squares

s^2 = unbiased estimate of σ^2

T = arbitrary power expressing upwelled radiance nonlinearity with P_C in optical interaction with P_B

X_A = concentration of atmospheric pollutant

Z_{90} = thickness of water layer from which 90 percent of the upwelled radiance is measured

$\alpha_{W,X}$ = expression defined by equation (C-10)

$\alpha_{W,Y}$ = expression defined by equation (C-10)

$\alpha_{Y,Z}$ = expression defined by equation (C-10)

β_W = expression defined by equation (C-15)

β_X = expression defined by equation (C-15)

θ = expression defined by equation (C-19)

ϕ = variable which is related to the instrument pointing angle and the solar elevation angle

σ = standard error of water constituent concentration

σ^2 = variance of water constituent concentration

σ_{Rad} = standard error of upwelled radiance measurement

$(\sigma_{Rad})^2$ = variance of upwelled radiance measurement

λ = wavelength

Subscripts:

i = ground truth observation number

p_{max} = quantity for equation with maximum number of estimated coefficients

W = value of wavelength

X = value of wavelength

Y = value of wavelength

Z = value of wavelength

APPENDIX C

SOLUTION TO SIGNAL RESPONSE EQUATIONS

Under the assumptions of this study, the equations for total radiance at wavelengths W, X, Y, and Z may be written:

$$Rad_W = A_W + B_W P_A + E_W P_B + H_W \phi^M + I_W + L_W X_A^N \quad (C\text{-}1)$$

$$Rad_X = A_X + B_X P_A + E_X P_B + H_X \phi^M + I_X + L_X X_A^N \quad (C\text{-}2)$$

$$Rad_Y = A_Y + B_Y P_A + E_Y P_B + H_Y \phi^M + I_Y + L_Y X_A^N \quad (C\text{-}3)$$

$$Rad_Z = A_Z = B_Z P_Z + E_Z P_B + H_Z \phi^M + I_Z + L_Z X_A^N \quad (C\text{-}4)$$

Multiplying (C-1) by L_X and (C-2) by L_W gives:

$$L_X Rad_W = L_X A_W + L_X B_W P_A + L_X E_W P_B + L_X H_W \phi^M + L_X I_W + L_X L_W X_A^N \quad (C\text{-}5)$$

$$L_W Rad_X = L_W A_X + L_W B_X P_A + L_W E_X P_B + L_W H_X \phi^M + L_W I_X + L_X L_W X_A^N \quad (C\text{-}6)$$

Subtracting (C-6) from (C-5):

$$\begin{aligned} L_X Rad_W - L_W Rad_X = {} & L_X(A_W + I_W) - L_W(A_X + I_X) \\ & + (L_X B_W - L_W B_X) P_A + (L_X E_W - L_W E_X) P_B \\ & + (L_X H_W - L_W H_X) \phi^M \end{aligned} \quad (C\text{-}7)$$

Performing similar operations first on equations (C-3) and (C-4), and second, on equations (C-1) and (C-3), one obtains:

$$L_Z Rad_Y - L_Y Rad_Z = L_Z(A_Y + I_Y) - L_Y(A_Z + I_Z) + (L_Z B_Y - L_Y B_Z)P_A + (L_Z E_Y - L_Y E_Z)P_B + (L_Z H_Y - L_Y H_Z)\phi^M \quad (C\text{-}8)$$

$$L_Y Rad_W - L_W Rad_Y = L_Y(A_W + I_W) - L_W(A_Y + I_Y) + (L_Y B_W - L_W B_Y)P_A + (L_Y E_W - L_W E_Y)P_B + (L_Y H_W - L_W H_Y)\phi^M \quad (C\text{-}9)$$

Equations (C-7), (C-8), and (C-9) represent three equations with three variables (P_A, P_B, ϕ). For convenience let:

$$\left.\begin{aligned} (L_X H_W - L_W H_X) &= \alpha_{W,X} \\ (L_Z H_Y - L_Y H_Z) &= \alpha_{Y,Z} \\ (L_Y H_W - L_W H_Y) &= \alpha_{W,Y} \end{aligned}\right\} \quad (C\text{-}10)$$

Multiplying (C-7) by $\alpha_{Y,W}$ and (C-8) by $\alpha_{W,X}$, one obtains:

$$\alpha_{Y,Z}L_X Rad_W - \alpha_{Y,Z}L_W Rad_X = \alpha_{Y,Z}L_X(A_W + I_W)$$
$$- \alpha_{Y,Z}L_W(A_X + I_X)$$
$$+ (\alpha_{Y,Z}L_X B_W - \alpha_{Y,Z}L_W B_X)P_A$$
$$+ (\alpha_{Y,Z}L_X E_W - \alpha_{Y,Z}L_W E_X)P_B$$
$$+ \alpha_{Y,Z}\alpha_{W,X}\phi^M \qquad \text{(C-11)}$$

$$\alpha_{W,X}L_Z Rad_Y - \alpha_{W,X}L_Y Rad_Z = \alpha_{W,X}L_Z(A_Y + I_Y)$$
$$- \alpha_{W,X}L_Y(A_Z + I_Z)$$
$$+ (\alpha_{W,X}L_Z B_Y - \alpha_{W,X}L_Y B_Z)P_A$$
$$+ (\alpha_{W,X}L_Z E_Y - \alpha_{W,X}L_Y E_Z)P_B$$
$$+ \alpha_{Y,Z}\alpha_{W,X}\phi^M \qquad \text{(C-12)}$$

Subtracting (C-12) from (C-11):

$$\alpha_{Y,Z}L_X Rad_W - \alpha_{Y,Z}L_W Rad_X - \alpha_{W,X}L_Z Rad_Y + \alpha_{W,X}L_Y Rad_Z =$$
$$+ \alpha_{Y,Z}L_X(A_W + I_W) - \alpha_{Y,Z}L_W(A_X + I_X)$$
$$- \alpha_{W,X}L_Z(A_Y + I_Y) + \alpha_{W,X}L_Y(A_Z + I_Z)$$
$$+ (\alpha_{Y,Z}L_X B_W - \alpha_{Y,Z}L_W B_X - \alpha_{W,X}L_Z B_Y + \alpha_{W,X}L_Y B_Z)P_A$$
$$+ (\alpha_{Y,Z}L_X E_W - \alpha_{Y,Z}L_W E_X - \alpha_{W,X}L_Z E_Y + \alpha_{W,X}L_Y F_Z)P_B \qquad \text{(C-13)}$$

Performing similar operations on (C-8) and (C-9):

$$\alpha_{W,Y}L_Z Rad_Y - \alpha_{W,Y}L_Y Rad_Z - \alpha_{Y,Z}L_Y Rad_W + \alpha_{Y,Z}L_W Rad_Y =$$

$$+ \alpha_{W,Y}L_Z(A_Y + I_Y) - \alpha_{Y,Z}L_Y(A_W + I_W)$$

$$- \alpha_{W,Y}L_Y(A_Z + I_Z) + \alpha_{Y,Z}L_W(A_Y + I_Y)$$

$$+ (\alpha_{W,Y}L_Z B_Y - \alpha_{W,Y}L_Y B_Z - \alpha_{Y,Z}L_Y B_W + \alpha_{Y,Z}L_W B_Y)P_A$$

$$+ (\alpha_{W,Y}L_Z E_Y - \alpha_{W,Y}L_Y E_Z - \alpha_{Y,Z}L_Y E_W + \alpha_{Y,Z}L_W E_Y)P_B \qquad \text{(C-14)}$$

Equations (C-13) and (C-14) represent two equations with two variables (P_A and P_B). For convenience, let:

$$\left.\begin{aligned}(\alpha_{Y,Z}L_X E_W - \alpha_{Y,Z}L_W E_X - \alpha_{W,X}L_Z E_Y + \alpha_{W,X}L_Y E_Z) &= \beta_W \\ (\alpha_{W,Y}L_Z E_Y - \alpha_{W,Y}L_Y E_Z - \alpha_{Y,Z}L_Y E_W + \alpha_{Y,Z}L_W E_Y) &= \beta_X\end{aligned}\right\} \qquad \text{(C-15)}$$

To solve for P_A, multiply equation (C-13) by β_X and equation (C-14) by β_W:

$$\beta_X\alpha_{Y,Z}L_X Rad_W - \beta_X\alpha_{Y,Z}L_W Rad_X - \beta_X\alpha_{W,X}L_Z Rad_Y + \beta_X\alpha_{W,X}L_Y Rad_Z =$$

$$+ \beta_X\alpha_{Y,Z}L_X(A_W + I_W) - \beta_X\alpha_{Y,Z}L_W(A_X + I_X)$$

$$- \beta_X\alpha_{W,X}L_Z(A_Y + I_Y) + \beta_X\alpha_{W,X}L_Y(A_Z + I_Z)$$

$$+ (\beta_X\alpha_{Y,Z}L_X B_W - \beta_X\alpha_{Y,Z}L_W B_X - \beta_X\alpha_{W,X}L_Z B_Y + \beta_X\alpha_{W,X}L_Y B_Z)P_A$$

$$+ (\beta_X\beta_W)P_B \qquad (C\text{-}16)$$

$$\beta_W\alpha_{W,Y}L_Z Rad_Y - \beta_W\alpha_{W,Y}L_Y Rad_Z - \beta_W\alpha_{Y,Z}L_Y Rad_W + \beta_W\alpha_{Y,Z}L_W Rad_Y =$$

$$+ \beta_W\alpha_{W,Y}L_Z(A_Y + I_Y) - \beta_W\alpha_{Y,Z}L_Y(A_W + I_W)$$

$$- \beta_W\alpha_{W,Y}L_Y(A_Z + I_Z) + \beta_W\alpha_{Y,Z}L_W(A_Y + I_Y)$$

$$+ (\beta_W\alpha_{W,Y}L_Z B_Y - \beta_W\alpha_{W,Y}L_Y B_Z - \beta_W\alpha_{Y,Z}L_Y B_W + \beta_W\alpha_{Y,Z}L_W B_Y)P_A$$

$$+ (\beta_X\beta_W)P_B \qquad (C\text{-}17)$$

Subtracting equations (C-17) from (C-16) and collecting like terms:

$$(\beta_X\alpha_{Y,Z}L_X + \beta_W\alpha_{Y,Z}L_Y)Rad_W - (\beta_X\alpha_{Y,Z}L_W)Rad_X$$

$$- (\beta_X\alpha_{W,X}L_Z + \beta_W\alpha_{W,Y}L_Z + \beta_W\alpha_{Y,Z}L_W)Rad_Y$$

$$+ (\beta_X\alpha_{W,X}L_Y + \beta_W\alpha_{W,Y}L_Y)Rad_Z =$$

$$(\beta_X\alpha_{Y,Z}L_X + \beta_W\alpha_{Y,Z}L_Y)(A_W + I_W) - (\beta_X\alpha_{Y,Z}L_W)(A_X + I_X)$$

$$- (\beta_X\alpha_{W,X}L_Z + \beta_W\alpha_{W,Y}L_Z + \beta_W\alpha_{Y,Z}L_W)(A_Y + I_Y)$$

$$+ (\beta_X\alpha_{W,X}L_Y - \beta_W\alpha_{W,Y}L_Y)(A_Z + I_Z) + (\beta_X\alpha_{Y,Z}L_XB_W$$

$$- \beta_X\alpha_{Y,Z}L_WB_X - \beta_X\alpha_{W,X}L_ZB_Y + \beta_X\alpha_{W,X}L_YB_Z$$

$$- \beta_W\alpha_{W,Y}L_ZB_Y + \beta_W\alpha_{W,Y}L_YB_Z + \beta_W\alpha_{Y,Z}L_YB_W$$

$$- \beta_W\alpha_{Y,Z}L_WB_Y)P_A \qquad (C\text{-}18)$$

For convenience, let:

$$(\beta_X\alpha_{Y,Z}L_XB_W - \beta_X\alpha_{Y,Z}L_WB_X - \beta_X\alpha_{W,X}L_ZB_Y + \beta_X\alpha_{W,X}L_YB_Z$$

$$- \beta_W\alpha_{W,Y}L_ZB_Y + \beta_W\alpha_{W,Y}L_YB_Z + \beta_W\alpha_{Y,Z}L_YB_W$$

$$- \beta_W\alpha_{Y,Z}L_WB_Y) = \theta \qquad (C\text{-}19)$$

Rearranging:

$$P_A = J + K_W(Rad_W) + K_X(Rad_X) + K_Y(Rad_Y) + K_Z(Rad_Z) \qquad (C\text{-}20)$$

where:

$$J = \frac{1}{\theta}\left[-(\beta_X\alpha_{Y,Z}L_X + \beta_W\alpha_{Y,Z}L_Y)(A_W + I_W)\right.$$

$$+ (\beta_X\alpha_{Y,Z}L_W)(A_X + I_X)$$

$$+ (\beta_X\alpha_{W,X}L_Z + \beta_W\alpha_{W,Y}L_Z + \beta_W\alpha_{Y,Z}L_W)(A_Y + I_Y)$$

$$\left. - (\beta_X\alpha_{W,X}L_Y - \beta_W\alpha_{W,Y}L_Y)(A_Z + I_Z)\right]$$

$$K_W = \frac{1}{\theta}\left[\beta_X\alpha_{Y,Z}L_X + \beta_W\alpha_{Y,Z}L_Y\right]$$

$$K_X = \frac{1}{\theta}\left[-\beta_X\alpha_{Y,Z}L_W\right]$$

$$K_Y = \frac{1}{\theta}\left[-\beta_X\alpha_{W,X}L_Z - \beta_W\alpha_{W,Y}L_Z - \beta_W\alpha_{Y,Z}L_W\right]$$

$$K_Z = \frac{1}{\theta}\left[\beta_X\alpha_{W,X}L_Y + \beta_W\alpha_{W,Y}L_Y\right]$$

TABLE 1

RADIANCE AND GROUND TRUTH DATA

FOR HOMOGENEOUS TEST CASE

Ground Truth Location	P_A	P_B	Rad_1	Rad_2	Rad_3	Rad_4	Rad_5
1	20	20	25.5	27.2	30.3	33.8	20.3
2	10	20	22.9	25.2	29.0	34.1	24.4
3	30	40	28.6	30.4	35.7	43.8	23.5
4	20	30	19.0	23.1	29.7	36.9	21.9
5	40	10	33.2	34.8	40.3	40.4	25.1
6	10	40	20.2	22.6	26.9	36.0	20.9
7	20	10	35.8	36.4	38.1	39.0	30.3
8	40	30	42.6	42.8	47.6	52.6	34.0

TABLE 2

ESTIMATES OF J,K COEFFICIENTS

FOR HOMOGENEOUS TEST CASE

FOR P_A

Bands Used	J	K_1	K_2	K_3	K_4	K_5
1	-7.3	1.09	0.	0.	0.	0.
2	-15.7	0.	1.30	0.	0.	0.
3	-27.6	0.	0.	1.48	0.	0.
4	-35.9	0.	0.	0.	1.51	0.
5	-9.5	0.	0.	0.	0.	1.33
1,2	-61.9	-7.49	9.86	0.	0.	0.
1,3	-45.5	-1.72	0.	3.41	0.	0.
1,4	-20.4	0.49	0.	0.	0.99	0.
1,5	11.1	2.03	0.	0.	0.	-1.80
2,3	-38.7	0.	-2.66	4.12	0.	0.
2,4	-31.1	0.	0.69	0.	0.86	0.
2,5	0.1	0.	2.69	0.	0.	-2.31
3,4	-28.9	0.	0.	1.40	0.11	0.
3,5	-17.0	0.	0.	2.82	0.	-2.28
4,5	-35.2	0.	0.	0.	1.79	-0.48
1,2,3	-27.5	2.57	-6.41	4.96	0.	0.
1,2,4	-63.5	-6.49	8.42	0.	0.43	0.
1,2,5	-49.7	-8.31	12.32	0.	0.	-2.53
1,3,4	-41.8	-2.03	0.	4.20	-0.57	0.
1,3,5	-26.8	-0.79	0.	3.50	0.	-1.94
1,4,5	-12.3	1.51	0.	0.	1.26	-2.27
2,3,4	-32.1	0.	-3.39	5.46	-0.78	0.
2,3,5	-23.6	0.	-1.14	3.73	0.	-1.90
2,4,5	-17.4	0.	2.09	0.	1.07	-2.57
3,4,5	-18.7	0.	0.	2.72	0.14	-2.28
1,2,3,4	0.6	6.66	-13.50	8.38	-1.22	0.
1,2,3,5	-30.6	-1.82	1.62	3.11	0.	-2.02
1,2,4,5	-51.4	-6.90	10.34	0.	0.62	-2.65
1,3,4,5	-26.2	-0.90	0.	3.73	-0.17	-1.89
2,3,4,5	-22.2	0.	-1.47	4.19	-0.26	-1.79
1,2,3,4,5	-26.9	-1.08	0.287	3.64	-0.15	-1.91

TABLE 3

ESTIMATES OF PRECISION

FOR HOMOGENEOUS TEST CASE.

FOR P_A

Bands Used	r	σ	$(F/F_{cr})_{.95}$	C_p	C_p/p
1	0.76	8.4	1.33	1404.	702.1
2	0.79	7.9	1.61	1252.	626.4
3	0.88	6.1	3.38	744.	372.5
4	0.79	7.8	1.67	1224.	612.3
5	0.53	10.8	0.40	2340.	1170.3
1,2	0.87	6.8	1.37	781.	260.6
1,3	0.93	4.9	3.11	398.	132.7
1,4	0.81	8.1	0.87	1088.	362.8
1,5	0.82	8.0	0.89	1066.	355.5
2,3	0.94	4.7	3.44	363.	121.0
2,4	0.83	7.9	0.93	1036.	345.5
2,5	0.88	6.6	1.52	725.	241.7
3,4	0.88	6.7	1.46	744.	248.3
3,5	0.99	2.0	21.74	61.	20.6
4,5	0.80	8.4	0.77	1177.	392.6
1,2,3	0.95	5.1	1.72	346.	86.5
1,2,4	0.88	7.4	0.70	737.	184.4
1,2,5	0.98	3.3	4.23	149.	37.5
1,3,4	0.95	5.1	1.70	349.	87.3
1,3,5	0.99	0.7	106.33	6.	1.6
1,4,5	0.91	6.6	0.96	573.	143.3
2,3,4	0.96	4.6	2.21	275.	68.9
2,3,5	0.99	0.9	56.50	11.	2.9
2,4,5	0.94	5.4	1.48	394.	98.5
3,4,5	0.99	2.1	10.81	60.	15.1
1,2,3,4	0.97	4.2	1.44	178.	35.7
1,2,3,5	0.99	0.6	77.55	5.	1.1
1,2,4,5	0.99	2.3	4.90	56.	11.2
1,3,4,5	0.99	0.5	132.30	4.	0.8
2,3,4,5	0.99	0.6	77.92	5.	1.1
1,2,3,4,5	0.99	0.5	33.98	6.	1.0

TABLE 4

ESTIMATES OF J,K COEFFICIENTS

FOR HOMOGENEOUS TEST CASE

FOR P_B

Bands Used	J	K_1	K_2	K_3	K_4	K_5
1	39.2	-0.50	0.	0.	0.	0.
2	42.3	0.	-0.57	0.	0.	0.
3	39.7	0.	0.	-0.42	0.	0.
4	8.4	0.	0.	0.	0.42	0.
5	42.0	0.	0.	0.	0.	-0.68
1,2	37.3	-0.81	0.35	0.	0.	0.
1,3	18.4	-2.03	0.	1.85	0.	0.
1,4	-19.4	-2.09	0.	0.	2.63	0.
1,5	34.6	-0.74	0.	0.	0.	0.46
2,3	24.4	0.	-3.63	3.18	0.	0.
2,4	-9.9	0.	-2.62	0.	2.89	0.
2,5	39.0	0.	-0.86	0.	0.	0.48
3,4	-9.3	0.	0.	-3.52	3.96	0.
3,5	42.3	0.	0.	-0.09	0.	-0.57
4,5	12.7	0.	0.	0.	2.05	-2.74
1,2,3	97.0	16.66	-27.88	8.62	0.	0.
1,2,4	25.0	6.99	-10.94	0.	3.35	0.
1,2,5	35.0	-0.66	-0.10	0.	0.	0.47
1,3,4	-8.4	0.14	0.	-3.72	4.00	0.
1,3,5	14.7	-2.21	0.	1.83	0.	0.39
1,4,5	-15.3	-1.84	0.	0.	2.69	-0.55
2,3,4	-9.2	0.	0.07	-3.60	3.97	0.
2,3,5	17.7	0.	-4.30	3.36	0.	0.85
2,4,5	-8.6	0.	-2.50	0.	2.91	-0.24
3,4,5	-6.4	0.	0.	-3.149	3.96	-0.65
1,2,3,4	11.9	4.30	-6.46	-1.72	3.69	0.
1,2,3,5	100.3	21.49	-36.68	10.64	0.	2.22
1,2,4,5	25.7	6.97	-10.83	0.	3.36	-0.16
1,3,4,5	-0.5	0.71	0.	-3.95	4.21	-0.96
2,3,4,5	-3.5	0.	1.18	-4.34	4.28	-1.04
1,2,3,4,5	-2.9	0.14	0.95	-4.26	4.26	-1.03

TABLE 5

ESTIMATES OF PRECISION

FOR HOMOGENEOUS TEST CASE

FOR P_B

Bands Used	r	σ	$(F/F_{cr})_{.95}$	C_p	C_p/p
1	0.34	12.1	0.13	485.	242.8
2	0.34	12.1	0.13	486.	243.2
3	0.25	12.5	0.07	516.	258.5
4	0.22	12.6	0.05	524.	262.4
5	0.27	12.4	0.08	510.	255.1
1,2	0.35	13.3	0.06	487.	162.5
1,3	0.46	12.6	0.11	437.	145.9
1,4	0.89	6.4	1.67	112.	37.4
1,5	0.35	13.2	0.06	483.	161.3
2,3	0.53	12.0	0.17	399.	133.1
2,4	0.93	5.1	2.86	71.	23.6
2,5	0.35	13.2	0.06	484.	161.5
3,4	0.98	2.5	13.39	15.	5.1
3,5	0.27	13.6	0.03	511.	170.6
4,5	0.73	9.6	0.49	257.	86.0
1,2,3	0.72	11.0	0.22	268.	67.2
1,2,4	0.99	2.5	7.62	14.	3.6
1,2,5	0.34	14.7	0.03	486.	121.5
1,3,4	0.99	2.8	6.39	17.	4.3
1,3,5	0.46	14.0	0.05	437.	109.3
1,4,5	0.90	7.0	0.83	109.	27.3
2,3,4	0.98	2.8	6.28	17.	4.3
2,3,5	0.55	13.2	0.09	389.	97.4
2,4,5	0.93	5.7	1.36	72.	18.0
3,4,5	0.99	1.9	13.62	8.	2.0
1,2,3,4	0.99	2.5	4.29	12.	2.4
1,2,3,5	0.80	11.0	0.15	202.	40.3
1,2,4,5	0.99	2.9	3.19	16.	3.2
1,3,4,5	0.99	1.1	21.98	4.	0.8
2,3,4,5	0.99	1.1	22.71	4.	0.8
1,2,3,4,5	0.99	1.3	5.73	6.	1.0

TABLE 6

RADIANCE DATA FOR HOMOGENEOUS TEST CASE

Ground Truth Location	Rad_1	Rad_2	Rad_3	Rad_4	Rad_5
9	23.3	25.9	28.9	37.1	20.7
10	27.7	28.7	31.3	35.2	20.2
11	31.6	34.1	39.2	40.5	25.1
12	33.9	34.8	35.5	36.1	24.1
13	37.8	40.0	44.9	46.8	32.2
14	23.6	26.8	29.9	36.7	24.1
15	28.0	30.9	36.7	43.4	24.6
16	28.2	30.2	33.5	35.6	20.1
17	24.3	26.3	27.8	32.1	18.6
18	22.7	27.3	35.8	42.7	24.1

TABLE 7

RADIANCE AND GROUND TRUTH DATA

FOR NON-HOMOGENEOUS TEST CASE

Ground Truth Location	P_A	P_B	Rad_1	Rad_2	Rad_3	Rad_4	Rad_5
19	15	0	23.1	25.3	26.3	25.2	16.4
20	22	0	27.5	28.3	29.8	28.0	17.6
21	37	0	31.5	33.9	38.2	36.1	23.5
22	23	0	33.9	34.7	34.8	32.6	22.8
23	38	0	37.7	39.7	43.8	41.8	30.4
24	12	0	23.9	26.8	28.0	28.3	21.1
25	32	0	27.8	30.4	34.4	32.7	20.7
26	29	0	28.1	29.9	32.4	30.2	18.1
27	14	0	24.2	25.9	26.2	24.8	16.1
28	35	0	22.5	26.8	33.6	32.6	20.5

TABLE 8

ESTIMATES OF J,K COEFFICIENTS

FOR NON-HOMOGENEOUS TEST CASE

FOR P_A

Bands Used	J	K_1	K_2	K_3	K_4	K_5
1	-9.2	1.17	0.	0.	0.	0.
2	-17.2	0.	1.36	0.	0.	0.
3	-24.9	0.	0.	1.44	0.	0.
4	-12.0	0.	0.	0.	1.00	0.
5	-4.1	0.	0.	0.	0.	1.21
1,2	-39.3	-4.46	6.28	0.	0.	0.
1,3	-28.2	-0.63	0.	2.07	0.	0.
1,4	-17.2	0.91	0.	0.	0.42	0.
1,5	-7.6	1.29	0.	0.	0.	-0.22
2,3	-25.6	0.	-0.80	2.18	0.	0.
2,4	-21.9	0.	1.13	0.	0.32	0.
2,5	-15.0	0.	1.72	0.	0.	-0.57
3,4	-22.4	0.	0.	1.72	-0.33	0.
3,5	-23.2	0.	0.	2.66	0.	-1.84
4,5	-12.1	0.	0.	0.	0.93	0.12
1,2,3	-31.3	-1.45	1.18	1.79	0.	0.
1,2,4	-39.8	-4.21	5.92	0.	0.11	0.
1,2,5	-41.6	-5.78	8.41	0.	0.	-1.07
1,3,4	-25.7	-1.47	0.	3.66	-0.90	0.
1,3,5	-27.5	-0.85	0.	3.58	0.	-1.94
1,4,5	-18.6	1.45	0.	0.	1.22	-1.84
2,3,4	-18.4	0.	-2.63	4.87	-1.18	0.
2,3,5	-24.2	0.	-1.17	3.82	0.	-1.96
2,4,5	-26.6	0.	1.89	0.	1.21	-2.17
3,4,5	-25.5	0.	0.	2.56	0.35	-2.13
1,2,3,4	-4.4	3.04	-7.32	6.48	-1.53	0.
1,2,3,5	-27.5	-0.85	0.01	3.58	0.	-1.95
1,2,4,5	-48.7	-5.09	7.77	0.	1.07	-2.43
1,3,4,5	-27.3	-0.94	0.	3.70	-0.10	-1.87
2,3,4,5	-22.6	0.	-1.56	4.29	-0.28	-1.76
1,2,3,4,5	-23.5	-0.18	-1.26	4.18	-0.25	-1.78

TABLE 9

ESTIMATES OF PRECISION

FOR NON-HOMOGENEOUS TEST CASE

FOR P_A

Bands Used	r	σ	$(F/F_{cr})_{.95}$	C_p	C_p/p
1	0.77	7.3	3.23	3706.	1853.2
2	0.81	6.8	4.19	3152.	1576.1
3	0.88	5.3	8.10	1960.	980.5
4	0.64	8.7	1.61	5258.	2629.3
5	0.57	9.4	1.08	6092.	3046.4
1,2	0.87	5.9	3.65	2243.	747.9
1,3	0.90	5.3	5.00	1754.	585.0
1,4	0.79	7.3	2.09	3309.	1103.2
1,5	0.77	7.6	1.76	3673.	1224.6
2,3	0.90	5.3	4.88	1790.	596.7
2,4	0.82	6.8	2.50	2944.	981.4
2,5	0.82	6.8	2.50	2940.	980.0
3,4	0.89	5.4	4.78	1822.	607.4
3,5	0.98	2.5	26.47	389.	129.7
4,5	0.64	9.1	0.87	5253.	1751.1
1,2,3	0.90	5.5	3.23	1739.	434.8
1,2,4	0.87	6.3	2.36	2221.	555.3
1,2,5	0.91	5.3	3.64	1578.	394.6
1,3,4	0.94	4.4	5.54	1101.	275.3
1,3,5	0.99	0.6	345.91	15.	3.8
1,4,5	0.87	6.3	2.31	2260.	565.2
2,3,4	0.95	4.0	6.95	899.	224.9
2,3,5	0.99	0.8	175.10	33.	8.3
2,4,5	0.91	5.2	3.77	1533.	383.4
3,4,5	0.98	2.2	23.71	280.	70.1
1,2,3,4	0.96	3.9	5.71	748.	149.7
1,2,3,5	0.99	0.6	231.81	17.	3.4
1,2,4,5	0.97	3.1	8.89	494.	98.9
1,3,4,5	0.99	0.5	312.53	12.	2.4
2,3,4,5	0.99	0.4	627.48	4.	0.9
1,2,3,4,5	0.99	0.4	452.69	6.	1.0

TABLE 10

ESTIMATES OF J,K COEFFICIENTS

FOR NON-HOMOGENEOUS TEST CASE

FOR P_B

Bands Used	J	K_1	K_2	K_3	K_4	K_5
1	35.0	-0.67	0.	0.	0.	0.
2	38.0	0.	-0.73	0.	0.	0.
3	24.3	0.	0.	-0.26	0.	0.
4	-24.8	0.	0.	0.	1.09	0.
5	6.6	0.	0.	0.	0.	0.37
1,2	31.4	-1.33	0.74	0.	0.	0.
1,3	7.1	-3.30	0.	3.03	0.	0.
1,4	-12.3	-2.19	0.	0.	2.49	0.
1,5	12.9	-2.32	0.	0.	0.	2.95
2,3	19.1	0.	-5.61	4.93	0.	0.
2,4	-1.7	0.	-2.63	0.	2.68	0.
2,5	24.8	0.	-2.87	0.	0.	3.34
3,4	-4.0	0.	0.	-3.45	3.76	0.
3,5	21.7	0.	0.	-2.10	0.	2.77
4,5	-21.7	0.	0.	0.	3.25	-3.47
1,2,3	68.4	12.62	-22.86	8.31	0.	0.
1,2,4	20.0	5.12	-8.45	0.	2.93	0.
1,2,5	39.1	3.11	-6.47	0.	0.	3.60
1,3,4	-3.3	0.31	0.	-3.86	3.88	0.
1,3,5	6.4	-3.03	0.	1.18	0.	2.38
1,4,5	-13.0	-1.94	0.	0.	2.86	-0.85
2,3,4	-4.5	0.	0.35	-3.87	3.87	0.
2,3,5	17.4	0.	-5.20	3.08	0.	2.22
2,4,5	-2.8	0.	-2.47	0.	2.88	-0.48
3,4,5	-5.0	0.	0.	-3.19	3.97	-0.66
1,2,3,4	4.5	1.95	-2.66	-2.84	3.65	0.
1,2,3,5	64.5	11.99	-21.64	6.45	0.	2.02
1,2,4,5	19.1	5.04	-8.28	0.	3.01	-0.23
1,3,4,5	-3.9	0.55	0.	-3.85	4.23	-0.82
2,3,4,5	6.6	0.	0.89	-4.16	4.32	-0.88
1,2,3,4,5	-4.4	0.45	0.16	-3.91	4.25	-0.83

TABLE 11

ESTIMATES OF PRECISION

FOR NON-HOMOGENEOUS TEST CASE

FOR P_B

Bands Used	r	σ	$(F/F_{cr})_{.95}$	C_p	C_p/p
1	0.31	15.5	0.23	3355.	1677.7
2	0.30	15.5	0.22	3367.	1683.8
3	0.11	16.2	0.03	3660.	1829.9
4	0.49	14.2	0.71	2820.	1410.2
5	0.12	16.2	0.03	3651.	1825.7
1,2	0.31	16.3	0.13	3353.	1117.8
1,3	0.57	14.1	0.58	2510.	836.7
1,4	0.92	6.5	7.10	537.	179.1
1,5	0.67	12.8	0.97	2065.	688.2
2,3	0.68	12.5	1.07	1969.	656.2
2,4	0.96	5.0	13.28	305.	101.8
2,5	0.70	12.2	1.16	1894.	631.4
3,4	0.99	2.1	80.14	49.	16.2
3,5	0.46	15.2	0.32	2939.	979.7
4,5	0.76	11.1	1.66	1567.	522.3
1,2,3	0.83	10.1	1.69	1165.	291.2
1,2,4	0.99	2.9	29.14	91.	22.9
1,2,5	0.71	12.6	0.81	1816.	454.2
1,3,4	0.99	2.1	58.15	44.	11.0
1,3,5	0.68	13.2	0.67	1986.	496.6
1,4,5	0.93	6.6	5.01	493.	123.4
2,3,4	0.99	2.1	54.42	47.	11.8
2,3,5	0.77	11.5	1.11	1517.	379.2
2,4,5	0.96	5.1	8.88	294.	73.5
3,4,5	0.99	1.5	111.83	21.	5.2
1,2,3,4	0.99	2.0	48.38	37.	7.3
1,2,3,5	0.89	8.9	1.91	794.	158.8
1,2,4,5	0.99	3.0	20.17	90.	18.1
1,3,4,5	0.99	0.8	274.72	4.	0.8
2,3,4,5	0.99	0.9	255.71	5.	0.9
1,2,3,4,5	0.99	0.9	186.73	6.	1.0

TABLE 12

RADIANCE AND CONCENTRATION DATA

FOR DUAL-CONSTITUENT TESTS

Test Number	Ball Clay (ppm)	Feldspar (ppm)	Rad_1	Rad_2	Rad_3	Rad_4	Rad_5
1	129	17	0.297	0.310	0.290	0.220	0.156
2	173	17	0.360	0.390	0.369	0.297	0.205
3	9	35	0.075	0.058	0.047	0.034	0.023
4	9	69	0.114	0.100	0.081	0.058	0.042
5	52	69	0.229	0.213	0.198	0.142	0.102
6	52	173	0.315	0.304	0.267	0.202	0.147
7	173	173	0.477	0.518	0.496	0.395	0.285
8	9	17	0.072	0.063	0.047	0.036	0.024
9	17	17	0.099	0.092	0.074	0.056	0.038
10	129	73	0.420	0.452	0.425	0.332	0.235
11	52	17	0.189	0.178	0.153	0.107	0.076
12	173	35	0.369	0.391	0.364	0.286	0.200
13	17	69	0.142	0.124	0.105	0.077	0.056
14	17	35	0.094	0.087	0.072	0.049	0.032
15	52	35	0.171	0.161	0.145	0.094	0.068
16	173	52	0.378	0.420	0.380	0.281	0.200

TABLE 13

RADIANCE AND CONCENTRATION DATA

FOR THREE-CONSTITUENT TESTS

Test Number	Ball Clay (ppm)	Feldspar (ppm)	Rad_1	Rad_2	Rad_3	Rad_4	Rad_5
1	9	17	0.094	0.096	0.094	0.053	0.028
2	9	17	0.039	0.093	0.140	0.078	0.027
3	9	35	0.105	0.100	0.097	0.056	0.033
4	17	35	0.121	0.127	0.120	0.080	0.047
5	9	35	0.044	0.100	0.143	0.078	0.029
6	17	35	0.054	0.101	0.154	0.099	0.039
7	17	35	0.116	0.134	0.155	0.091	0.045
8	17	52	0.138	0.148	0.167	0.101	0.052
9	17	52	0.099	0.148	0.190	0.110	0.050
10	52	52	0.177	0.192	0.252	0.170	0.090
11	17	52	0.059	0.105	0.165	0.102	0.044
12	52	52	0.113	0.133	0.212	0.154	0.080
13	173	129	0.406	0.428	0.437	0.370	0.260
14	173	129	0.388	0.347	0.429	0.390	0.256
15	52	129	0.232	0.230	0.304	0.218	0.128
16	129	129	0.359	0.323	0.439	0.362	0.220
17	173	129	0.359	0.300	0.440	0.407	0.256
18	52	129	0.147	0.155	0.245	0.188	0.095
19	129	129	0.246	0.213	0.355	0.313	0.188
20	173	129	0.299	0.263	0.444	0.426	0.256
21	173	173	0.459	0.470	0.475	0.395	0.267
22	173	173	0.432	0.379	0.495	0.404	0.267
23	173	173	0.387	0.322	0.464	0.415	0.267
24	129	173	0.260	0.225	0.376	0.334	0.197
25	173	173	0.290	0.250	0.420	0.386	0.244

TABLE 14

ESTIMATES OF J,K COEFFICIENTS

FOR DUAL-CONSTITUENT MIXTURES

FOR BALL CLAY SEDIMENT

Bands Used	J	K_1	K_2	K_3	K_4	K_5
1	-38.6	480.53	0.	0.	0.	0.
2	-28.7	0.	432.67	0.	0.	0.
3	-22.7	0.	0.	451.68	0.	0.
4	-18.9	0.	0.	0.	571.70	0.
5	-18.2	0.	0.	0.	0.	803.90
1,2	10.7	-1462.21	1709.52	0.	0.	0.
1,3	25.4	-1195.25	0.	1535.61	0.	0.
1,4	10.5	-598.95	0.	0.	1254.52	0.
1,5	18.2	-748.87	0.	0.	0.	2017.54
2,3	-11.6	0.	-739.88	1220.43	0.	0.
2,4	-15.9	0.	-118.62	0.	726.83	0.
2,5	-26.3	0.	328.77	0.	0.	193.78
3,4	-18.2	0.	0.	-75.52	666.89	0.
3,5	-30.2	0.	0.	1314.64	0.	-1545.45
4,5	-18.7	0.	0.	0.	4829.20	-6035.00
1,2,3	21.1	-1400.87	835.25	854.23	0.	0.
1,2,4	15.6	-1386.44	1347.28	0.	390.36	0.
1,2,5	13.5	-1463.01	1594.42	0.	0.	215.98
1,3,4	26.0	-1274.41	0.	1898.30	-367.98	0.
1,3,5	17.8	-1195.39	0.	2399.50	0.	-1546.89
1,4,5	-51.1	664.16	0.	0.	7123.71	-10360.73
2,3,4	-12.5	0.	-484.76	616.85	428.20	0.
2,3,5	-16.4	0.	-1090.38	2740.41	0.	-2069.87
2,4,5	-56.8	0.	1537.39	0.	7167.0	-12198.87
3,4,5	-36.2	0.	0.	1901.18	5547.13	-10449.23
1,2,3,4	21.5	-1409.12	792.64	974.82	-87.08	0.
1,2,3,5	16.3	-1326.64	533.25	1821.35	0.	-1290.57
1,2,4,5	-54.4	-61.11	1560.61	0.	6991.25	-11893.93
1,3,4,5	-35.8	-9.33	0.	1906.45	5516.88	-10400.69
2,3,4,5	-55.4	0.	1391.06	239.57	7035.01	-12168.42
1,2,3,4,5	-51.9	-84.22	1401.94	274.13	6773.67	-11743.80

TABLE 15

ESTIMATES OF PRECISION

FOR DUAL-CONSTITUENT MIXTURES

FOR BALL CLAY SEDIMENT

Bands Used	r	σ	$(F/F_{cr})_{.95}$	C_p	C_p/p
1	0.91	30.6	9.20	21.	10.5
2	0.93	26.5	12.96	14.	6.9
3	0.93	25.8	13.74	13.	6.3
4	0.94	25.4	14.28	12.	6.0
5	0.93	26.7	12.71	14.	7.1
1,2	0.96	21.1	12.72	6.	2.1
1,3	0.96	20.9	12.95	6.	2.1
1,4	0.95	24.0	9.57	10.	3.4
1,5	0.94	25.5	8.37	12.	4.0
2,3	0.94	26.7	7.49	14.	4.7
2,4	0.94	26.7	7.52	14.	4.6
2,5	0.93	27.9	6.80	16.	5.2
3,4	0.94	26.7	7.49	14.	4.7
3,5	0.94	26.5	7.66	14.	4.5
4,5	0.96	21.2	12.56	7.	2.2
1,2,3	0.96	21.5	8.53	8.	1.9
1,2,4	0.96	21.9	8.26	8.	2.0
1,2,5	0.96	22.3	7.92	8.	2.1
1,3,4	0.96	22.0	8.16	8.	2.0
1,3,5	0.97	21.1	8.81	7.	1.8
1,4,5	0.96	21.6	8.51	8.	1.9
2,3,4	0.94	28.2	4.70	16.	3.9
2,3,5	0.94	27.0	5.17	14.	3.5
2,4,5	0.98	15.6	16.89	2.	0.5
3,4,5	0.98	17.3	13.55	3.	0.9
1,2,3,4	0.96	23.0	5.53	10.	1.9
1,2,3,5	0.97	22.3	5.90	9.	1.8
1,2,4,5	0.98	16.7	10.97	4.	0.8
1,3,4,5	0.98	18.5	8.79	5.	1.1
2,3,4,5	0.98	16.6	10.99	4.	0.8
1,2,3,4,5	0.98	18.0	7.09	6.	1.0

TABLE 16

ESTIMATES OF J,K COEFFICIENTS

FOR DUAL-CONSTITUENT MIXTURES

FOR FELDSPAR SEDIMENT

Bands Used	J	K_1	K_2	K_3	K_4	K_5
1	31.4	95.75	0.	0.	0.	0.
2	38.2	0.	65.73	0.	0.	0.
3	40.5	0.	0.	62.15	0.	0.
4	42.1	0.	0.	0.	71.81	0.
5	40.5	0.	0.	0.	0.	115.41
1,2	-36.2	2758.13	-2342.77	0.	0.	0.
1,3	-67.9	2697.12	0.	-2383.78	0.	0.
1,4	-45.4	1783.59	0.	0.	-1961.52	0.
1,5	-58.4	2040.53	0.	0.	0.	-3191.53
2,3	-11.4	0.	3457.28	-3530.07	0.	0.
2,4	07.4	0.	1392.70	0.	-1749.51	0.
2,5	21.4	0.	776.99	0.	0.	-1326.52
3,4	28.4	0.	0.	1479.19	-1792.50	0.
3,5	50.4	0.	0.	-1081.50	0.	2048.13
4,5	41.6	0.	0.	0.	-10134.35	14467.23
1,2,3	-70.9	2552.56	587.22	-2862.81	0.	0.
1,2,4	-50.3	2538.10	-1290.86	0.	-1133.55	0.
1,2,5	-53.7	2763.20	-1613.46	0.	0.	-1368.45
1,3,4	-68.8	2800.78	0.	-2858.70	481.84	0.
1,3,5	-57.9	2697.31	0.	-3529.41	0.	2051.37
1,4,5	36.9	96.34	0.	0.	-9801.54	13839.78
2,3,4	-11.1	0.	3381.27	-3350.24	-127.58	0.
2,3,5	-10.0	0.	4141.38	-6496.74	0.	4039.96
2,4,5	72.7	0.	-1253.46	0.	-12040.46	19492.74
3,4,5	62.2	0.	0.	-2242.63	-10981.22	19674.25
1,2,3,4	-74.6	2631.57	995.69	-4018.76	834.71	0.
1,2,3,5	-61.2	2401.33	1202.50	-4833.17	0.	2629.36
1,2,4,5	40.2	824.44	-1566.70	0.	-9668.56	15378.96
1,3,4,5	13.8	1110.08	0.	-2869.59	-7382.94	13899.94
2,3,4,5	56.3	0.	430.40	-2756.74	-10520.86	19142.33
1,2,3,4,5	10.5	1094.65	288.88	-3205.94	-7123.97	13623.18

TABLE 17

ESTIMATES OF PRECISION

FOR DUAL-CONSTITUENT MIXTURES

FOR FELDSPAR SEDIMENT

Bands Used	r	σ	$(F/F_{cr})_{.95}$	C_p	C_p/p
1	0.28	44.4	0.17	23.	11.3
2	0.22	45.1	0.10	24.	11.8
3	0.20	45.3	0.08	24.	11.9
4	0.18	45.5	0.07	24.	12.0
5	0.21	45.2	0.09	24.	11.9
1,2	0.74	32.7	1.29	9.	3.0
1,3	0.83	27.1	2.36	4.	1.4
1,4	0.75	32.5	1.33	9.	3.0
1,5	0.70	34.8	1.02	11.	3.6
2,3	0.52	41.5	0.40	18.	6.0
2,4	0.46	43.3	0.28	20.	6.7
2,5	0.28	46.8	0.09	25.	8.2
3,4	0.34	45.8	0.14	23.	7.8
3,5	0.26	47.0	0.08	25.	8.3
4,5	0.82	27.7	2.23	5.	1.6
1,2,3	0.83	28.5	1.50	6.	1.5
1,2,4	0.78	32.1	1.05	9.	2.2
1,2,4	0.76	33.5	0.91	10.	2.5
1,3,4	0.83	28.5	1.50	6.	1.5
1,3,5	0.85	27.4	1.69	5.	1.3
1,4,5	0.82	29.3	1.38	7.	1.7
2,3,4	0.52	44.0	0.25	20.	5.0
2,3,5	0.62	40.8	0.40	17.	4.2
2,4,5	0.86	26.2	1.90	5.	1.1
3,4,5	0.89	24.0	2.39	3.	0.8
1,2,3,4	0.84	29.9	1.03	8.	1.5
1,2,3,5	0.86	28.3	1.20	7.	1.3
1,2,4,5	0.87	27.0	1.36	6.	1.2
1,3,4,5	0.91	23.6	1.91	4.	0.8
2,3,4,5	0.89	25.5	1.57	5.	1.0
1,2,3,4,5	0.91	25.4	1.24	6.	1.0

TABLE 18

ESTIMATES OF J,K COEFFICIENTS

FOR THREE-CONSTITUENT MIXTURES

FOR BALL CLAY SEDIMENT

Bands Used	J	K_1	K_2	K_3	K_4	K_5
1	-27.1	485.74	0.	0.	0.	0.
2	-36.1	0.	515.33	0.	0.	0.
3	-56.6	0.	0.	484.88	0.	0.
4	-29.6	0.	0.	0.	491.89	0.
5	-15.5	0.	0.	0.	0.	709.15
1,2	-22.3	633.02	-166.25	0.	0.	0.
1,3	-52.0	116.74	0.	377.49	0.	0.
1,4	-31.5	108.00	0.	0.	394.33	0.
1,5	-12.3	-79.96	0.	0.	0.	816.09
2,3	-56.4	0.	56.75	438.98	0.	0.
2,4	-34.5	0.	98.06	0.	415.48	0.
2,5	-13.2	0.	-34.07	0.	0.	748.85
3,4	-22.3	0.	0.	-120.00	610.93	0.
3,5	-2.3	0.	0.	-144.38	0.	913.15
4,5	-15.7	0.	0.	0.	5.18	701.79
1,2,3	-48.6	214.20	-103.15	371.27	0.	0.
1,2,4	-33.8	33.60	71.86	0.	405.54	0.
1,2,5	-13.8	-147.41	62.61	0.	0.	833.39
1,3,4	-9.4	186.46	0.	-388.60	708.97	0.
1,3,5	1.5	-83.90	0.	-150.11	0.	1033.46
1,4,5	-.5	-172.20	0.	0.	-260.28	1308.85
2,3,4	-4.1	0.	234.43	-613.65	918.00	0.
2,3,5	-1.1	0.	-26.48	-138.14	0.	935.17
2,4,5	-8.1	0.	-60.72	0.	-104.93	928.76
3,4,5	-.4	0.	0.	-227.50	180.35	774.65
1,2,3,4	-4.3	-59.46	285.79	-636.14	954.00	0.
1,2,3,5	2.0	-200.93	107.82	-183.50	0.	1111.59
1,2,4,5	-2.2	-215.07	44.75	0.	-245.23	1292.72
1,3,4,5	1.9	-105.77	0.	-122.21	-63.78	1113.80
2,3,4,5	-3.0	0.	195.62	-552.38	785.25	147.37
1,2,3,4,5	-.4	-131.38	211.89	-448.60	532.29	516.50

TABLE 19

ESTIMATES OF PRECISION

FOR THREE-CONSTITUENT MIXTURES

FOR BALL CLAY SEDIMENT

Bands Used	r	σ	$(F/F_{cr})_{.95}$	C_p	C_p/p
1	0.95	25.1	17.1	116.	58.2
2	0.91	32.0	9.7	194.	97.2
3	0.97	17.7	36.26	54.	27.1
4	0.99	12.7	72.6	24.	12.0
5	0.99	8.4	169.5	6.	2.9
1,2	0.95	25.9	9.4	114.	37.9
1,3	0.98	17.8	21.2	50.	16.7
1,4	0.99	11.8	49.1	19.	6.3
1,5	0.99	8.1	104.7	6.	1.9
2,3	0.97	18.4	19.6	54.	18.1
2,4	0.99	11.7	50.4	18.	6.7
2,5	0.99	8.6	93.0	7.	2.4
3,4	0.99	13.1	39.6	25.	8.2
3,5	0.99	8.0	109.6	5.	1.8
4,5	0.99	8.8	88.8	8.	2.6
1,2,3	0.98	18.5	13.6	50.	12.6
1,2,4	0.99	12.3	31.5	20.	5.0
1,2,5	0.99	8.4	68.6	7.	1.8
1,3,4	0.99	10.0	48.2	12.	3.0
1,3,5	0.99	7.5	85.5	5.	1.2
1,4,5	0.99	7.8	80.9	5.	1.4
2,3,4	0.99	6.8	105.7	3.	0.8
2,3,5	0.99	8.3	70.3	7.	1.7
2,4,5	0.99	9.0	59.7	9.	2.2
3,4,5	0.99	7.8	79.2	6.	1.4
1,2,3,4	0.99	7.1	72.4	5.	1.0
1,2,3,5	0.99	7.3	68.4	5.	1.1
1,2,4,5	0.99	8.2	54.2	7.	1.4
1,3,4,5	0.99	8.0	55.7	7.	1.4
2,3,4,5	0.99	7.2	69.7	5.	1.0
1,2,3,4,5	0.99	7.1	53.5	6.	1.0

TABLE 20

ESTIMATES OF J,K COEFFICIENTS

FOR THREE-CONSTITUENT MIXTURES

FOR FELDSPAR SEDIMENT

Bands Used	J	K_1	K_2	K_3	K_4	K_5
1	15.2	356.39	0.	0.	0.	0.
2	9.8	0.	372.46	0.	0.	0.
3	-8.0	0.	0.	361.40	0.	0.
4	14.6	0.	0.	0.	355.23	0.
5	25.9	0.	0.	0.	0.	503.14
1,2	22.4	572.63	-244.10	0.	0.	0.
1,3	-6.8	30.92	0.	332.95	0.	0.
1,4	12.4	119.53	0.	0.	247.26	0.
1,5	21.8	104.68	0.	0.	0.	363.12
2,3	-8.1	0.	-32.75	387.98	0.	0.
2,4	11.0	0.	72.20	0.	298.97	0.
2,5	24.4	0.	22.84	0.	0.	476.53
3,4	-18.2	0.	0.	545.13	-185.57	0.
3,5	-24.9	0.	0.	557.80	0.	-285.00
4,5	13.4	0.	0.	0.	398.90	-62.97
1,2,3	-.5	209.92	-189.45	321.54	0.	0.
1,2,4	15.8	232.27	-108.89	0.	230.27	0.
1,2,5	25.6	273.00	-156.23	0.	0.	319.96
1,3,4	-17.5	13.36	0.	525.88	-178.55	0.
1,3,5	-30.4	119.53	0.	565.97	0.	-456.42
1,4,5	-34.5	542.32	0.	0.	1234.98	-1974.86
2,3,4	-25.5	0.	-91.99	738.84	-306.07	0.
2,3,5	-24.6	0.	-7.97	559.68	0.	-278.37
2,4,5	-15.2	0.	229.90	0.	815.83	-922.44
3,4,5	-25.4	0.	0.	579.64	-47.38	-248.62
1,2,3,4	-24.8	360.29	-403.18	875.10	-524.22	0.
1,2,3,5	-31.8	467.00	-320.10	665.10	0.	-688.39
1,2,4,5	-31.8	607.46	-67.98	0.	1212.11	-1950.36
1,3,4,5	-36.1	495.23	0.	86.62	1095.69	-1836.62
2,3,4,5	-23.2	0.	-170.47	862.74	-574.50	298.00
1,2,3,4,5	-33.7	523.68	-235.30	449.07	433.77	-1173.33

TABLE 21

ESTIMATES OF PRECISION

FOR THREE-CONSTITUENT MIXTURES

FOR FELDSPAR SEDIMENT

Bands Used	r	σ	$(F/F_{cr})_{.95}$	C_p	Cp/p
1	0.88	28.9	6.95	3.	1.7
2	0.84	33.6	4.63	7.	3.7
3	0.92	23.8	11.17	0.	0.1
4	0.90	26.1	8.99	1.	0.6
5	0.90	27.2	8.10	2.	1.1
1,2	0.89	29.5	3.95	5.	1.6
1,3	0.92	25.1	5.88	2.	0.6
1,4	0.91	26.6	5.10	3.	0.9
1,5	0.90	28.3	4.38	4.	1.3
2,3	0.92	25.1	5.89	2.	0.6
2,4	0.91	27.1	4.89	3.	1.0
2,5	0.90	28.7	4.25	4.	1.4
3,4	0.92	24.8	6.08	2.	0.5
3,5	0.92	24.6	6.17	1.	0.5
4,5	0.90	27.5	4.71	3.	1.1
1,2,3	0.93	25.9	3.89	3.	0.8
1,2,4	0.91	28.0	3.22	5.	1.1
1,2,5	0.90	29.6	2.81	6.	1.3
1,3,4	0.92	26.3	3.75	4.	0.9
1,3,5	0.93	25.5	4.03	3.	0.8
1,4,5	0.94	24.0	4.64	2.	0.6
2,3,4	0.93	25.9	3.89	3.	0.8
2,3,5	0.92	26.1	3.83	3.	0.9
2,4,5	0.92	27.4	3.38	4.	1.1
3,4,5	0.92	26.0	3.83	3.	0.9
1,2,3,4	0.94	25.7	2.98	4.	1.1
1,2,3,5	0.94	25.2	3.13	4.	0.8
1,2,4,5	0.94	25.5	3.04	4.	0.8
1,3,4,5	0.94	25.6	3.02	4.	0.9
2,3,4,5	0.93	27.6	2.54	5.	1.1
1,2,3,4,5	0.94	27.1	2.04	6.	1.0

TABLE 22

ESTIMATES OF J,K COEFFICIENTS

FOR THREE-CONSTITUENT MIXTURES

FOR RHODAMINE WT DYE

Bands Used	J	K_1	K_2	K_3	K_4	K_5
1	2.565	-1.077	0.	0.	0.	0.
2	2.615	0.	-1.281	0.	0.	0.
3	2.336	0.	0.	0.002	0.	0.
4	2.329	0.	0.	0.	0.035	0.
5	2.404	0.	0.	0.	0.	-0.525
1,2	2.642	-1.252	-2.629	0.	0.	0.
1,3	1.916	-10.706	0.	9.851	0.	0.
1,4	2.482	-8.242	0.	0.	7.480	0.
1,5	2.793	-9.790	0.	0.	0.	12.569
2,3	2.305	0.	-8.277	6.697	0.	0.
2,4	2.634	0.	-6.052	0.	4.751	0.
2,5	2.818	0.	-6.160	0.	0.	6.651
3,4	2.441	0.	0.	-1.844	1.865	0.
3,5	1.144	0.	0.	13.816	0.	-20.045
4,5	1.609	0.	0.	0.	25.277	-36.396
1,2,3	1.948	-9.795	-0.965	9.793	0.	0.
1,2,4	2.421	-10.251	1.940	0.	7.783	0.
1,2,5	2.772	-10.749	0.890	0.	0.	12.815
1,3,4	1.677	-11.097	0.	14.141	-3.970	0.
1,3,5	1.579	-9.444	0.	13.170	0.	-6.502
1,4,5	1.771	-1.835	0.	0.	22.448	-29.928
2,3,4	1.621	0.	-10.604	20.486	-12.025	0.
2,3,5	1.465	0.	-7.012	15.467	0.	-14.211
2,4,5	1.550	0.	0.472	0.	26.133	-38.161
3,4,5	1.384	0.	0.	3.356	22.693	-37.471
1,2,3,4	1.605	-7.679	-3.972	17.582	-7.376	0.
1,2,3,5	1.568	-6.677	-2.549	13.960	0.	-8.349
1,2,4,5	1.668	-4.314	2.588	0.	23.318	-30.861
1,3,4,5	1.556	-7.974	0.	11.295	4.287	-11.902
2,3,4,5	1.446	0.	-4.733	11.217	8.057	-22.294
1,2,3,4,5	1.596	-7.514	-3.803	17.153	-6.411	-1.181

TABLE 23

ESTIMATES OF PRECISION

FOR THREE-CONSTITUENT MIXTURES

FOR RHODAMINE WT DYE

Bands Used	r	σ	$(F/F_{cr})_{.95}$	C_p	C_p/p
1	0.31	0.51	0.21	263.	131.5
2	0.33	0.50	0.24	258.	129.2
3	0.	0.53	0.	291.	145.4
4	0.01	0.53	0.	291.	145.4
5	0.11	0.53	0.02	287.	143.7
1,2	0.34	0.53	0.14	259.	86.2
1,3	0.96	0.15	13.28	16.	5.3
1,4	0.86	0.29	2.92	73.	24.5
1,5	0.76	0.37	1.41	122.	40.7
2,3	0.84	0.31	2.49	83.	27.8
2,4	0.73	0.39	1.17	136.	45.2
2,5	0.61	0.44	0.64	181.	60.2
3,4	0.07	0.56	0.	291.	97.1
3,5	0.66	0.42	0.83	161.	53.8
4,5	0.93	0.20	7.03	33.	11.0
1,2,3	0.96	0.16	8.59	17.	4.3
1,2,4	0.86	0.30	1.91	72.	18.1
1,2,5	0.76	0.39	0.88	123.	30.9
1,3,4	0.97	0.13	12.17	11.	2.8
1,3,5	0.98	0.12	15.59	8.	2.0
1,4,5	0.94	0.21	4.73	32.	8.1
2,3,4	0.93	0.22	4.16	37.	9.2
2,3,5	0.95	0.18	6.26	24.	6.1
2,4,5	0.93	0.21	4.41	35.	8.7
3,4,5	0.94	0.20	5.08	30.	7.5
1,2,3,4	0.99	0.09	20.64	4.	0.8
1,2,3,5	0.99	0.10	17.71	5.	1.0
1,2,4,5	0.95	0.20	3.69	29.	5.8
1,3,4,5	0.98	0.12	11.05	9.	1.8
2,3,4,5	0.96	0.19	4.42	24.	4.8
1,2,3,4,5	0.99	0.10	13.34	6.	1.0

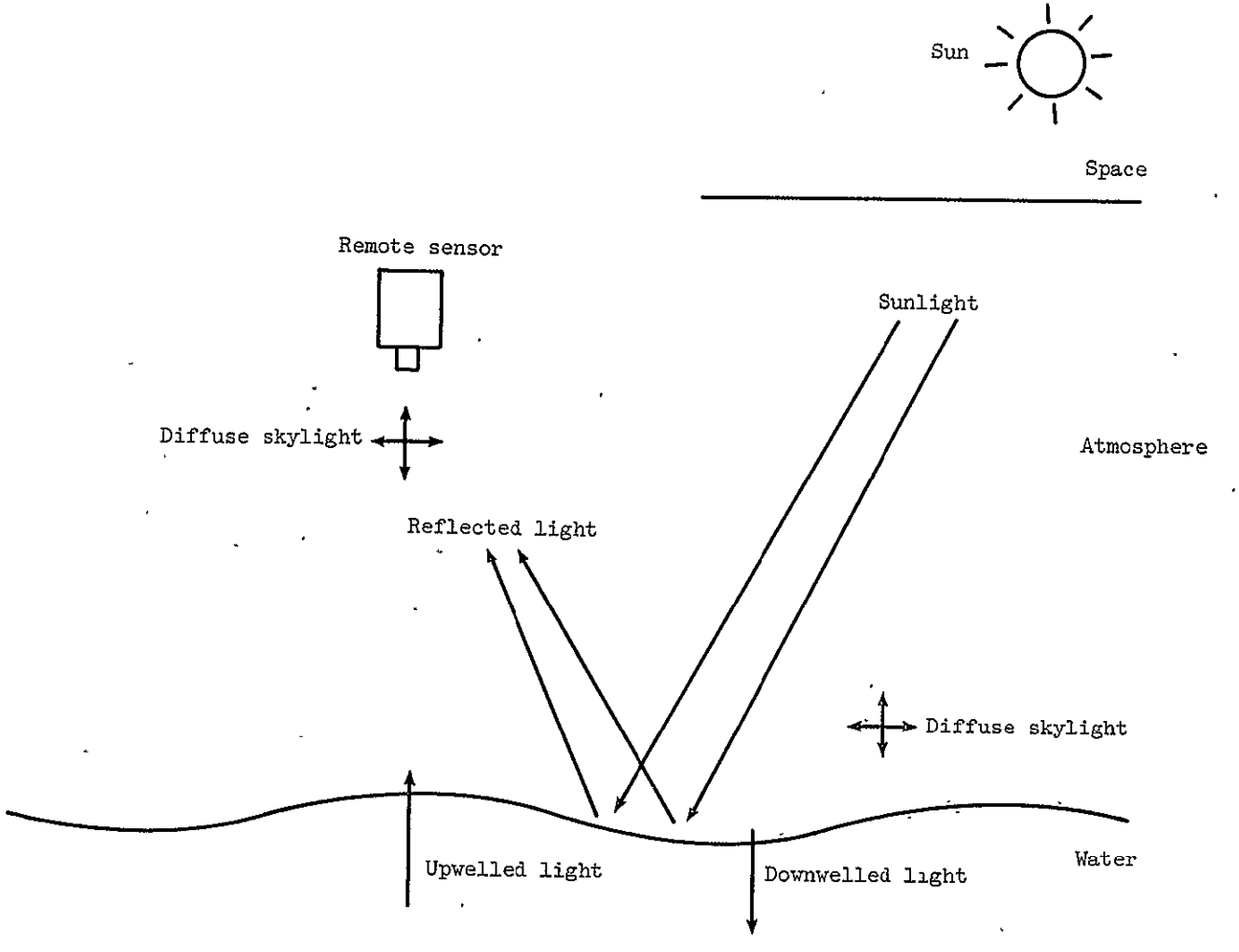

Figure 1.- Optical processes involved in passive remote sensing of water parameters.

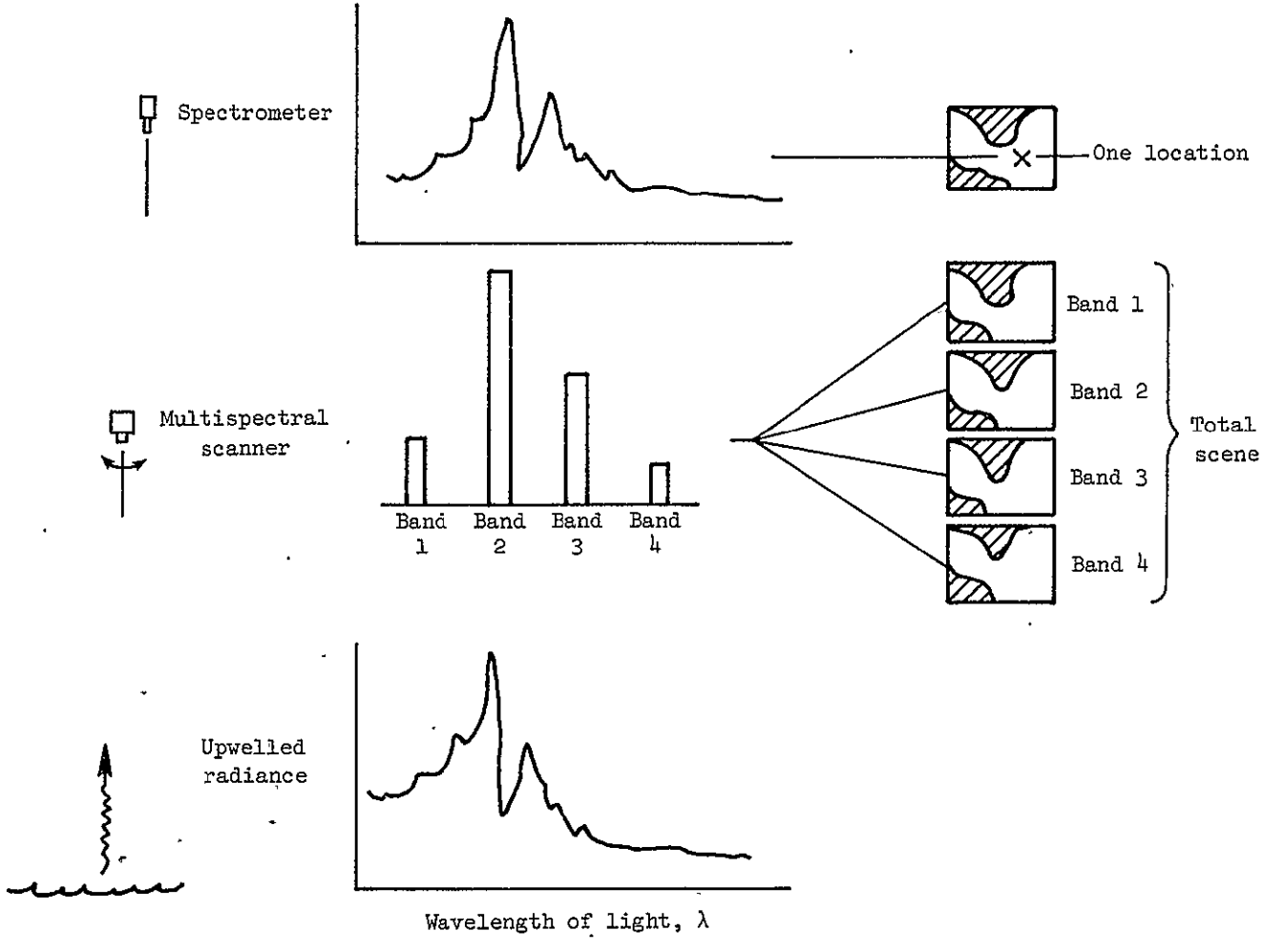

Figure 2.- Spectroradiometric measurement systems.

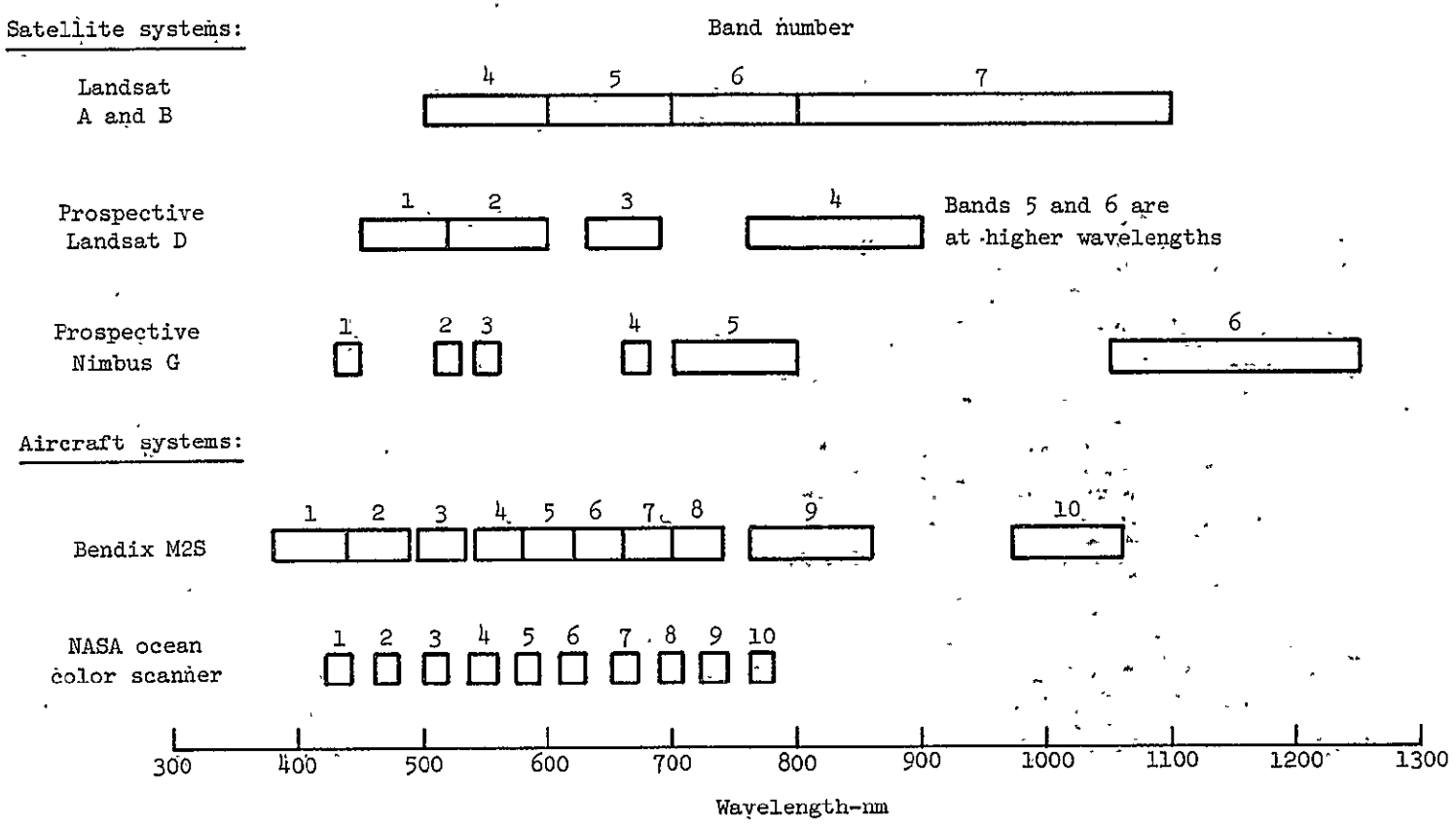

Figure 3.- Typical multispcetral scanner measurement ranges.

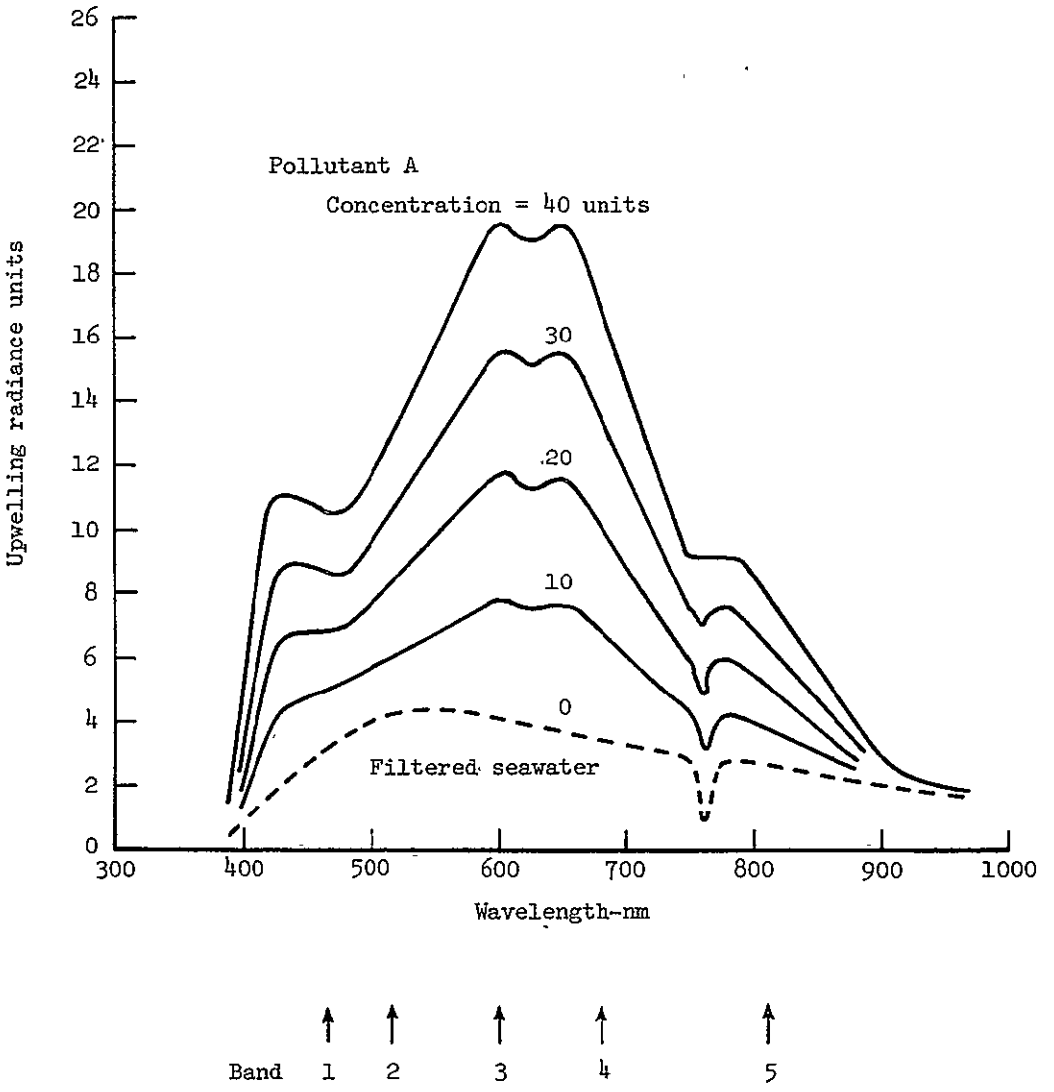

Figure 4.- Hypothetical radiance spectra for various pollutant A concentrations.

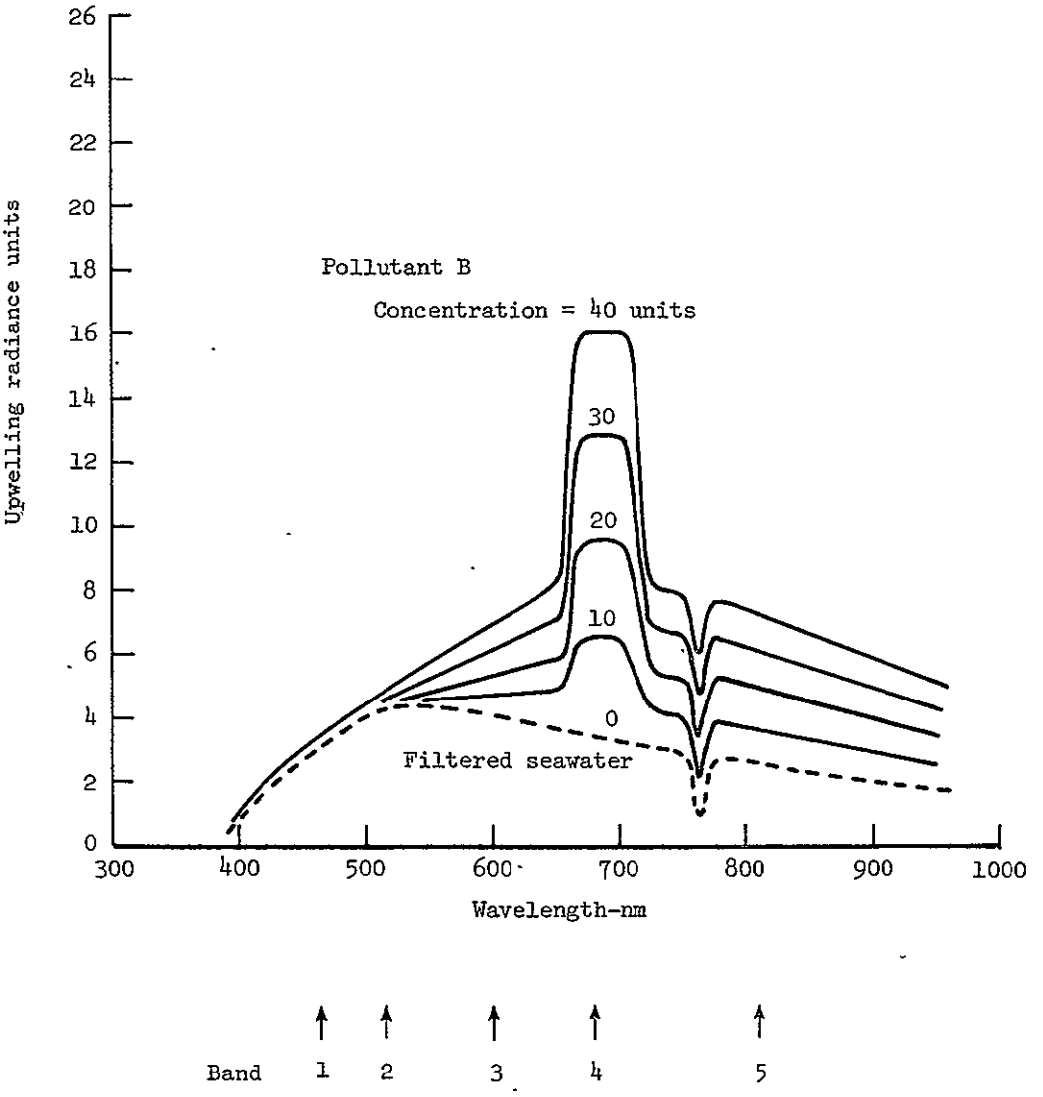

Figure 5.- Hypothetical radiance spectra for pollutant B.

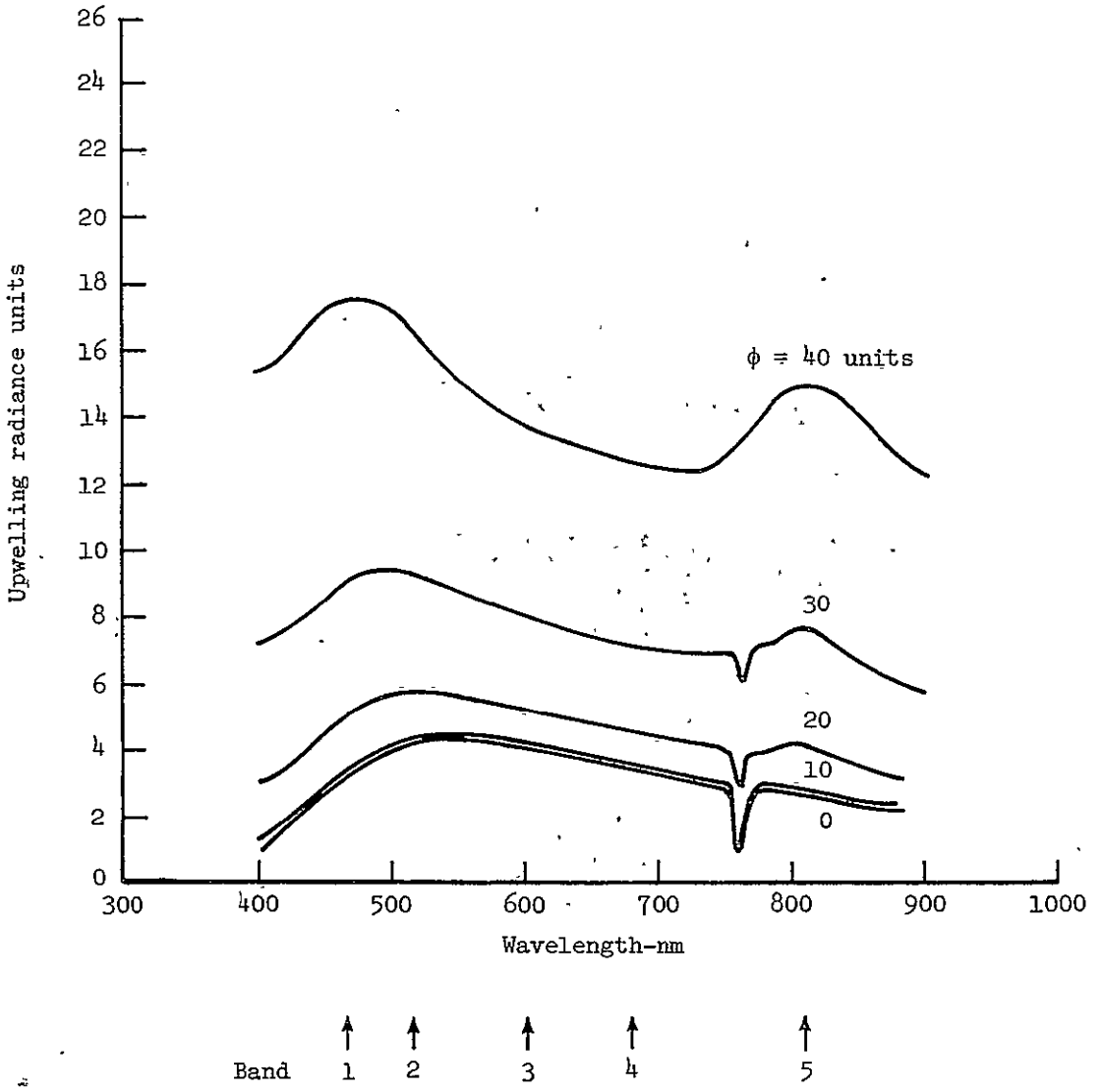

Figure 6.- Hypothetical radiance spectra for surface reflection.

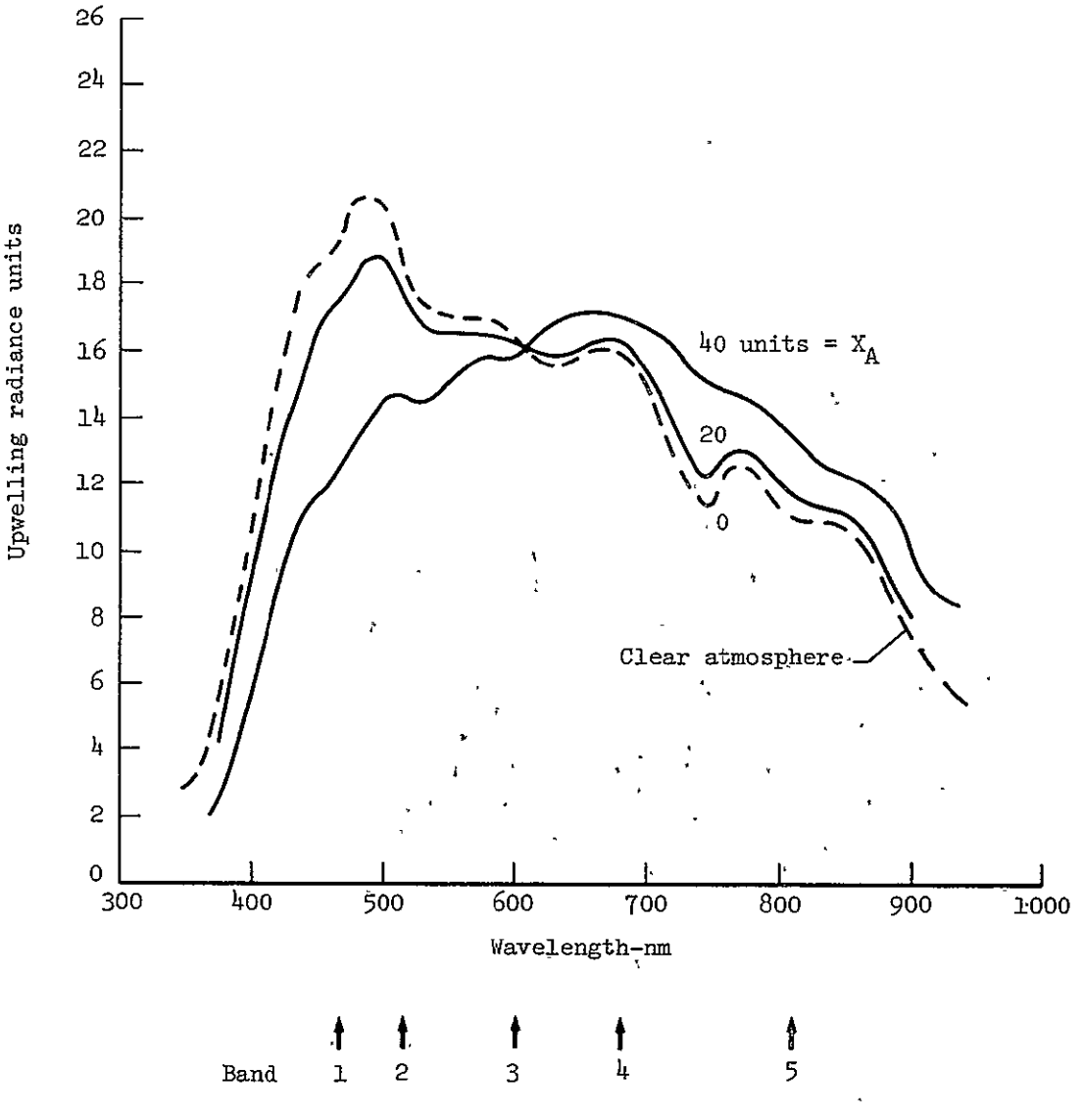

Figure 7.- Hypothetical radiance spectra for atmosphere.

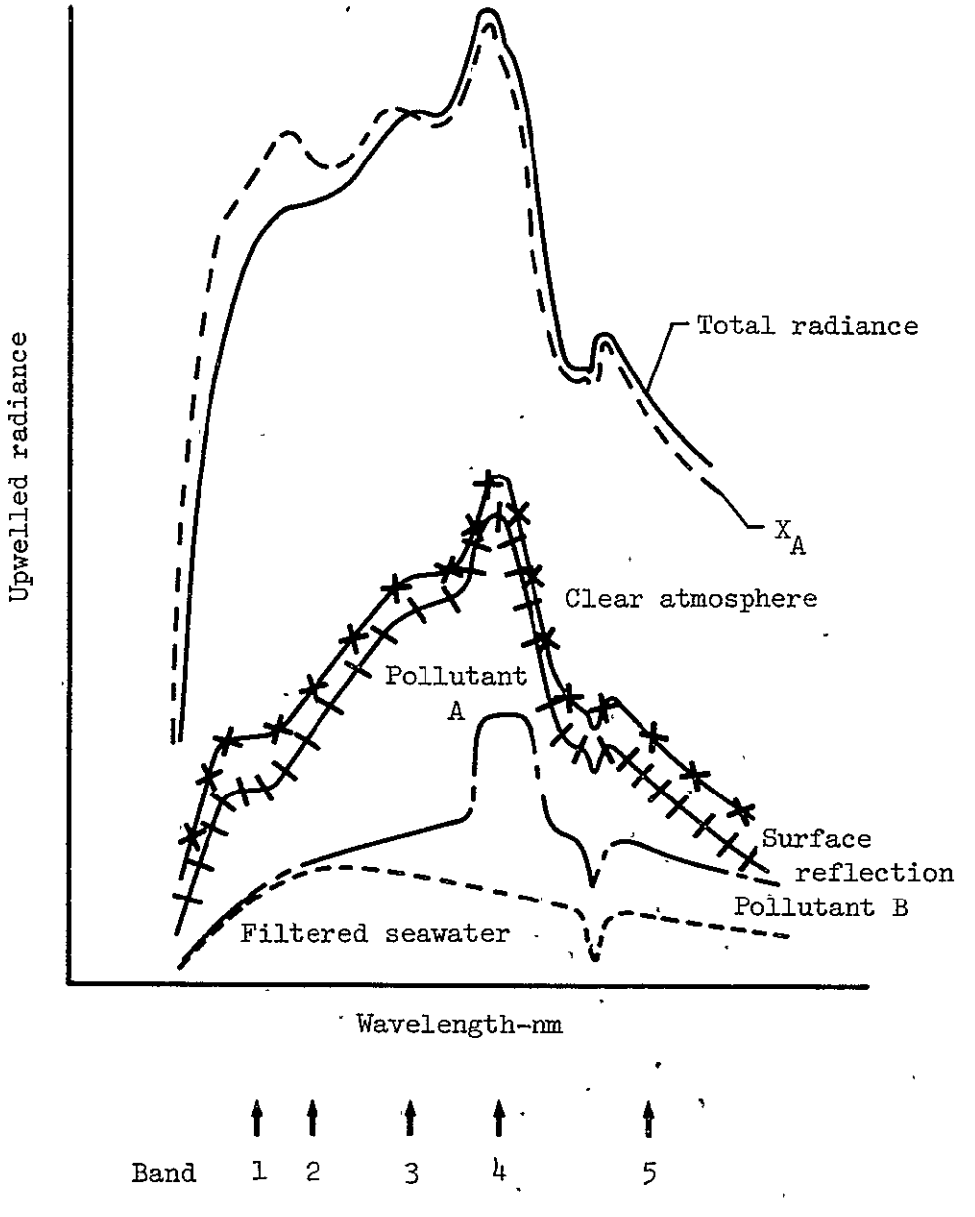

Figure 8.- Components of upwelled radiance for ground truth location 1.

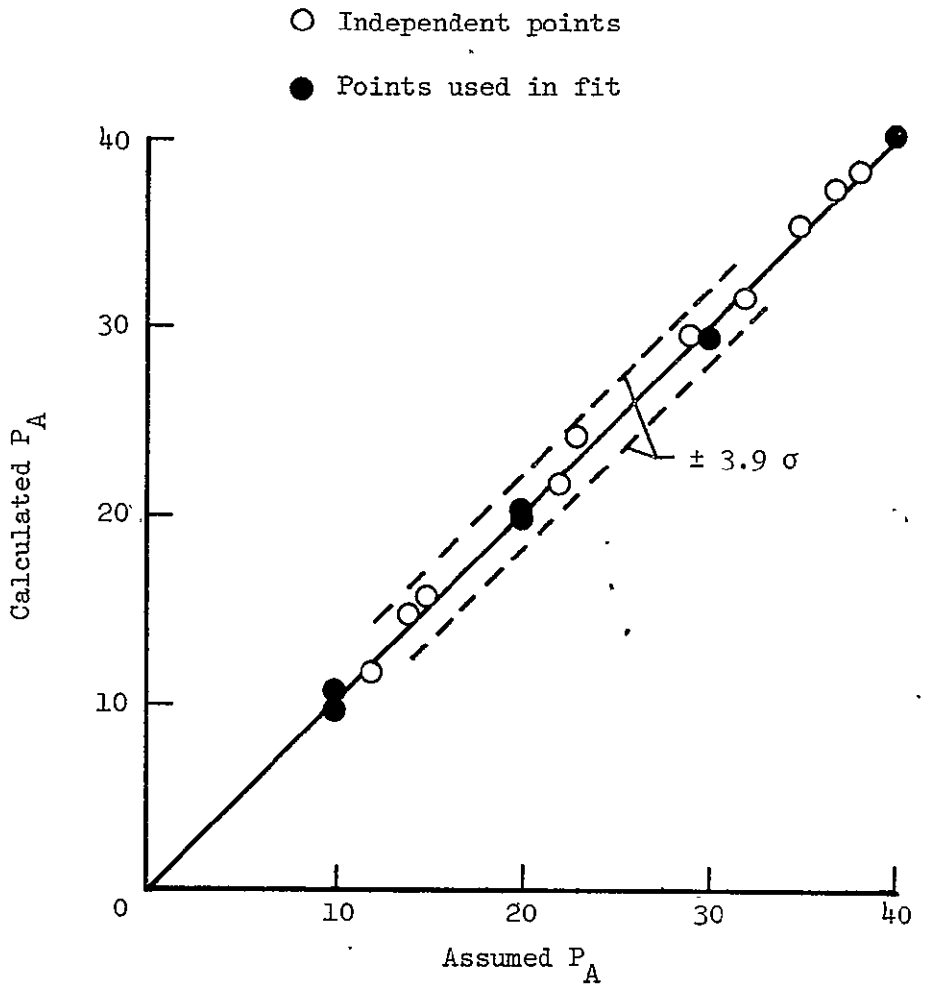

Figure 9.- Comparison of calculated and assumed P_A values for homogeneous test case.

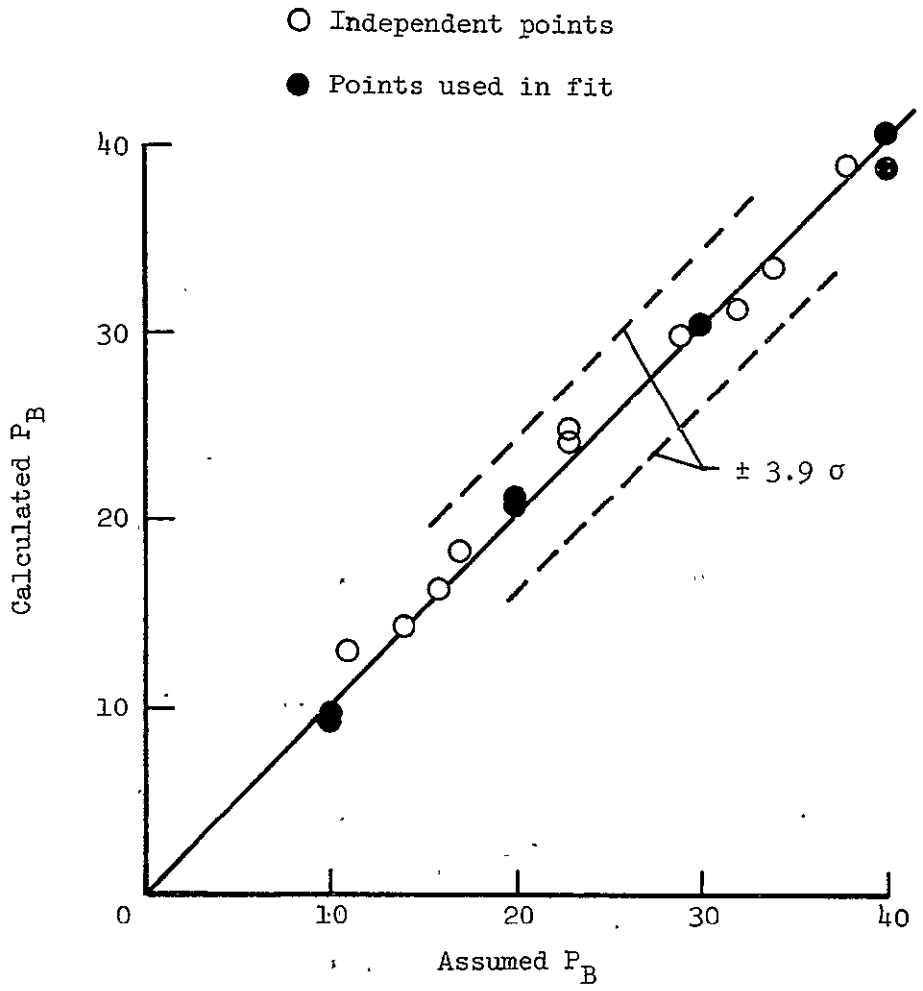

Figure 10.- Comparison of calculated and assumed P_B values for homogeneous test case.

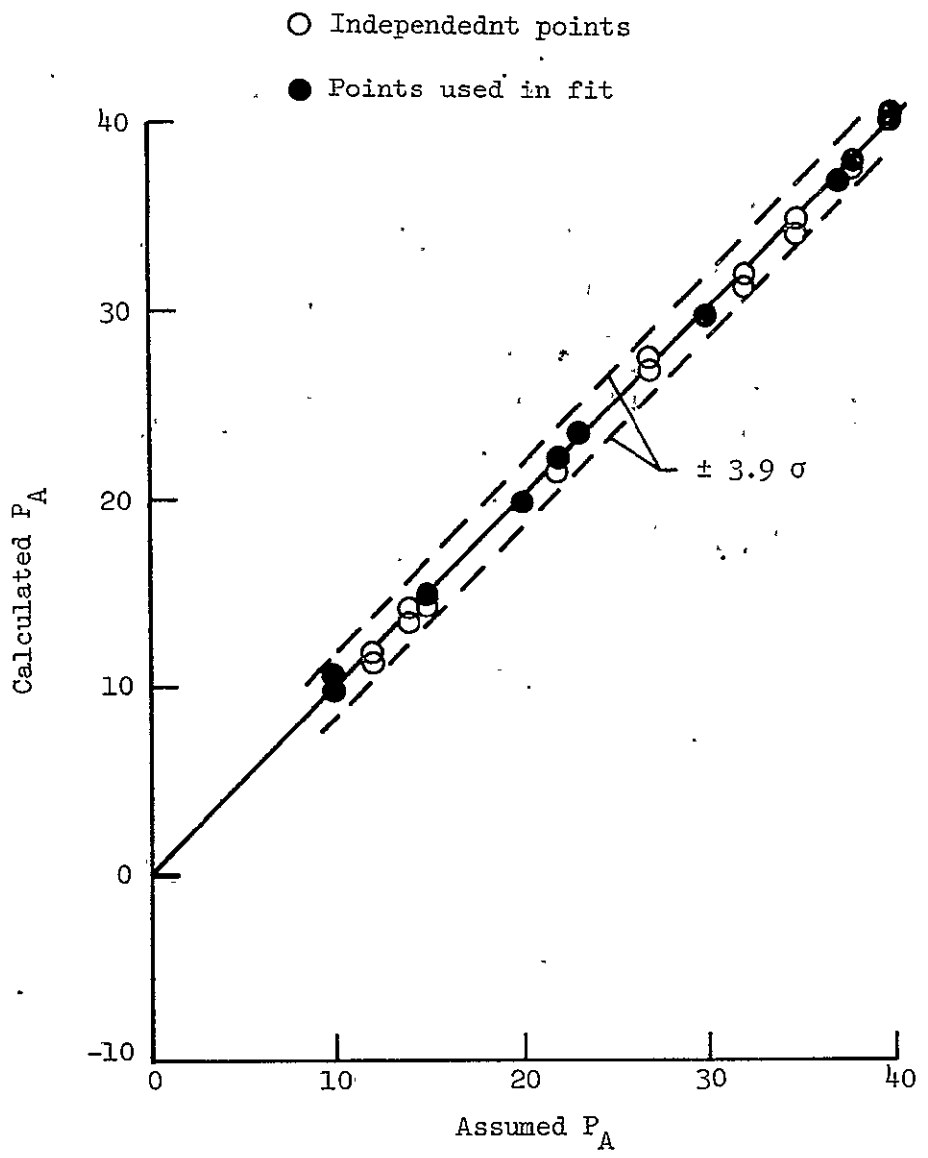

Figure 11.- Comparison of calculated and assumed P_A values for non-homogeneous test case.

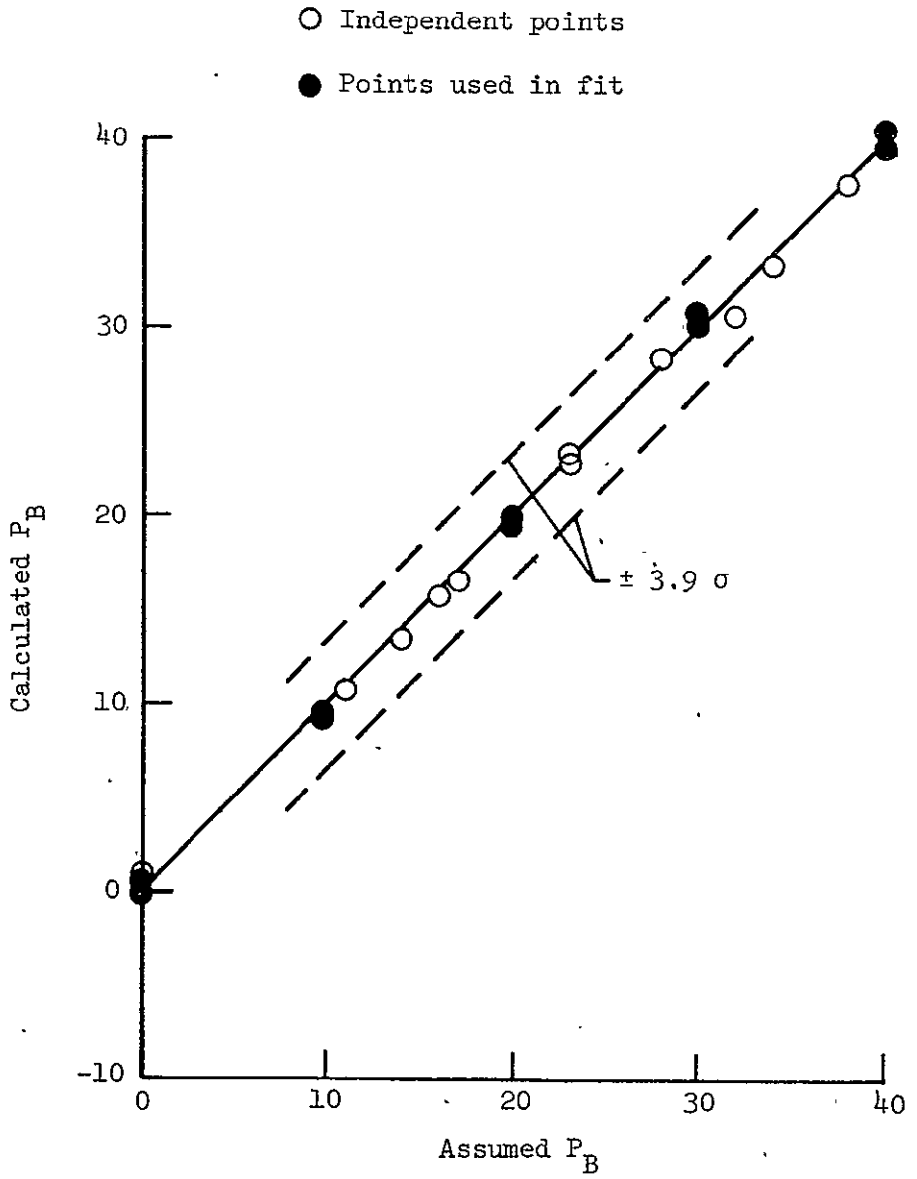

Figure 12.- Comparison of calculated and assumed P_B values for non-homogeneous test case.

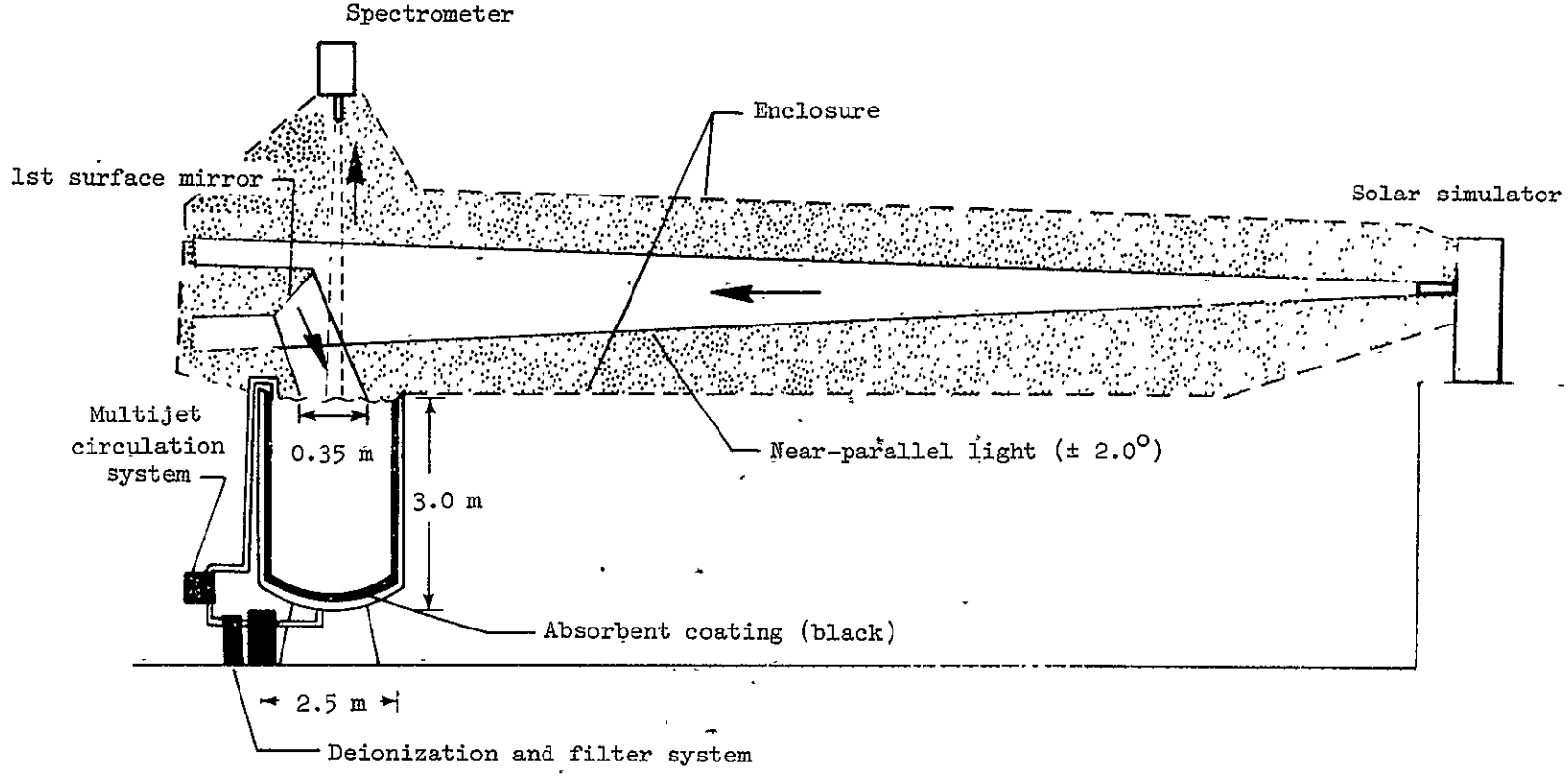

Figure 13.- Laboratory set-up.

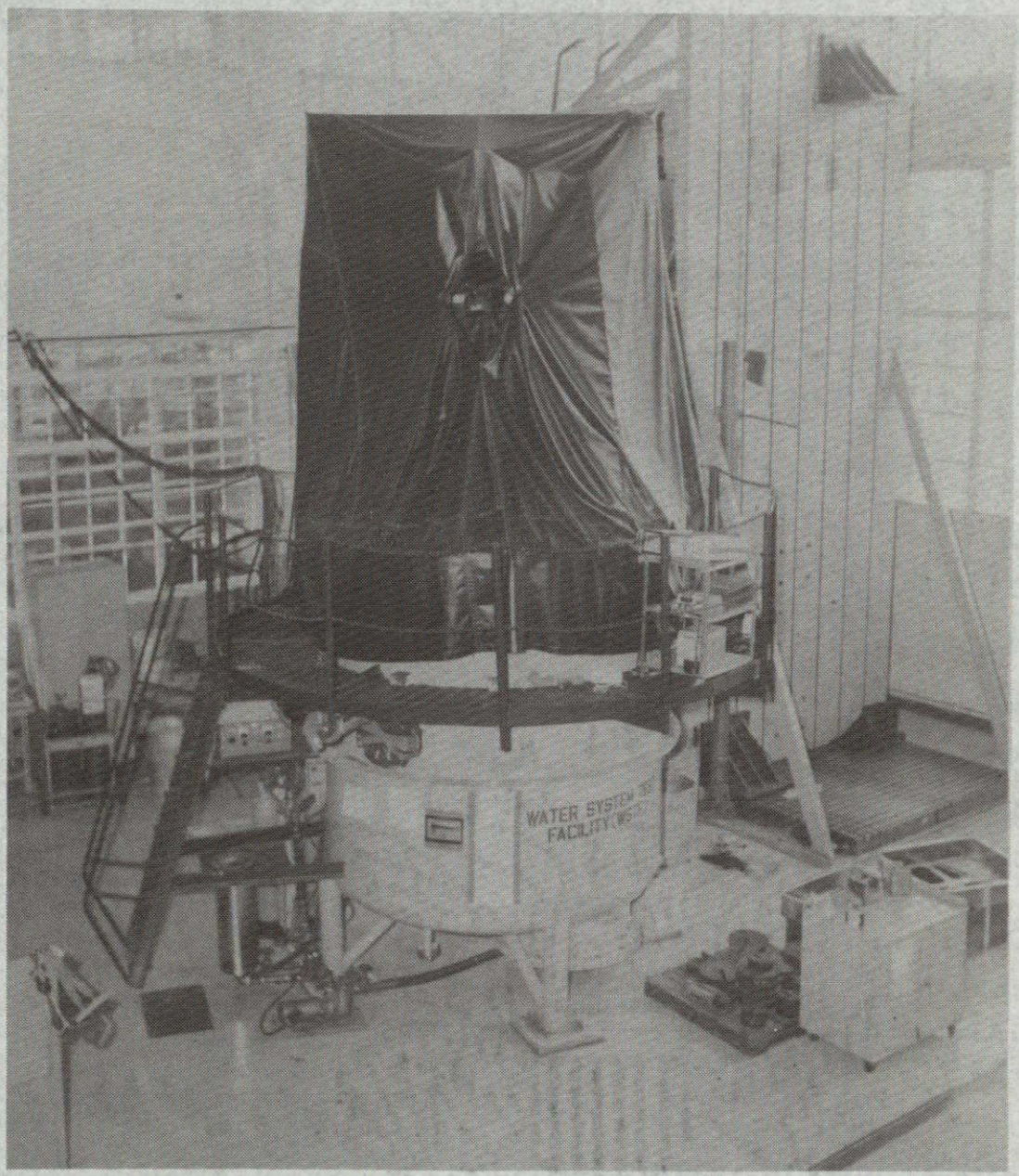

Figure 14.- View of tank and partial enclosure from solar simulator.

Figure 15.- View of solar simulator.

"Page missing from available version"

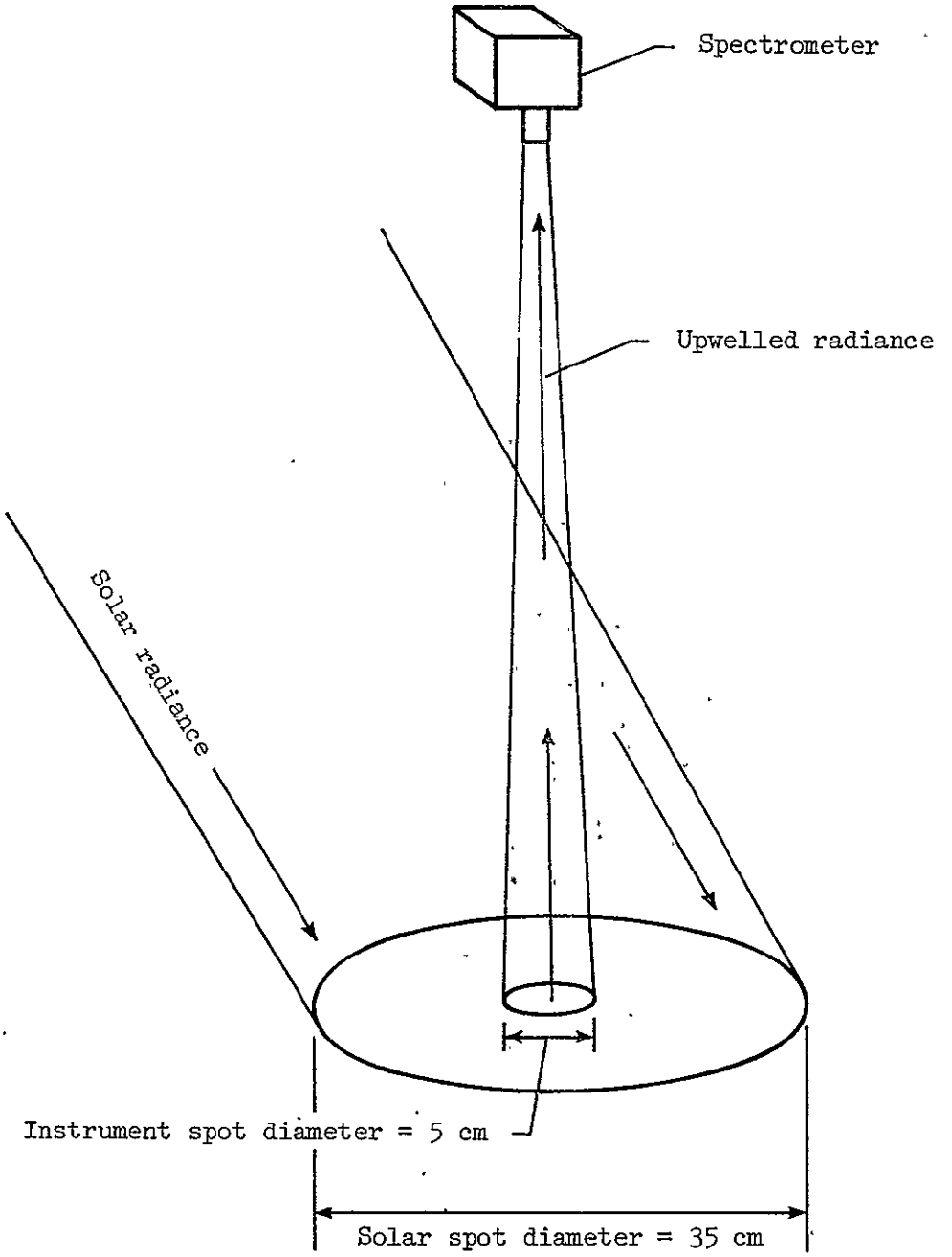

Figure 17.- Illumination geometry on water surface.

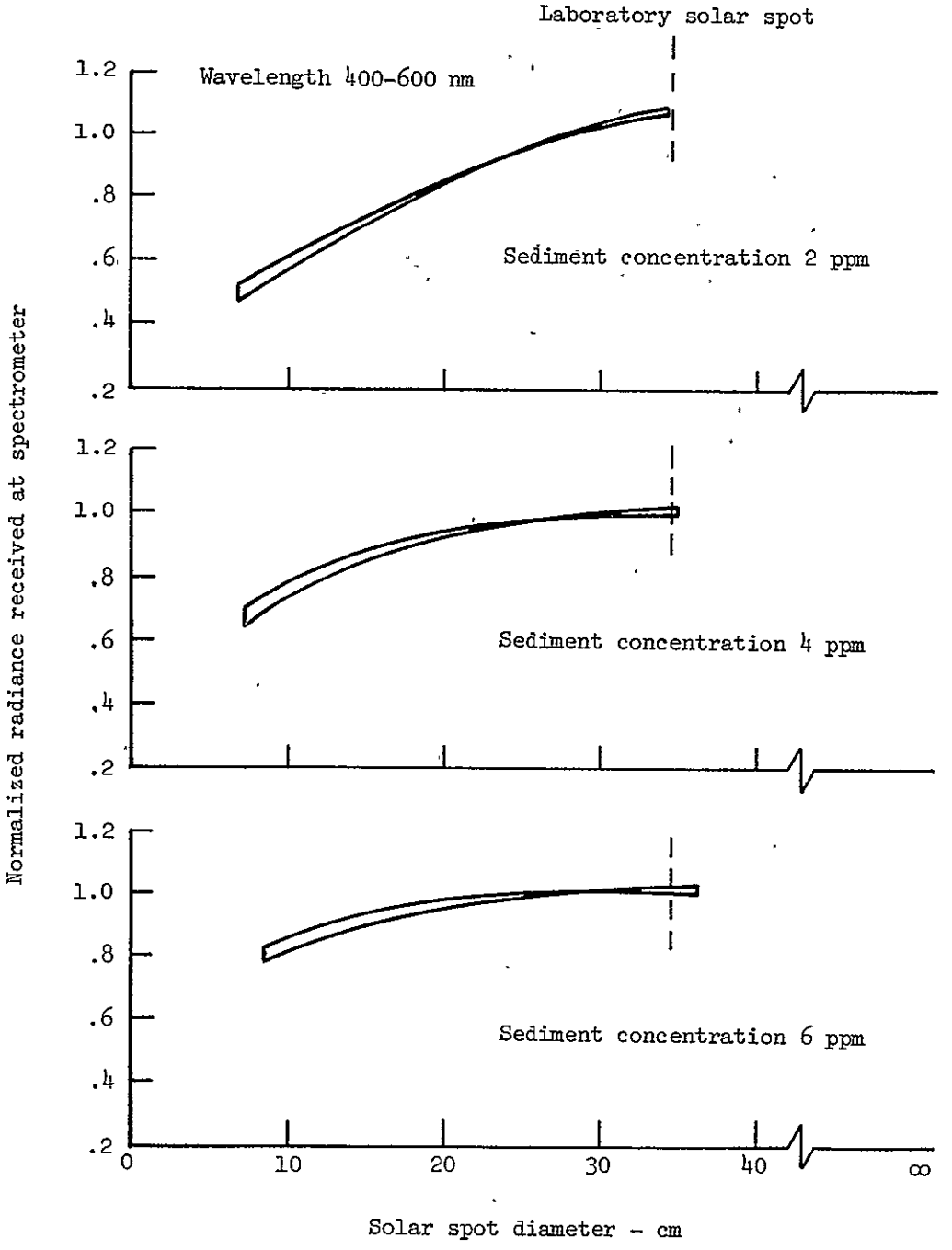

Figure 18.- Results from optical modeling study.

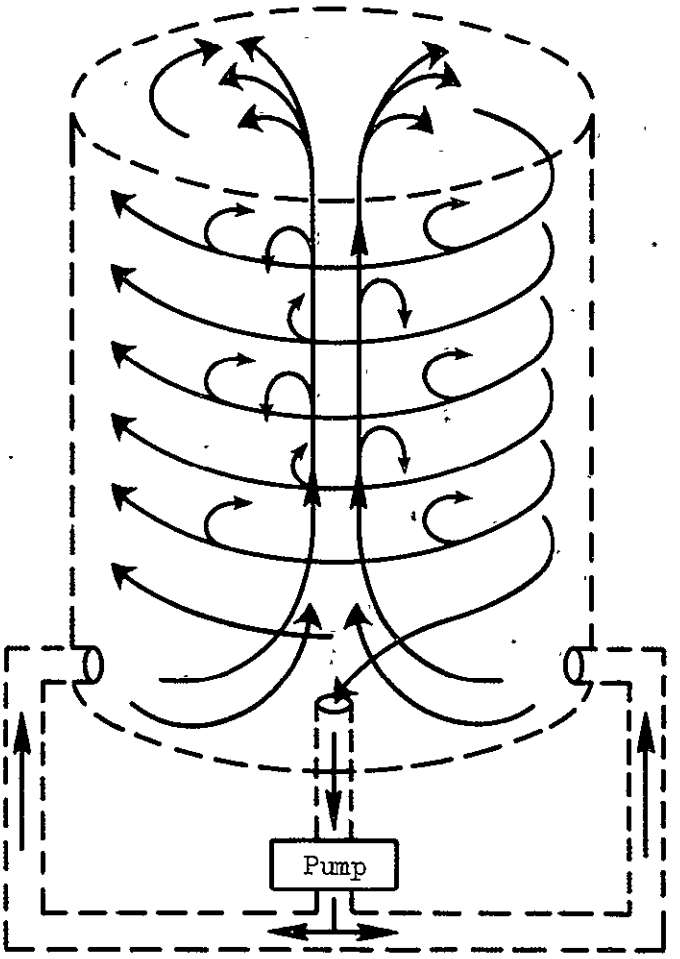

Figure 19.- Schematic of tank circulation system.

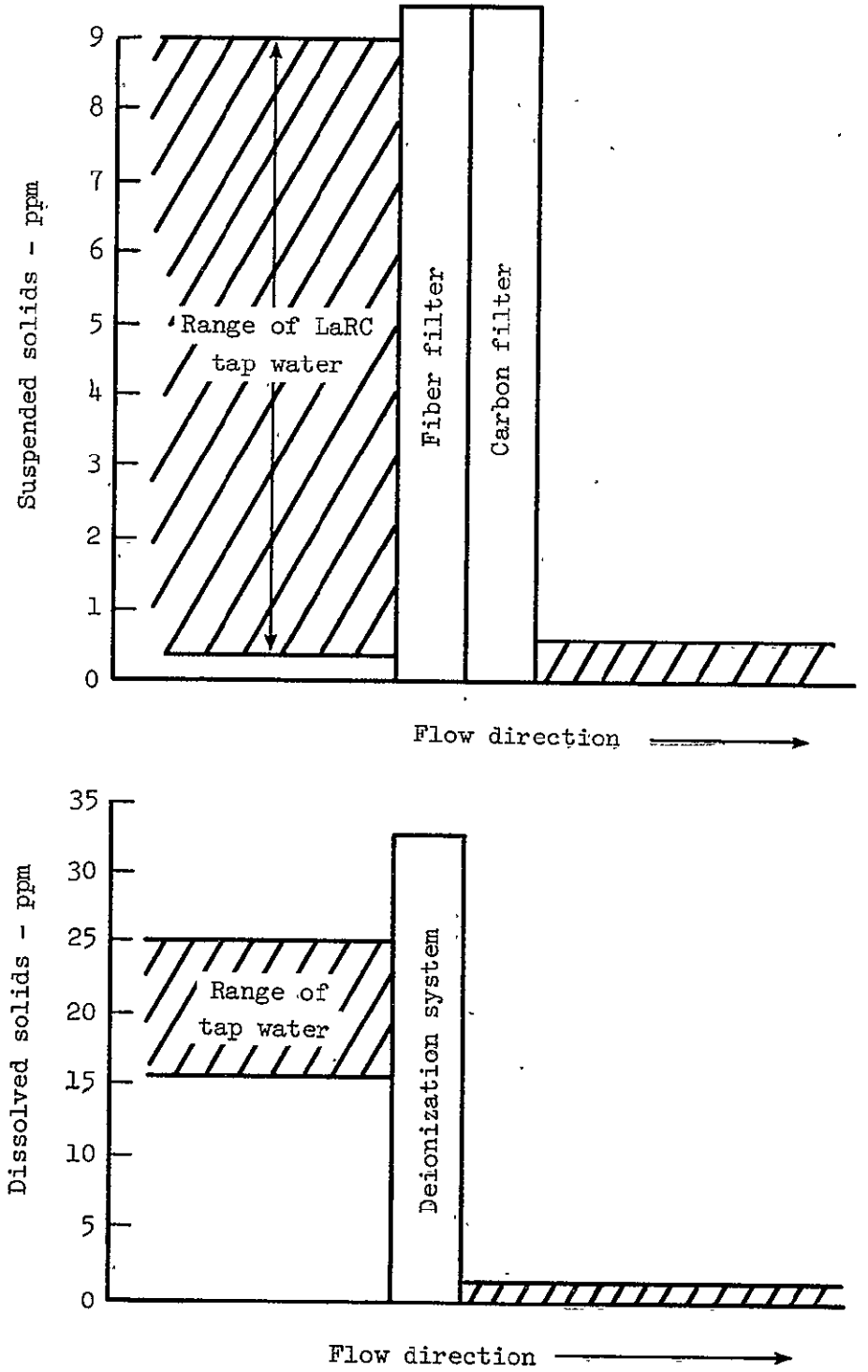

Figure 20.- Performance of deionization and filter system.

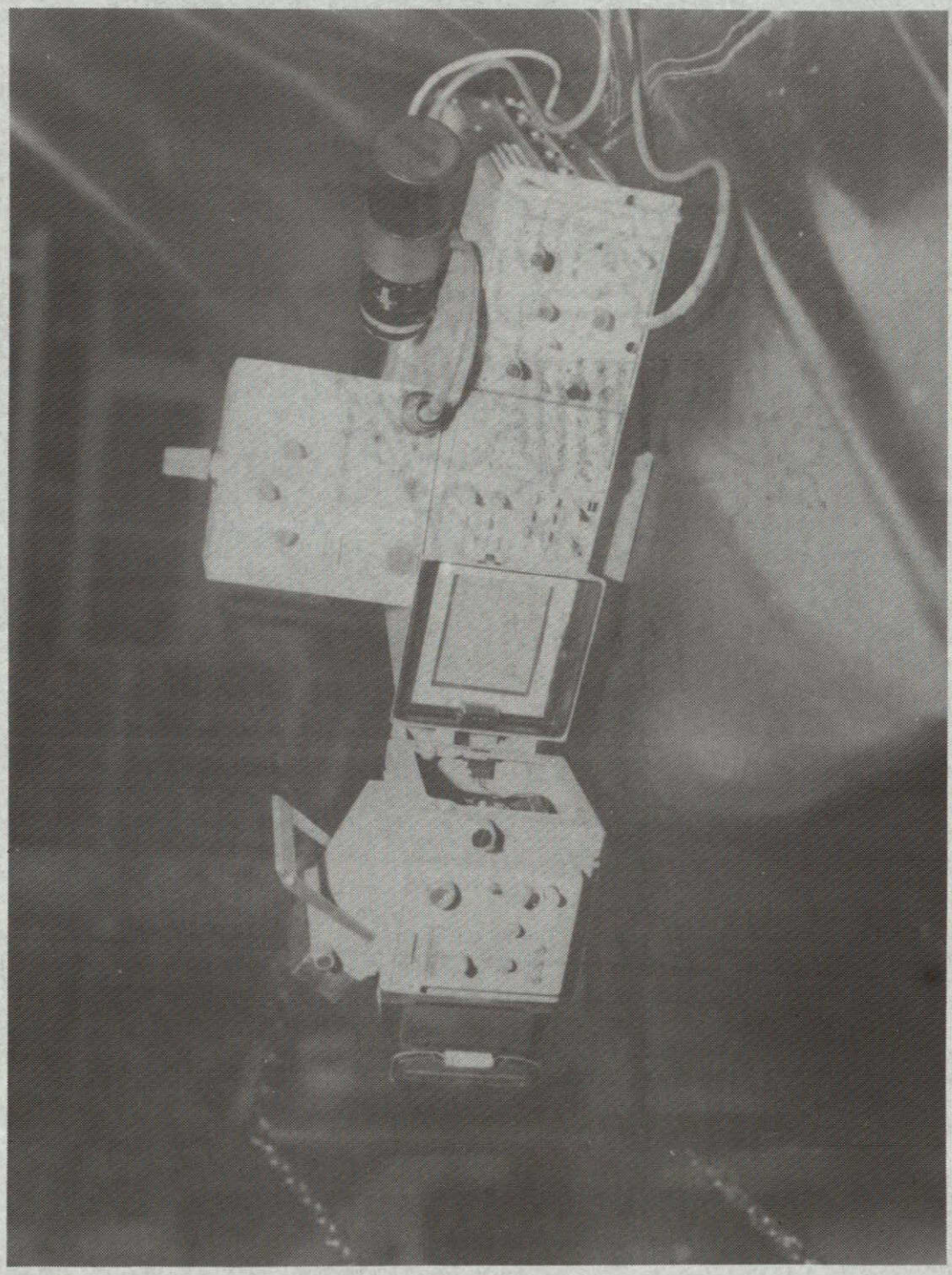

Figure 21.- View of spectrometer system.

"Page missing from available version"

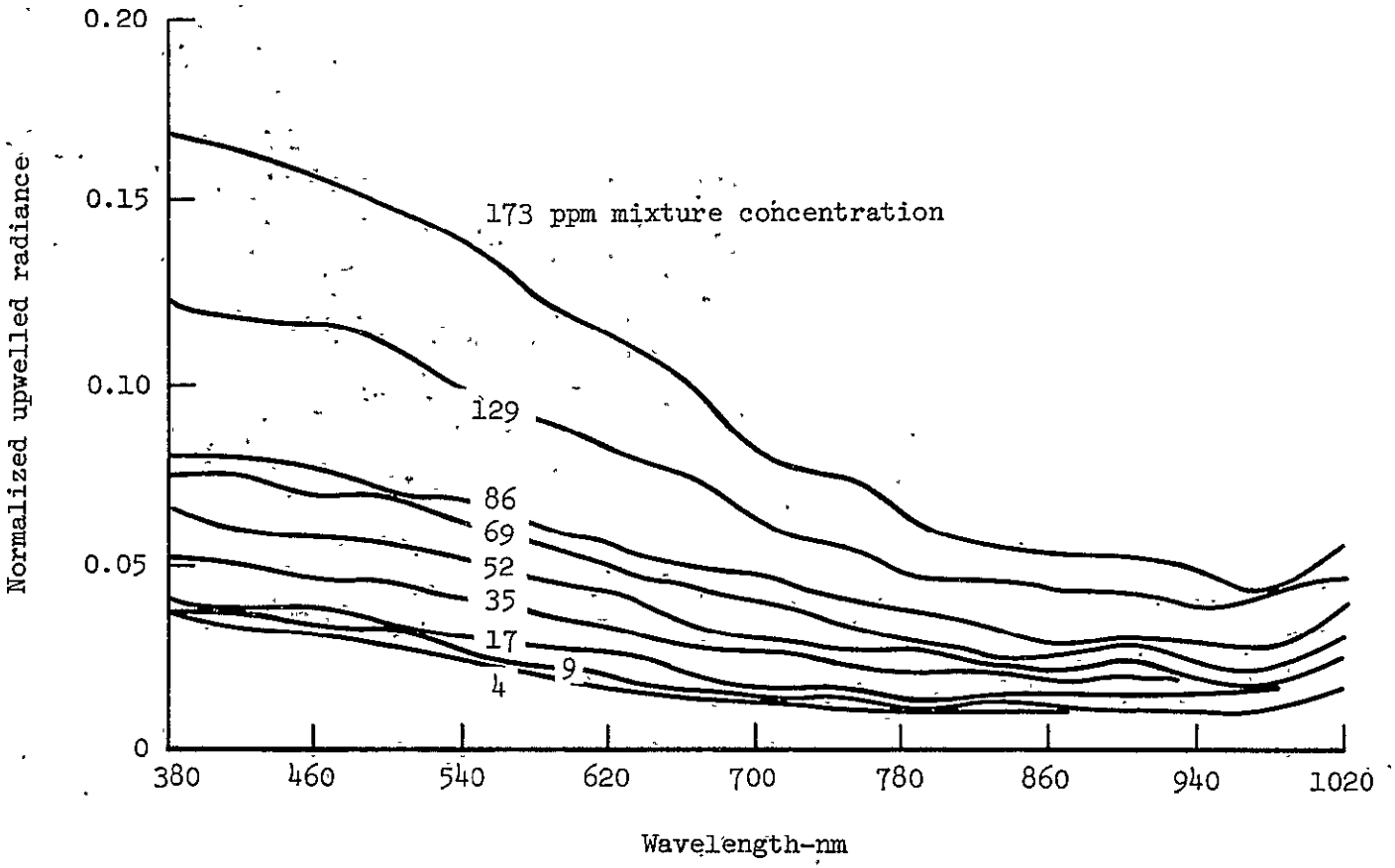

Figure 23.- Wide-band spectra for Feldspar sediment.

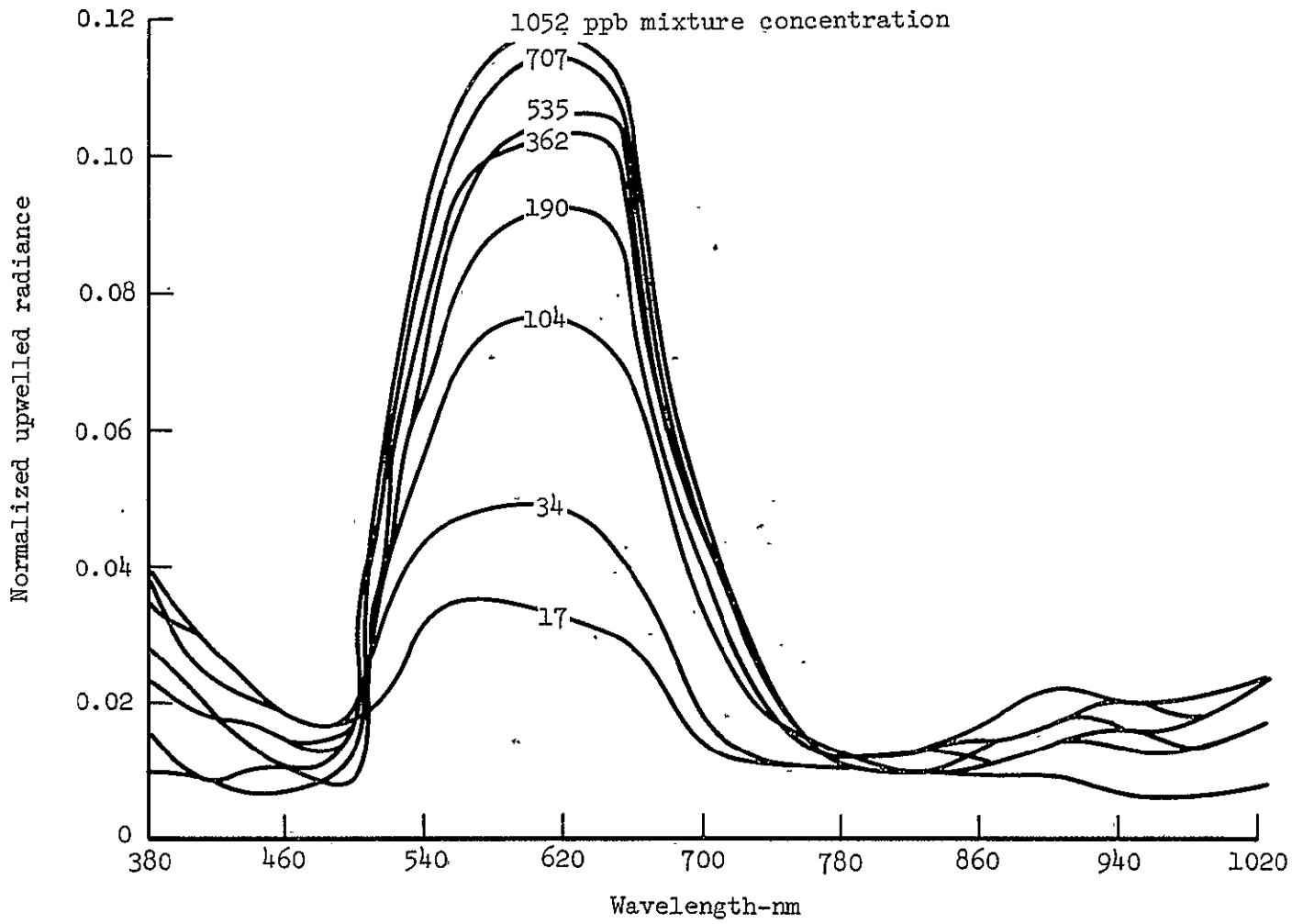

Figure 24.- Wide-band spectra for Rhodamine WT dye.

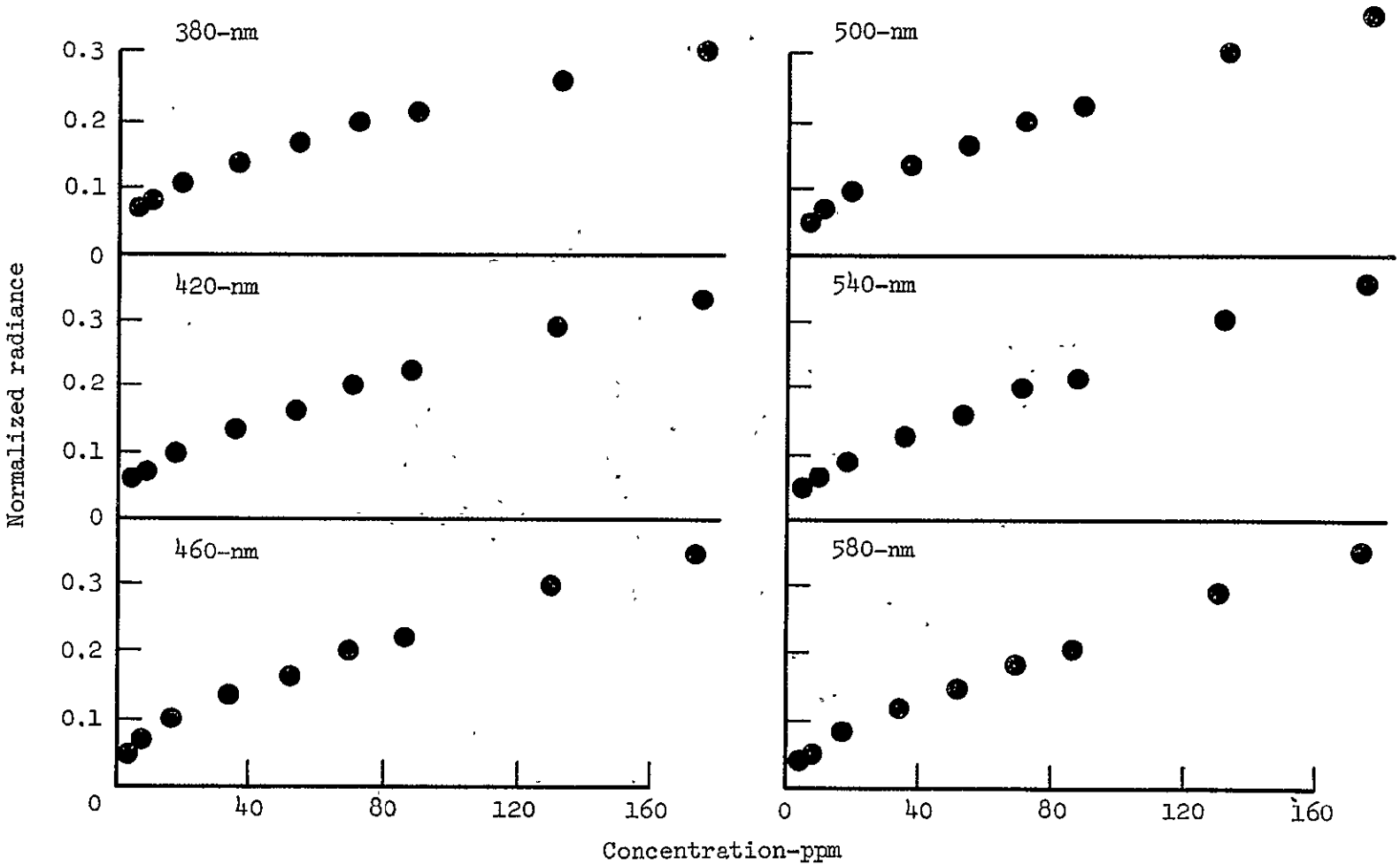

Figure 25.- Linearity of Ball Clay sediment.

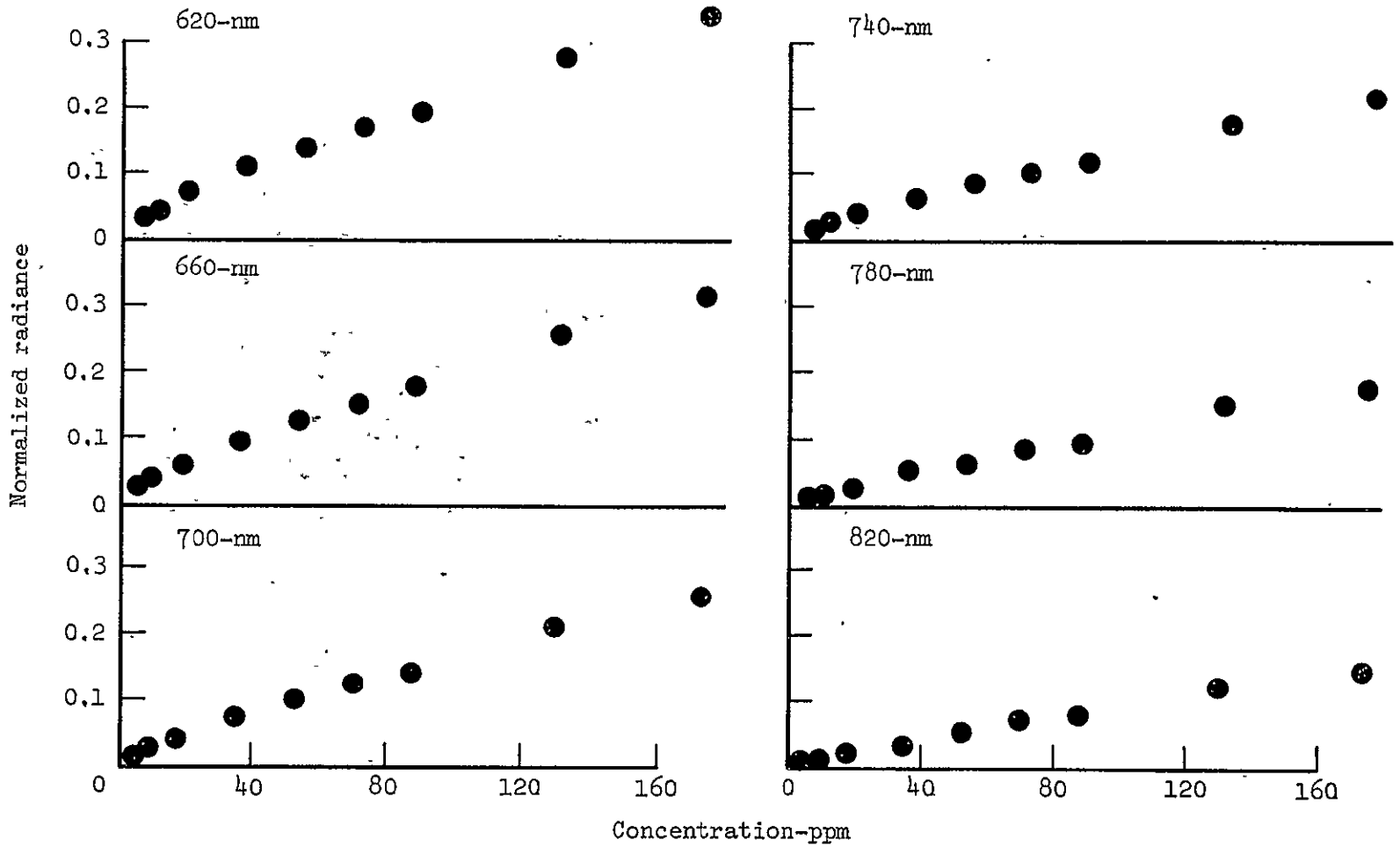

Figure 25.- Continued.

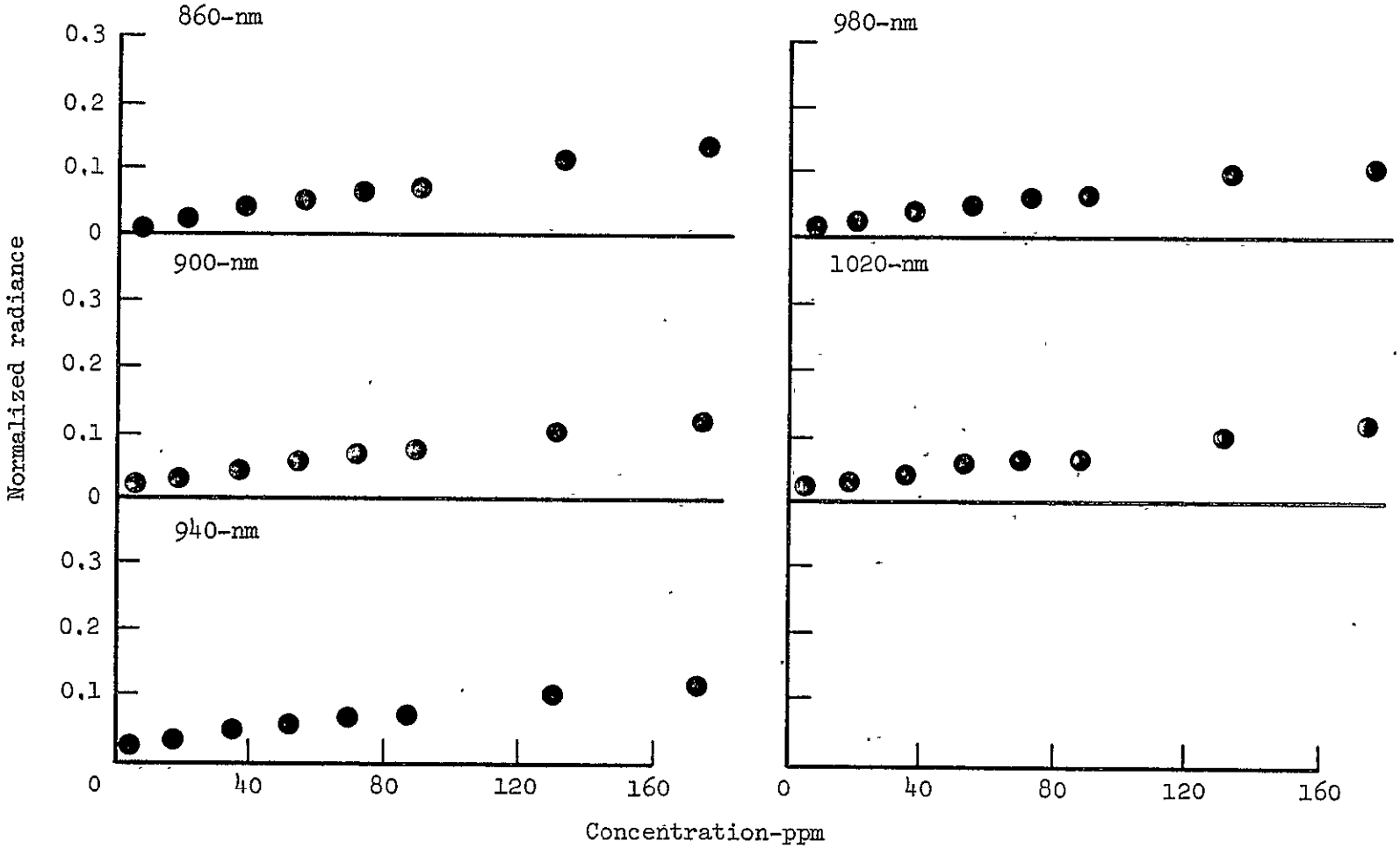

Figure 25.- Concluded.

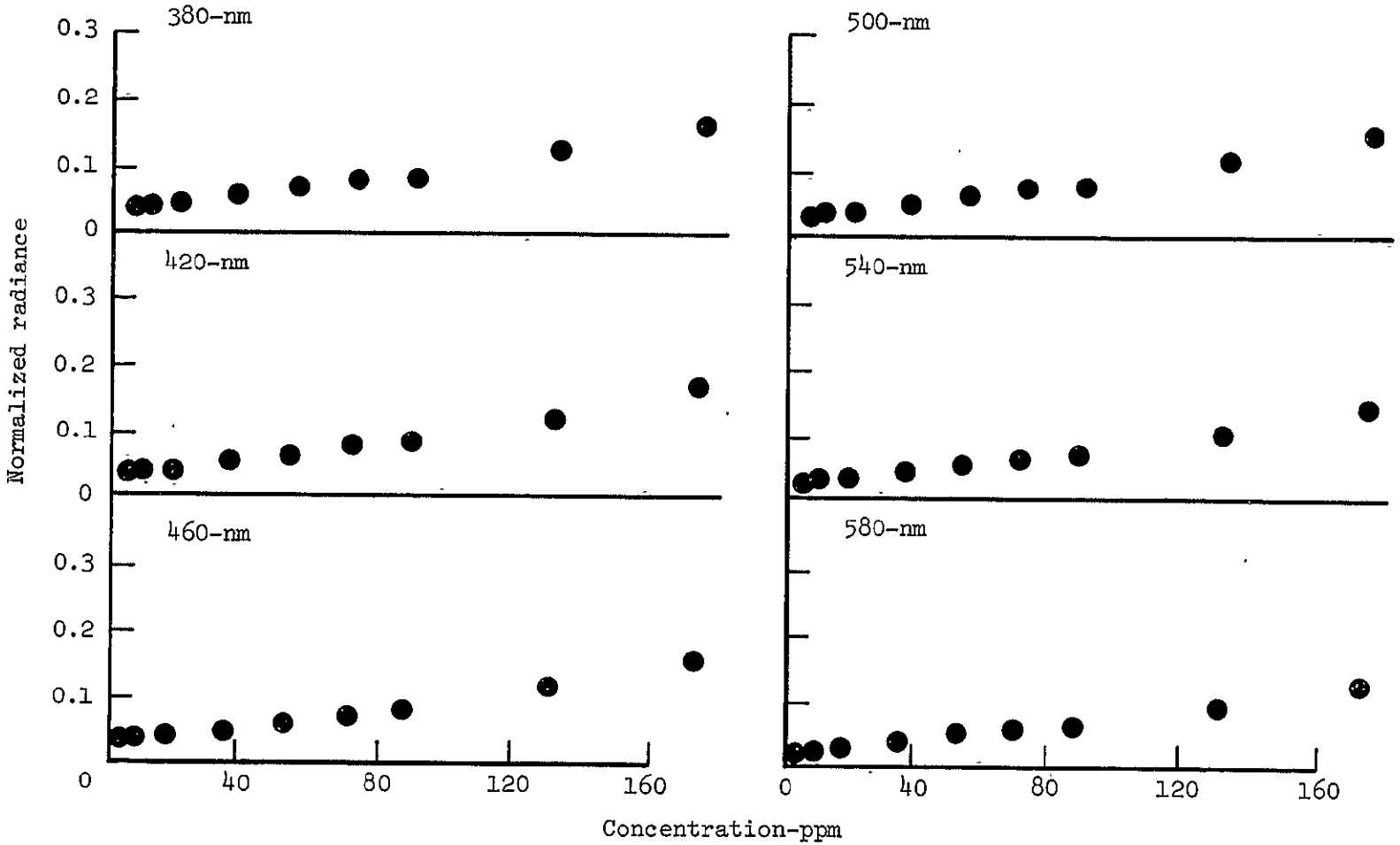

Figure 26.- Linearity of Feldspar sediment.

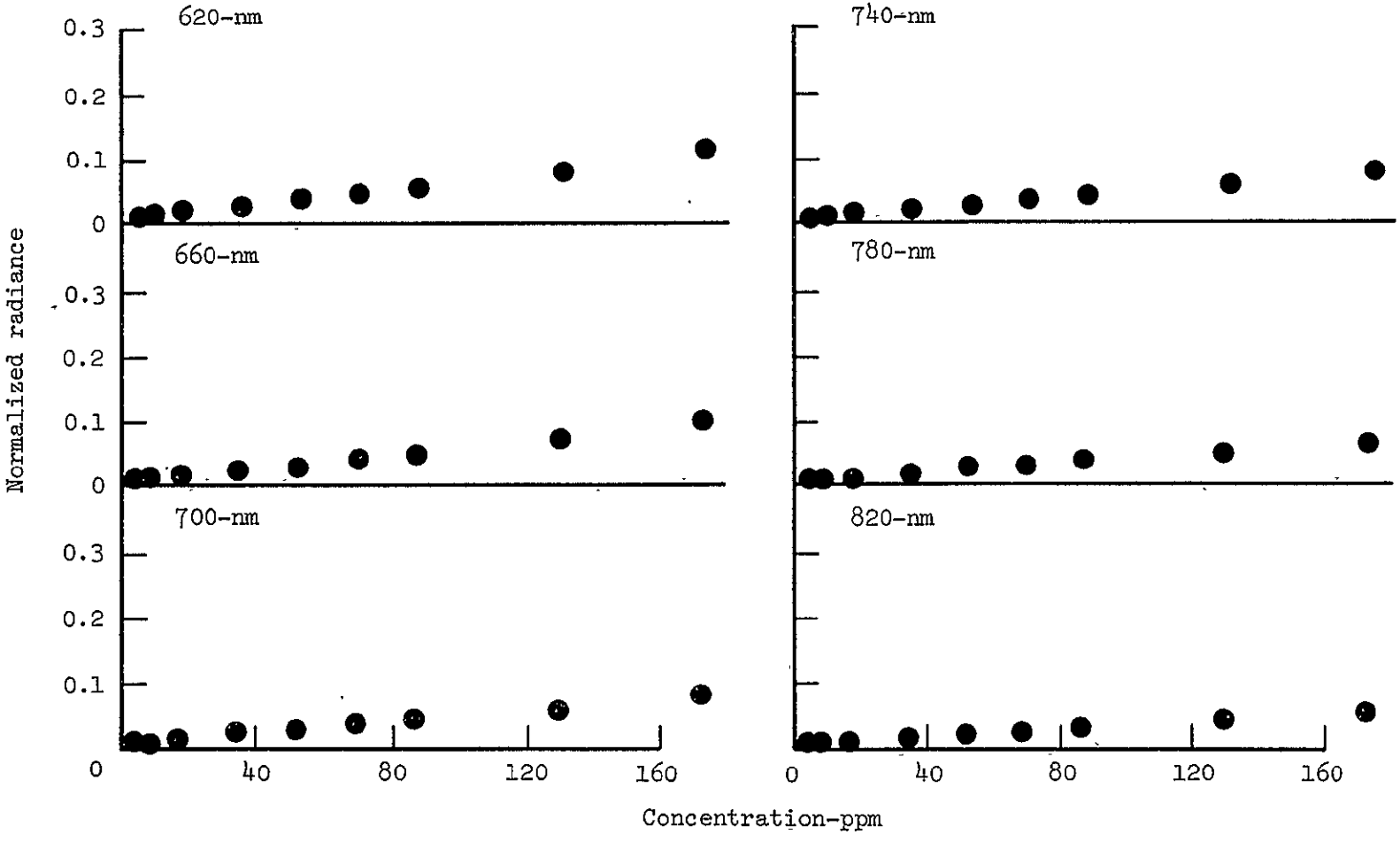

Figure 26.- Continued.

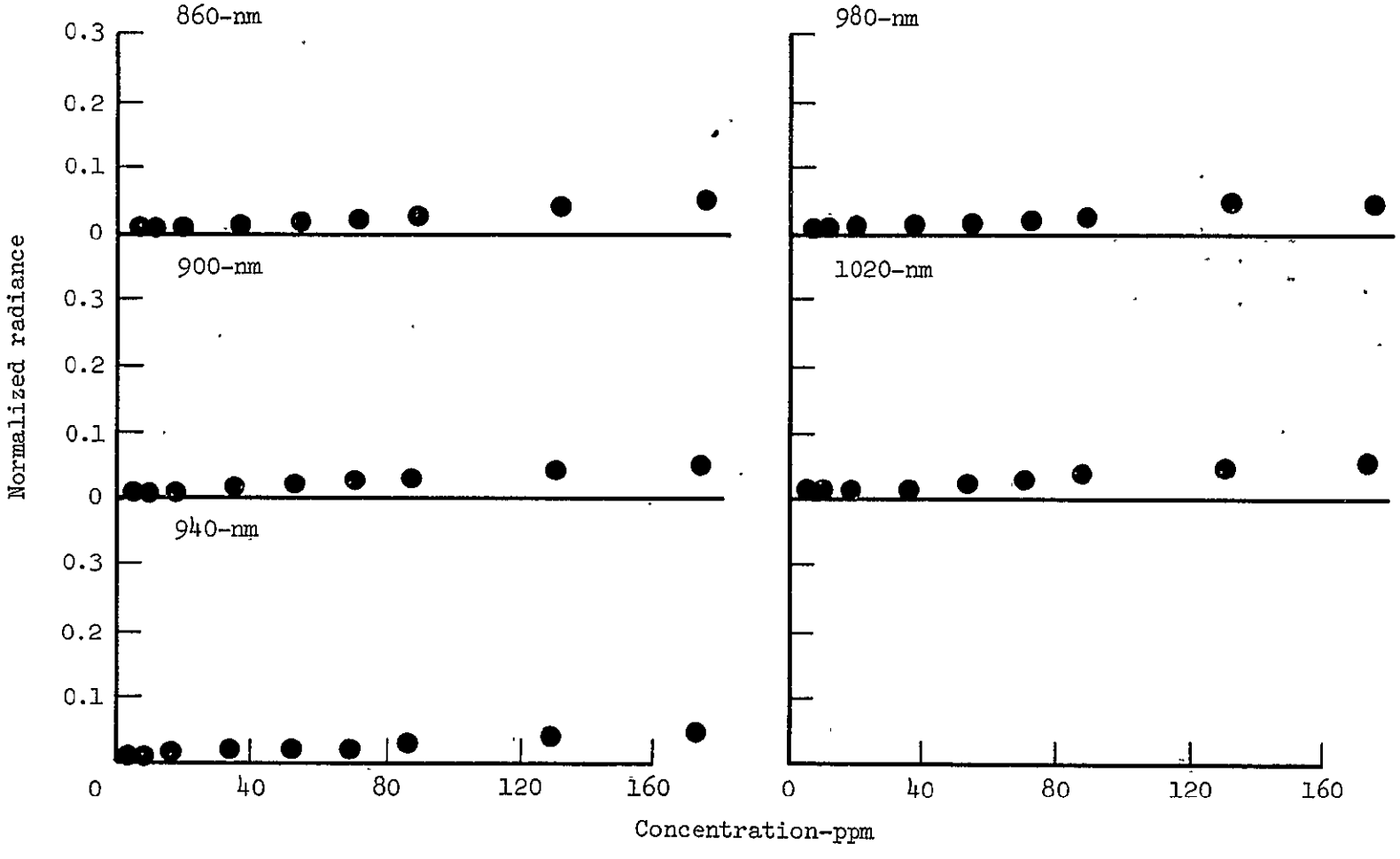

Figure 26.- Concluded.

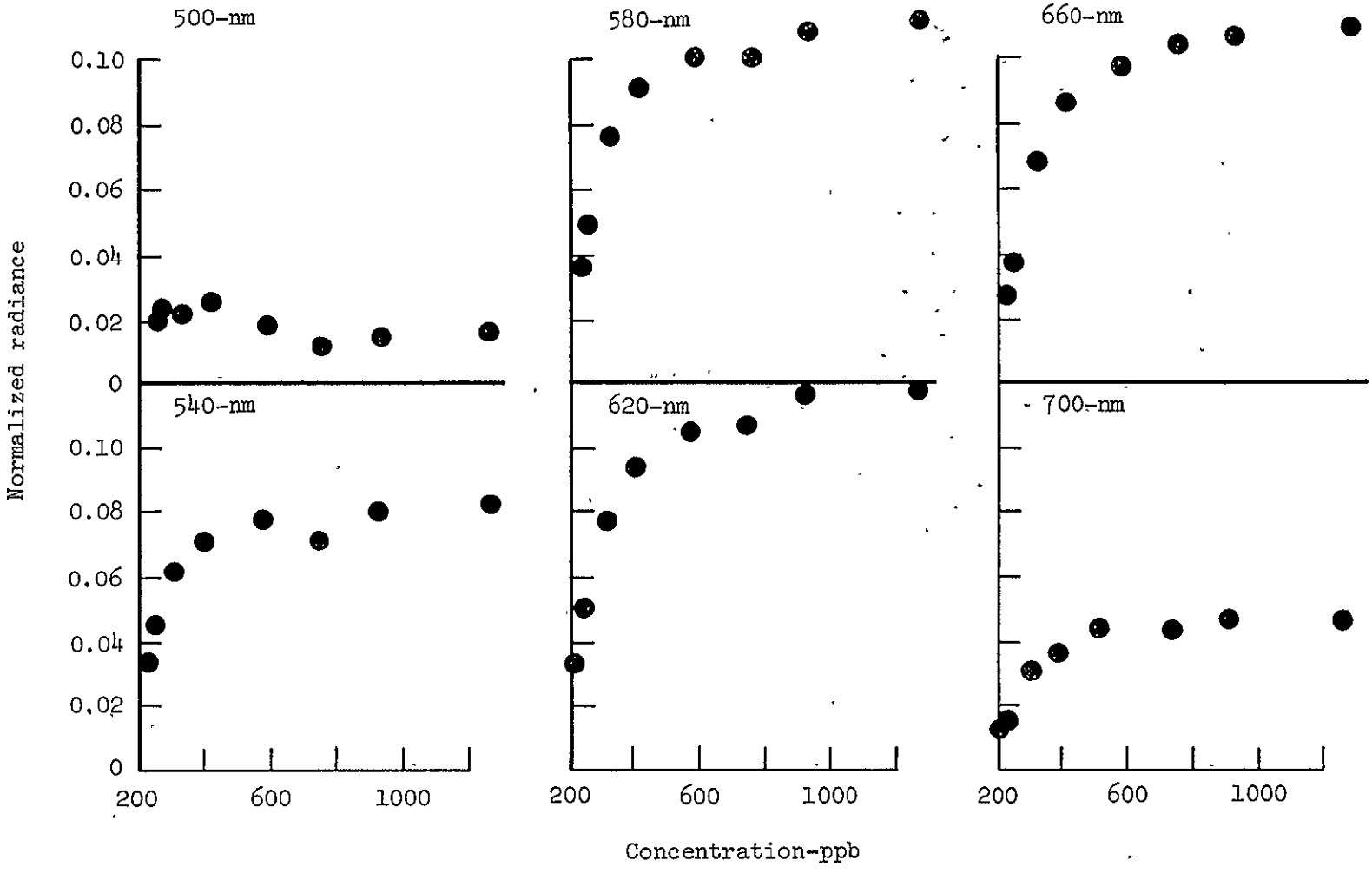

Figure 27.- Linearity of Rhodamine WT dye.

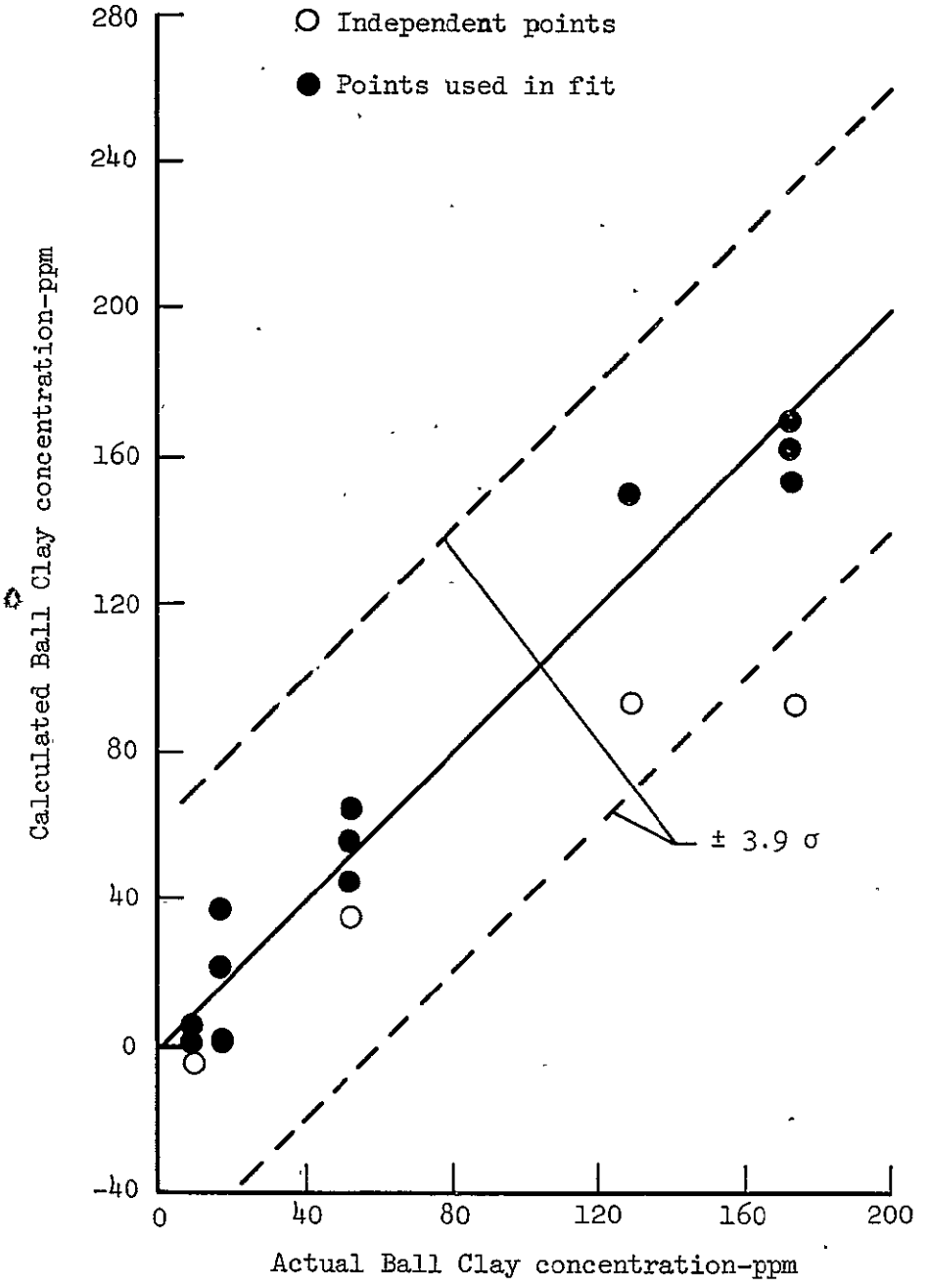

Figure 28.- Comparison of calculated and actual Ball Clay concentration for dual-constituent mixture tests.

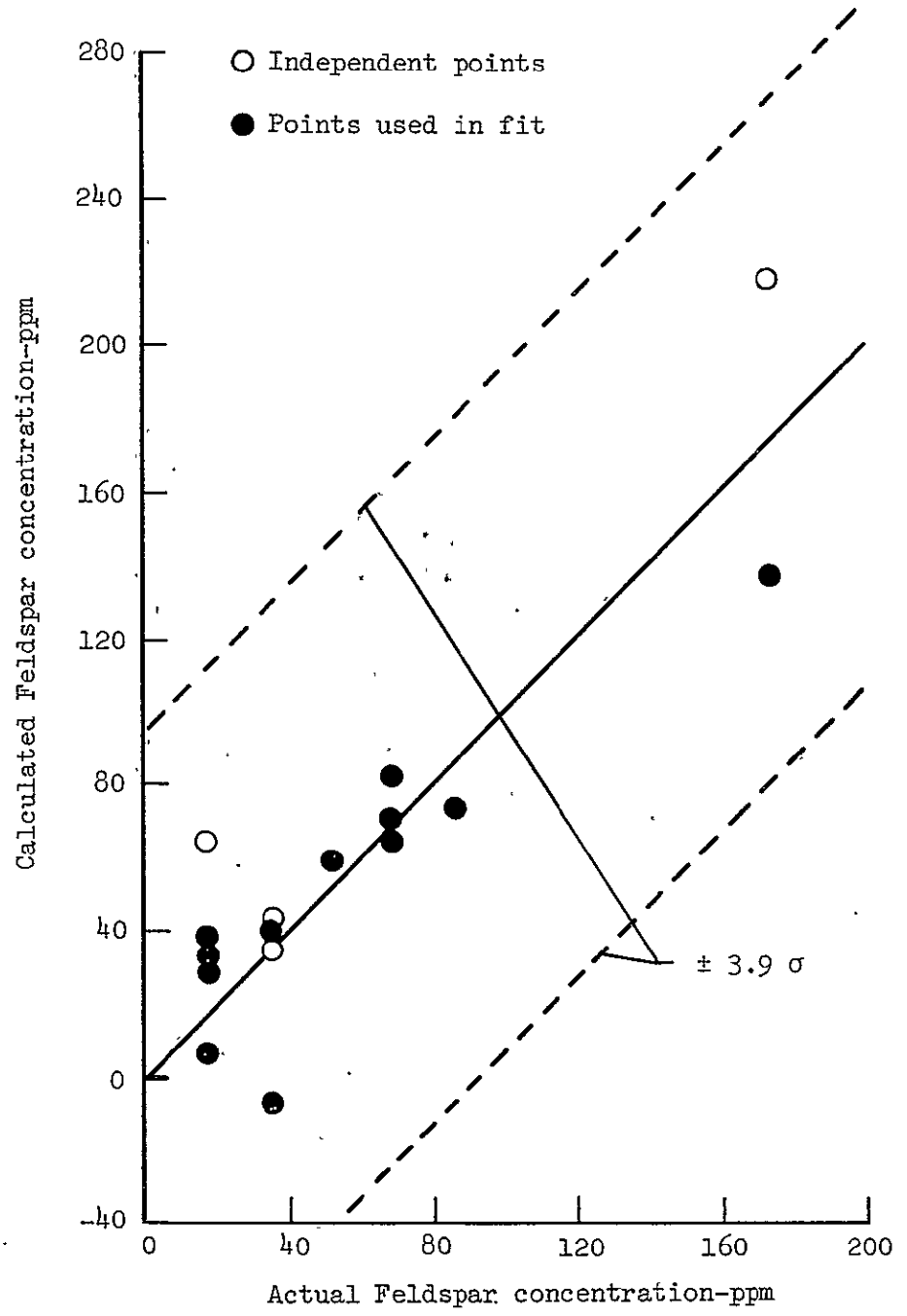

Figure 29.- Comparison of calculated and actual Feldspar concentration for dual-constituent mixture tests.

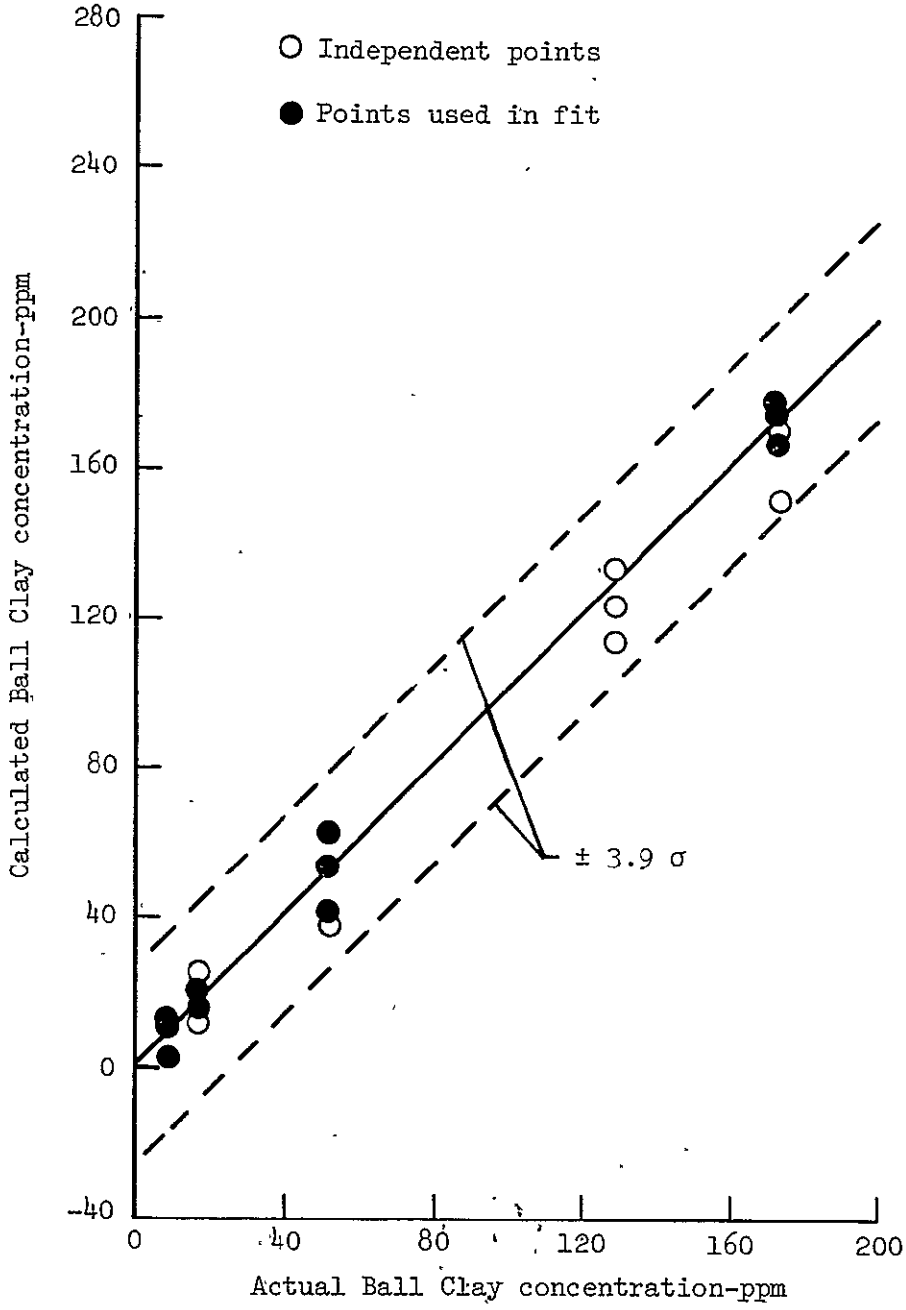

Figure 30.- Comparison of calculated and actual Ball Clay concentrations for three-constituent mixture tests.

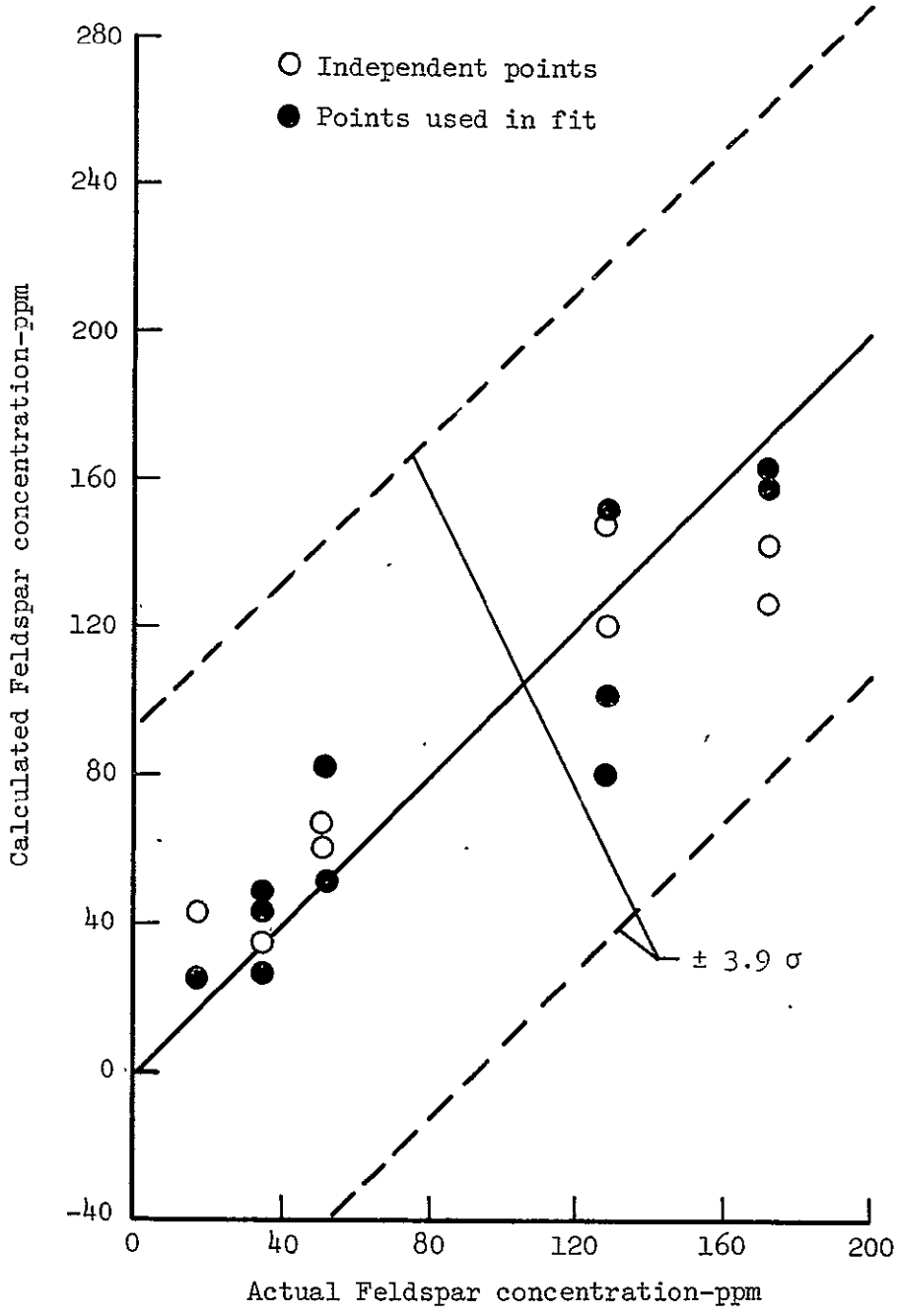

Figure 31.- Comparison of calculated and actual Feldspar concentration for three-constituent mixture tests.

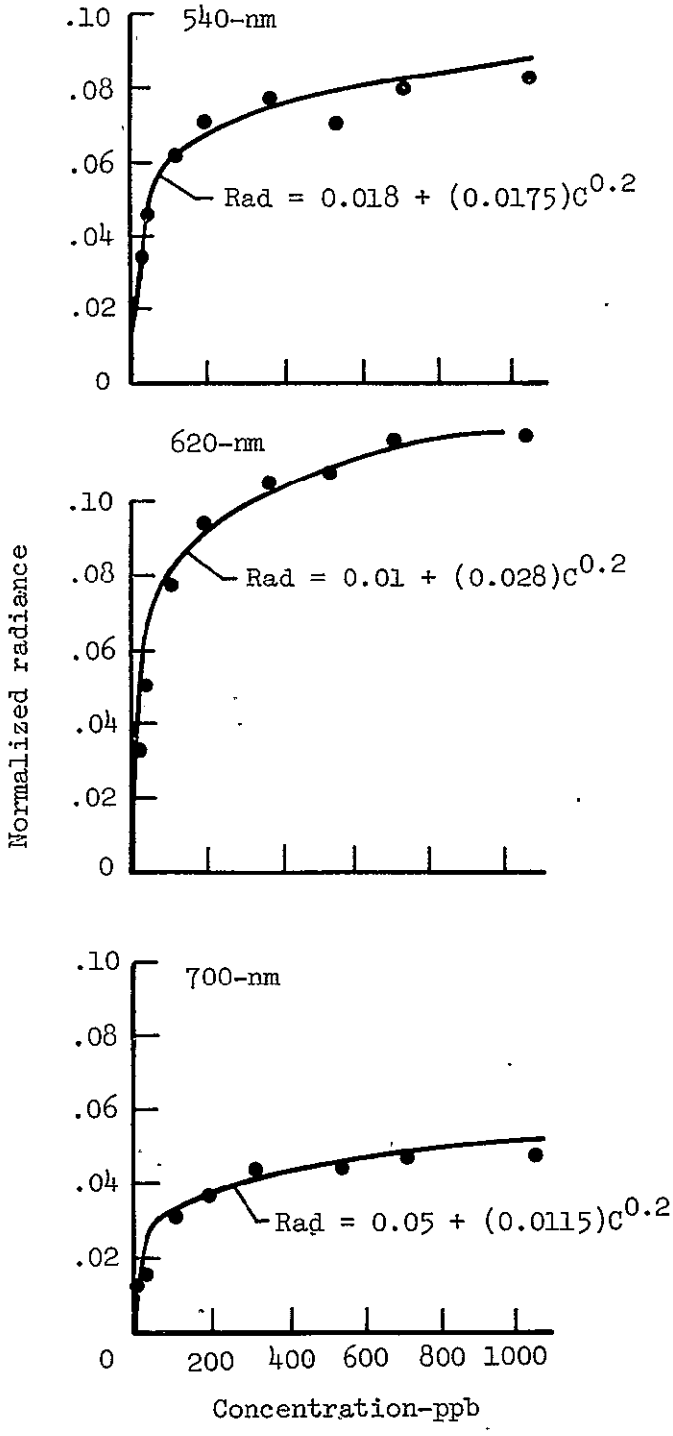

Figure 32.- Power-law fit to Rhodemine WT data.

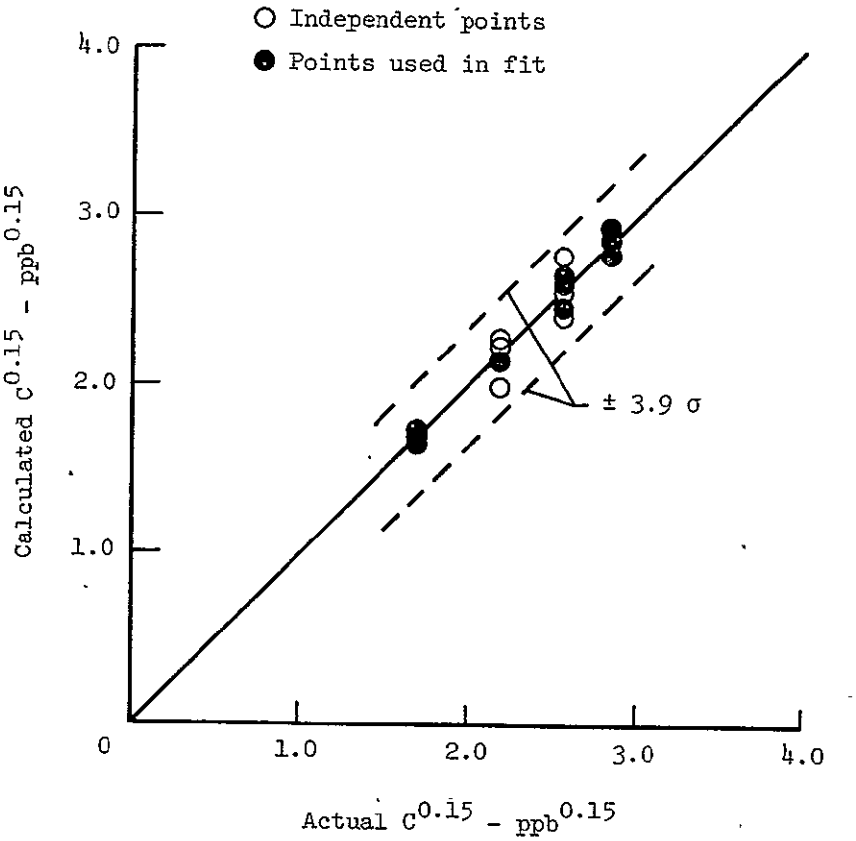

Figure 33.- Comparison of calculated and actual Rhodamine WT concentration to 0.15 power for three-constituent mixture tests.

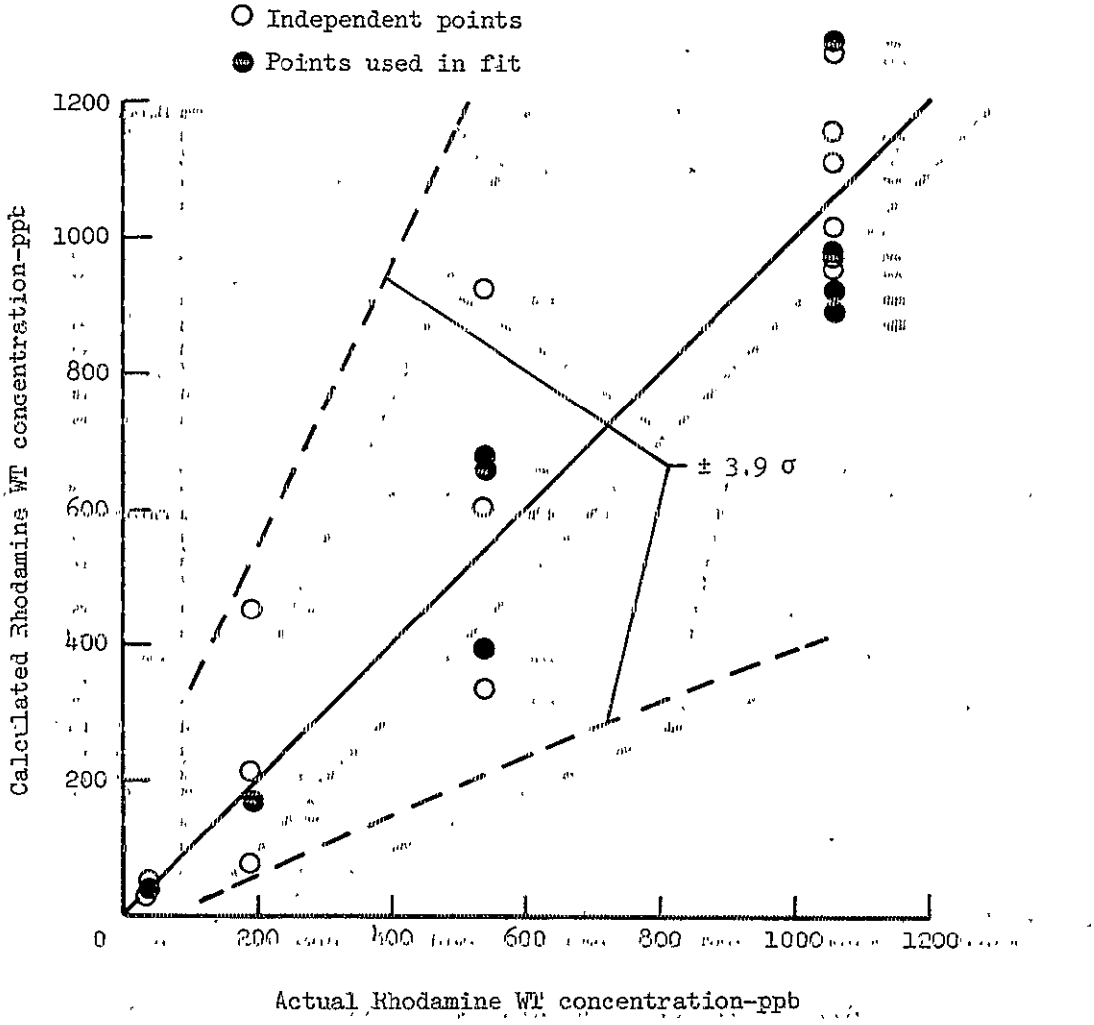

Figure 34.- Comparison of calculated and actual Rhodamine WT concentration for three-constituent mixture tests.

BIOGRAPHY

Charles Henry Whitlock III

Born:

[redacted]

Education:

B.A.E. June 1961, University of Virginia
M.A.E. June 1965, University of Virginia
M.B.A. June 1970, College of William and Mary
Ph.D. Candidate, January 1976 to Present, Old Dominion University

Appointments and Positions:

NASA Langley Research Center. Research Aerospace Engineer (1961-1970), Head of System Dynamics Section (1970-1972), Assistant Head of Marine Analysis Section (1972-1974), Head of Data Analysis Section (1974-1976), Research Aerospace Engineer (1976-Present).

Honors and Awards:

Nine NASA awards for technical accomplishments.

Publications

1. Whitlock, Charles H.: Comparison of Steady-Stage and Six-Degree-of-Freedom Analyses of Pitch-Roll Resonance Conditions for a Long Slender Sounding Rocket. NASA TN D-1816, 1963.

2. Whitlock, Charles H., and Murrow, Harold N.: Performance Characteristics of a Pre-Formed Elliptical Parachute at Altitudes Between 200,000 and 100,000 Feet Obtained by In-Flight Photography. NASA TN D-2183, 1964.

3. Lawrence, George F., Whitlock, Charles H., and Walton, Thomas E., Jr.: Aerothermal Measurements of Damaged Reentry Bodies Obtained in Free Flight at Mach Numbers from 11.0 to 2.0. NASA TM X-966, 1964.

4. Whitlock, Charles H.: A Data Reduction Technique for Determining Reentry Motions Using Body-Fixed Rate Gyro-Accelerometer Data. M. S. Thesis University of Virginia, June 1965 (NASA TM X-57004).

5. Whitlock, Charles H.: A Data Reduction Technique for Determining Reentry Motions Using Body-Fixed Rate Gyro and Accelerometer Data. AIAA Paper No. 65-438, Presented at the AIAA Second Annual Meeting, San Francisco, Calif., July 26-29, 1965.

6. Whitlock, Charles H. and Bendura, R. J.: A Limited Study of the Dynamic Stability Derivatives on Sharp, Right Circular Cones at Hypersonic Speeds. Langley Working Paper 156, Oct. 1965.

7. Whitlock, Charles H. (With Appendix by John D. Shaughnessy): Approximation of Reentry Angles of Attack for a Spinning Body from Rate Gyro and Accelerometer Data. NASA TN D-3492, 1966.

8. Bendura, Richard J., and Whitlock, Charles H.: A Dispersion and Motion Analysis of the Balloon-Launched Phase of the Planetary Entry Parachute Project. Langley Working Paper 290, Oct. 1966.

9. Whitlock, Charles H., Bendura, Richard J., and Coltrane, Lucille C.: Performance of a 26-Meter Diameter Ringsail Parachute in a Simulated Martian Environment. NASA TM X-1356, 1967.

10. Whitlock, Charles H., Henning, Allen B., and Coltrane, Lucille C.: Performance of a 16.6 Meter Diameter Modified Ringsail Parachute in a Simulated Martian Environment. NASA TM X-1500, 1968.

11. Whitlock, Charles H., and Bendura, Richard J.: Dynamic Stability of a 4.6-Meter-Diameter 120° Conical Spacecraft at Mach numbers from 0.78 to 0.48 in a Simulated Martian Environment. NASA TN D-4558, 1968.

12. Whitlock, Charles H.: Low Dynamic Pressure Parachute Deployment Technology for Mars Lander Missions. Langley Working Paper 596, April 1968.

13. Bendura, Richard J., and Whitlock, Charles H.: Preliminary Results of Low Subsonic Dynamic Stability Tests of Three Blunted 55° Half-Angle Cone Configurations with Various Afterbodies. Presented at the Third Technical Workshop on Dynamic Stability Problems. Moffett Field, Calif., Nov. 4-7, 1968.

14. Whitlock, Charles H., Bendura, Richard J., and Henning, Allen B.: Dynamic Stability Characteristics of Large-Size 120° Blunted Conical Spacecraft in a Simulated Martian Environment. AIAA Paper No. 69-104, Presented at the AIAA 7th Aerospace Sciences Meeting, New York, N.Y., Jan. 20-22, 1969.

15. Whitlock, Charles H.: Wind-Tunnel Investigation of Inflation of Disk Gap-Band and Modified Ringsail Parachutes at Dynamic Pressures Between 0.24 and 7.07 Pounds Per Square Foot. NASA TM X-1786, 1969.

16. Whitlock, Charles H., and Bendura, Richard J.: Inflation and Performance of Three Parachute Configurations from Supersonic Flight Tests in a Low Density Environment. NASA TN D-5296, 1969.

17. Whitlock, Charles H., Bendura, Richard J., and Henning, Allen B.: Damping Derivatives of 120° Conical Spacecraft from Flights in a Low Density Environment. Journal of Spacecraft and Rockets, Vol. 6, No. 8, August 1969, pp. 937-939.

18. Whitlock, Charles H.: Structural Load Capability and Margins of Safety of PEPP and SPED I Test Parachutes. Langley Working Paper LWP-776, July 1969.

19. Bendura, Richard J. and Whitlock, Charles H.: Subsonic Dynamic Stability Tests of 140° Cones with Various Afterbodies. Langley Working Paper LWP-785, August 1969.

20. Whitlock, Charles H.: Simulation of PEPP Aeroshell Motions Using Ground-Facility Aerodynamic Coefficients. Langley Working Paper LWP-847, February 1970.

21. Whitlock, Charles H.: A By-Product of NASA; Transfer of New Technology to Various Sectors of the Economy. MBA Thesis, College of William and Mary, April 1970. (NASA TMX-66393).

22. Talay, T. A.; Poole, L. R.; and Whitlock, C. H.: The Effect of Suspension Line Length on Viking Parachute Inflation Loads. LWP-985, September 1971.

23. Poole, L. R. and Whitlock, C. H.: Approximate Unfurling Dynamics During Viking Decelerator Deployment. LWP-997, September 1971.

24. Whitlock, C. H.: Decelerator Angular Motions During Deployment for the LADT #3 Flight Test. LWP-1052, May 1972.

25. Whitlock, C. H., and Siemers, P. M., III: Parameters Influencing Dynamic Stability Characteristics of Viking-Type Entry Configurations at Mach 1.76. Journal of Spacecraft and Rockets, Vol. 9, No. 7, July 1972, pp. 558-560.

26. Whitlock, C. H.: Advances in the Modeling of Aerodynamic Decelerator Dynamics. Astronautics and Aeronautics, Vol. 11, No. 4, April 1973, pp. 67-71.

27. Talay, T. A., Morris, W. D., and Whitlock, C. H.: An Advanced Technique for the Prediction of Decelerator System Dynamics. AIAA Paper No. 73-460, Presented at the AIAA 4th Aerodynamic Deceleration Systems Conference, Palm Springs, Calif., May 21-23, 1973.

28. Whitlock, C. H., Poole, L. R., and Talay, T. A.: Post-Flight Simulation of Parachute Deployment Dynamics of Viking Qualification Flight Tests. NASA TN D-7415, 1973.

29. Talay, T. A.; Morris, W. D.; and Whitlock, C. H.: An Advanced Technique for the Prediction of Decelerator System Dynamics. Journal of Spacecraft and Rockets, Vol. 10, No. 12, Dec. 1973, pp. 817-819.

30. Young, G. R.; Whitlock, C. H.; Rees, T. H.; Suttles, J. T.; Turner, R. W.; and Woodbury, G. E.: An Integrated Approach to the Study of Pollution Transport and Waves in the Coastal Zone - Part II: Modeling. Proceedings of the IEEE International Conference on Engineering in the Ocean Environment, Halifax, Nova Scotia, Canada, August 21-23, 1974.

31. Whitlock, C. H.; and Talay, T. A.: The Influence of Surface Waves on Water Circulation of the Mid-Atlantic Continental Shelf. NASA TN D-7771, 1974.

32. Goldsmith, V.; Morris, W. D.; Byrne, R. J.; and Whitlock, C. H.: Wave Climate Model of the Mid-Atlantic Continental Shelf and Shoreline. NASA SP 358, 1974.

33. Talay, T. A.; and Whitlock, C. H.: Wave Modeling and Experimental Activities in the Baltimore Canyon Region. Proceedings of the BLM Conference on Marine Environmental Implications of Offshore Oil and Gas Development in the Baltimore Canyon Region of the Mid-Atlantic Coast, College Park, Maryland, December 2-4, 1974.

34. Whitlock, C. H.: Coastal Wave Modeling for Application to Advance Hurricane Wave Forecasting Systems. Presented to the Earth and Ocean Dynamics Applications Program Modeling Conference, Washington, D. C., November 18, 1975.

35. Whitlock, C. H.: An Estimate of the Influence of Sediment Concentration and Type of Remote Sensing Penetration Depth for Various Coastal Waters. NASA TMX-73906, 1976.